University of Alberta

Concentration and Mixing Effects on the Production of Amine Hydrochloride Salts in a Confined Impinging Jet Reactor

by

Navid Farrokhzad Ershad

A thesis submitted to the Faculty of Graduate Studies and Research
in partial fulfillment of the requirements for the degree of

Master of Science
in
Chemical Engineering

Chemical and Materials Engineering Department

Fall 2013
Edmonton, Alberta

Abstract

A Confined Impinging Jet Reactor (CIJR) was used to react 4, 4'-methylene dianiline (MDA) with hydrogen chloride (HCl) in order to study formation of the aminehydrochloride (AHC) salts, unwelcome byproducts in the manufacture of polyurethanes.

The effects of several processing variables (local concentration of MDA and HCl and the intensity of local mixing) on the formation of AHC salts were studied. The precipitated solids were characterized using a wide range of analytical techniques: elemental analysis, FTIR, TGA, DSC, optical microscopy, SEM and EDX. The effects of each process variable on the solid compounds and composition, thermal properties, morphology and average particle size are discussed.

Results show that formation of AHC salts more than anything depends on local concentration of MDA and it dominates the structure of product in terms of formation of MDA.HCl or MDA.2HCl. Mixing intensity affects product purity of and evenness of shape and average size.

Acknowledgement

I would like to express the deepest appreciation to my academic supervisor, Prof. Suzanne M. Kresta. Without her guidance and persistent help this thesis would not have been possible. No doubt that you are the kindest person I have ever met in Canada among very nice people here, Dr. Kresta.

This work is enabled by the generous support of Huntsman Polyurethanes. I particularly thank Dr. Archie Eaglesham, Mr. Michael A Schultz, and Don H. Jones for their advice during development of this project. Don, I truly appreciate your inspiring emails full of good comments and questions.

Additionally, I would like to thank Mr. Wayne L. Anthon, for his kind support and contributions to this project at the first steps with his good advice and help on both technical and personal level. Many thanks go to all the other colleagues who helped me in many ways.

I also would like to acknowledge the support of administrative staff of Chemical & Materials Engineering Department at University of Alberta, especially, beautiful Lily Laser for her kindness and endless help and Gayle Hatchard for her generous help with SEM.

Last, but by no means least, I would like to thank my family and friends. Above all, endless gratitude and love to my dearest family, Alireza and Fouzieh, my parents; and Nima and Naeim my brothers and lifetime friends. Special thanks to my dear friend, Samaneh, who helped me with statistical part of the thesis and made the long and cold Edmonton winter days a little warmer!

Table of Contents

List of Figures

List of Tables

Nomenclature

Roman characters

C,c	concentration (M)
C^*	critical concentration (M)
D	diameter (mm)
d_P	particle diameter (μm)
F	F value in ANOVA
F_{crit}	critical value for F-test in ANOVA
H	height (mm)
S	supersaturation (unitless)
S_{crit}	critical supersaturation (unitless)
t	time (s)
t_R	reaction time (s)
t_M	total mixing time (s)
T	temperature (K)
u_{max}	maximum velocity (ms^{-1})
v_{jet}	jet velocity(ms^{-1})
wt	weight percent (%)
Y	product yield (unitless)
%Cl	degree of chlorination (%)

Greek characters

ε	energy dissipation (W/kg)
σ	standard deviation (μm- same unit as in d_P)
τ_{res}	residence time(ms)
μ	dynamic viscosity(Nm^{-2})
ρ	density(kgm^{-3})

Abbreviations

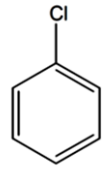	MCB	monochlorobenzene
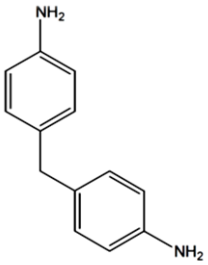	MDA (DADPM)	4,4’-methylene dianiline (4,4'-diamino diphenyl methane)
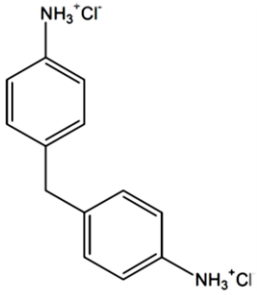	MDA.2HCl	4,4’-methylene dianiline dihydrochloride
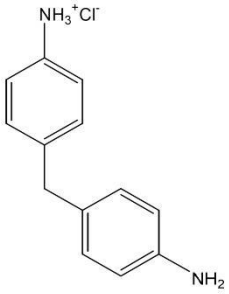	MDA.HCl	4,4’-methylene dianiline monohydrochloride
	AHC	Aminehydrochloride
	ANOVA	Analysis of Variance

1 Introduction

1.1 Polyurethanes

Polyurethanes (PU) are a class of common industrially produced materials that are ubiquitous in our everyday lives. Although knowledge of market size is difficult to estimate with great accuracy, the total size of PU industrial activity was approximately 8 million tons in 2000 [1]. During WWII the reaction was very useful to German scientists allowing them to produce adhesives, coatings, drying oils for paints and foams. Since then the polyurethane world market has grown enormously [2]. In the near future much of the growth is expected to be generated within developing economies. The largest volume participation is, in order of market size: 1) furniture and bedding, 2) building and construction, 3) CASE (coatings, adhesives, sealants, and elastomers), 4) appliances, 5) automotive seating, and 6) footwear [3]. There are also numerous other smaller applications. Polyurethanes have also found medical uses as catheters and artificial heart-assisting devices, most commonly made from flexible (MDI) derived polyurethanes.

Urethanes were first discovered by C. A. Wurtz (1848) when he reported the first synthesis of an organic isocyanate, but later in the 1930s diisocyanates became commercially important when the addition polymerization of difunctional isocyanates and polyols to produce polyurethanes was discovered by O. Bayer and coworkers in Leverkusen, Germany [4].

The richness of polyurethane chemistry has allowed for a tremendous amount of chemical exploration and innovation. Over the past couple of decades, the rapid improvement in analytical techniques has vastly improved our knowledge about polyurethane phase structure and the underlying factors that affect it. This underlying structure is the basis for the resulting

useful broad range of properties we take for granted in our day-to-day lives [1].

1.2 Manufacturing Polyurethanes

1.2.1 Isocyanates

Isocyanates represent a class of chemicals that are characterized by their high reactivity and their versatility. This combination of positive attributes has contributed greatly to the broad application of polyurethane materials, but is part and parcel of the complications associated with isocyanates. The most chemically relevant attribute of isocyanate chemistry is its reactivity with other molecules having active hydrogen atoms.

Such active hydrogen atoms are typically found on molecules having alcohol and amine functionalities and also water. Since addition polymerization requires that monomers be able to propagate a chain by undergoing multiple reactions, polymerizable isocyanate monomers have at least two isocyanate functionalities. The growth of polyurethane technology has been associated with the ability to produce isocyanate monomers at low cost. The low cost requirement has driven the chemistry to employ available and low cost building blocks and industrial production has been optimized to an exceptional extent. The two highest volume diisocyanates are based in one case on toluene to make toluene diisocyanate (commonly referred to as TDI) and in the other case on aniline and formaldehyde to make methylene bis (phenyl diisocyanate) (commonly referred to as MDI)[1].

Methylene diphenyl diisocyanate (MDI) and toluene diisocyanate (TDI) are the major isocyanates used to make polyurethanes [5]. They dominate the global annual isocyanates production of 4.4 million tonnes, having respective shares of 60 and 34%. The furniture industry mainly uses polyurethanes based on TDI whereas most other applications use MDI polyurethanes.[6]

The primary intermediate for MDI is methylene dianiline (MDA), also referred to as diamino diphenyl methane (DADPM), all shown in Figure 1-1. More than 2 million tonnes of MDA was produced in Europe and the USA annually by 2000.[7]

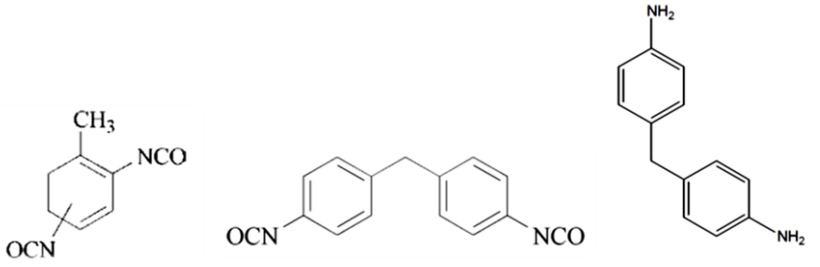

Figure 1-1- Left: TDI, Middle: MDI, Right: MDA

1.2.2 Industrial Isocyanate Synthesis

The production chain to polyurethanes using TDI and/or MDI is portrayed in Figure 1-2. The MDI route is discussed in more detail because the side reaction in the phosgenation step of MDI synthesis is the focus of this research project.

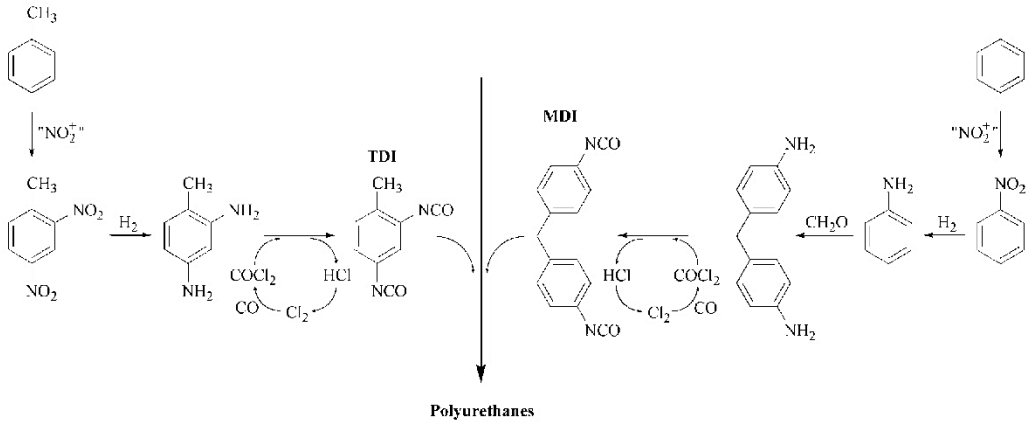

Figure 1-2- Industrial route to MDI and TDI [4]

Toluene is the primary raw material for industrial TDI manufacture. The classical dinitration of toluene with mixed acid produces a mixture of the 2,4-

and 2,6-dinitro isomers in a ratio of 80:20. Catalytic reduction of these derivatives under hydrogen pressure leads to the corresponding diamines TDA, which are subsequently treated with phosgene to give TDI [4].

In industrial MDI manufacturing, benzene is first nitrated to mononitrobenzene in a heterogeneous liquid-liquid reaction using sulfuric acid as a catalyst. The nitration of benzene is highly exothermic with a heat of reaction of -117 kJ mol^{-1}. An adiabatic process uses this heat to remove water from the reaction mixture, the final temperature reaching 393–403 K [8].

Catalytic hydrogenation of nitrobenzene to aniline is highly exothermic (-443 kJ mol^{-1}) and normally carried out over a solid supported Cu or Ni catalyst in the gas phase [9].

Aniline is reacted with formaldehyde and stoichiometric amounts of hydrochloric acid at 333–353 K to produce MDA. 4,4´-MDA production is favored by high aniline to formaldehyde ratios and low temperatures [7]. Other isomers are also formed, 3-5% of the product mixture is the 2,4´- and 2,2´-isomers, and 20-25 % is the higher molecular weight polymeric MDA [11].

The phosgenation of MDA to MDI occurs in the liquid phase either in a sequence of agitated vessels or a continuously operated series of towers at normal or slightly elevated pressures and temperatures (293 – 453 K). An excess of phosgene (50 – 200%), high dilution, and intense mixing of the reagents allows the reaction to proceed without the need for a catalyst [8]. However, this reaction first forms a carbamyl chloride and HCl, which then decomposes to form the desired MDI and more HCl. Removal of excess phosgene and distillation produces pure MDI [2]. Alternative, phosgene free, heterogeneously catalyzed routes to produce MDI have been investigated but not adopted in industry, mainly due to catalyst instability and poor selectivity [8].

Monomeric MDI is obtained from PMDI by continuous thin-film distillation. The residual crude oligomeric isocyanate product (PMDI) is used mainly in the production of rigid polyurethane or polyisocyanurate foams that usually find use in insulation, construction, or automotive applications [4].

1.2.3 Polyurethane Market

Polyurethanes have found many applications in recent years (reported in 2000); the furniture industry has the largest demand, accounting for 29% of the total polyurethane produced globally, followed by the construction and automotive sectors both using 18%; insulation applications and footwear constitute most of the remainder. As an example of their versatility, the automotive industry puts a variety of polyurethane types to use, flexible foams in car seats and head rests, semi-rigid foams in energy absorption parts, integral skin foams in bumpers, dashboards and steering wheels; and polyurethane based coatings which can provide enhanced corrosion and impact resistance of lacquers [2].

In 1998 the worldwide consumption of plastics was estimated at 150 Mt/a, of which PU-based materials accounted for 5% (7.5 Mt/a). Total consumption of diisocyanates in 2000 exceeded 3.4 Mt. The total size of PU industrial activity is expected to grow to 9.6 million tons by 2015[1]. After years of providing polyurethane precursor materials such as MDI, TDI, or polyols, polyurethane producers appear to be moving towards becoming fully integrated polyurethane providers, with the acquisition of ICI's urethane business by Huntsman and, more recently, Bayer's acquisition of Lyondell's polyols business. The companies are making their moves as the polyurethane industry undergoes an extended period of growth [3].

Present day polyurethane technology is highly optimized and widely disseminated. Current trends in polyurethane technology generally focus on correcting perceived deficits in current practice. These include applications of alternative feedstocks, improving environmental, health, and safety

profiles, incremental improvements in properties by design of polymer structure, and employing efficiencies to further reduce cost.

1.2.4 A Problem Encountered in Isocyanate Synthesis

During the industrial manufacture of methylene diphenyl diisocyanate (MDI) ($C_{15}H_{10}N_2O_2$), a complicating feature of the phosgenation of MDA process in a solvent such as chlorobenzene is the formation of unwelcome amine hydrochloride (AHC) salts [11].

In this undesired side reaction hydrogen chloride (HCl) is formed as a by-product by the phosgenation of polymeric amines and also by the subsequent decomposition of the carbamyl chloride. "HCl readily reacts with the polymeric amine to form an unwanted and highly insoluble amine hydrochloride salt." The reaction between amines and HCl in the solution phase to form an amine hydrochloride is a side reaction in the manufacture of isocyanates which causes loss of starting material and can also require extensive reprocessing [12].

1.3 Aminehydrochlorides

Amine hydrochlorides, as a group of compounds, are useful, especially in the pharmaceutical industry. Approximately half of the compounds used in medicine are administered as salts with over 40% of these being hydrochlorides. "Their common therapeutic use is due to the physiological acceptability of the Cl^- ion and ready availability of hydrochloric acid." However, their bioavailability may not always be as good as other salt forms due to the high concentration of Cl^- ions found in the gastrointestinal fluid which would limit the solubility of these hydrochloride salts [13].

AHCs are a major problem in the manufacture of isocyanates, as they cause loss of starting material and costly reprocessing. The more basic the amine is,

the greater this problem becomes, as the amine hydrochlorides that are produced are less soluble than their less basic counterparts [2]. Investigation of the hydrochloride salts and their back reaction to form the amine starting material is the focus of this project.

As far as we could determine, there was not any open literature published reporting the characteristics of these AHC salts, except for the publications of Emma K. Gibson et al. [11, 12, 14] which are used in many sections of this project. Chapter 3 provides characteristics of methylene dianiline dihydrochloride (MDA.2HCl) and methylene dianiline monohydrochloride (MDA.HCl), the main AHC salts made by the mentioned side reaction.

1.4 Mixing and Micromixing

"Mixing is a broad, generic term, which obviously includes reducing the variability of concentration, temperature, and so forth." [15] It is essential to understand mixing when considering the product distribution of many fast multiple reactions. "The ability to influence the yield of a reaction product not only by chemical means (catalysis, solvent, reagent stoichiometry, temperature, etc.) but also by physical means (agitation intensity, reactor type, viscosity of solvent, rate and location of adding reagents, etc.) is economically and ecologically significant." [15] In addition to considering homogenization, it is helpful to regard the scale at which variability exists and the rate at which various mixing mechanisms reduce variability.

"The way in which reagents are mixed can have a large influence on the product distribution of a complex chemical reaction." [16] This effect has been analyzed in detail when mixing on the molecular scale (micromixing or mixing in the viscous-convective and viscous-diffusive parts of the concentration spectrum) is the controlling mixing step [17]. In liquids, micromixing takes place by molecular diffusion, laminar deformation of striations below the Kolmogorov scale and the mutual engulfment of regions having different compositions leading to growth of the micromixed volume.

“Reaction is a molecular-scale process and micromixing should always be considered, although mixing on a larger scale can also be controlling.” [16]

In a general concept of mixing, three phases can be distinguished, namely (i) large scale mixing, (ii) meso-mixing, and (iii) micro-mixing [18, 19]. While large scale mixing, sometimes referred to as macro-mixing, is determined by the large scale motions of the turbulent flow field and the scalar integral scale (e.g. the initial conditions), meso-mixing is the process of reducing the scalar length scale down to the length scale range between the Kolmogorov and the Batchelor scale, the latter being determined by the Schmidt number. Molecular mixing or so-called micro-mixing is defined as the destruction of concentration fluctuations by molecular diffusion [18]. The large scale turbulent motions are a result of the large scale instabilities of the flow occurring in the specific geometry under specific flow conditions. Thus they are, along with the initial conditions of the scalar field, determined by the mixer design. The small scale motions are produced by the large scale motions in a cascade process, during which the individual characteristics of the large scales are mainly lost. Consequently, they are considered to assume a universal behavior which can be described by the theory of isotropic turbulence (Kolmogorov, 1941). “The total mixing time t_M is the total time required to reduce the initial spatial segregation of the reactants over the cascade of macro-mixing, meso-mixing, and micro-mixing down to a molecular segregation scale where the reactants can react.” [21]

To have a better understanding of mixing mechanisms in a simple stirred vessel, as an example, macromixing refers to attaining homogeneity at the scale of the vessel. At the opposite extreme, chemical reaction and its precursor, molecular diffusion, are molecular-scale phenomena. Between these limits two further scales (micro- and meso-) have been identified and will subsequently be explained. In the context of a particular problem it is usually necessary to decide which scale and mixing mechanism determines the final product distribution. Some mixing times in large reaction vessels are

longer than at the laboratory scale, and the most relevant mixing mechanism can be scale-dependent, making such reactions more difficult to scale-up while securing constant product yield and quality [15]

To minimize the process sensitivity to mixing, one must bring the mixing characteristic times, including macromixing, mesomixing, and micromixing, below the characteristic time of the process. Macro-mixing occurs on the scale of the vessel, meso-mixing on the scale of the intermediate turbulent eddies, and micro-mixing on the scale of molecular diffusion in stretching fluid lamellae [17,18, 22].

1.5 Mixing and Reaction

"Many desirable organic reactions are accompanied by side reactions and undesired by-products, which waste raw materials and complicate product work-up and isolation. By enhancing the competition between reactions to obtain more selective syntheses, ecological and economic benefits may be expected. The most effective way to do this is usually catalysis. Recently, however, more has been learned about the role of reactive mixing, which refers here to bringing reagents together on the molecular scale. When chemical knowledge (especially reaction kinetics and physical organic chemistry) is combined with that of mixing, significant improvements to the selectivity of some syntheses can be achieved."[15]

Comparing time constants, or characteristic times, for mixing and reaction is a practical framework for classifying mixing-sensitive reactions. Take two simple examples to compare: A neutralization time constant is orders of magnitude shorter than that for mixing; mixing is rate-determining, and neutralization is instantaneous relative to mixing. Ester hydrolysis, on the other hand, is the opposite: reaction kinetics determines its rate, and hydrolysis is slow relative to mixing [15].

Johnson and Prud'homme in 2003 reported a thorough report of examples of mixing-sensitive processes initiated by the combination of two fluid streams [31]. In all of these cases, the process kinetics and resulting product quality can be determined by the rate and intimacy of contacting two initially separate fluids [31].

By faster mixing, the observed rates of single mixing-controlled reactions, which are the most common case in organic material synthesis, can be significantly increased, thus saving time and reducing reactor volume. In the case where the possibility of multiple reactions taking place in a system exists, mixing can influence not only reaction rates but also the distribution of reaction products. "In some cases mixing can raise product yields, suppress by-product formation, simplify product isolation and purification, and improve conversion of raw materials to products. Such practical considerations dictate that this text treats the influence of mixing on the product distribution of multiple liquid-phase reactions, typically taking place in a solvent and in a semi-batch reactor. The product distributions of sufficiently fast reactions respond similarly to inadequate mixing rates irrespective of whether the reagents are fully miscible (single-phase reactions) or partially miscible (two-phase reactions)." [15]

1.5.1 Precipitation Reactions

"Precipitation typically consists of (turbulent) mixing of two liquid streams and, therefore, mixing affects generation of super-saturation (S), influences its redistribution, and causes transport of previously formed particles in regions of high supersaturation."[32] Precipitation is the result of several mechanisms, namely, nucleation, molecular growth, and secondary processes, such as aggregation (or agglomeration) and breakage, and the driving force is super-saturation [33,34]. Small particles are produced by high nucleation rates, which can be obtained if high mixing rates are realized.

"Since precipitation processes are very fast, the effect of mixing is significant down to the micro-scale level and, therefore, nanoparticles can be produced in mixing devices characterized by extremely short contact and mixing time scales." [32]

Supersaturation and Nucleation

To obtain very fine particles through a fast precipitation reaction, high supersaturation is necessary. Fast mixing in a fast precipitation reaction generates high local supersaturation, inducing rapid nucleation and facilitating small particle precipitation [35,36,37,38]. Supersaturation is created by mixing of controlled chemical reaction, it is consumed by precipitation; and also decreased due to mixing with a less supersaturated environment. The supersaturation distribution determines the local rates of nucleation and growth and strongly affects agglomeration processes because the supersaturated solution supplies the material necessary to bond colliding particles [34].

Nucleation step is the formation of the solid phase and occurs when a critical number of molecules join together to form an embryo. Then, stable embryos form nuclei that grow into bigger particles through molecular growth. "Nucleation and growth are competing phenomena since both consume solute molecules and, therefore, particle size is the result of this competition. Very small particles are produced by high nucleation rates whereas, on the contrary, big particles are produced by low nucleation rates." [32]

Growth and Agglomeration

Both local nucleation rates and nucleic growth depend on local reactant concentration, and increase with an increase in concentration. The reagent concentration corresponding to the critical supersaturation, S_{crit} (minimum

required for nucleation) and above is released via nucleation while the remaining supersaturation ($1 < S < S_{crit}$) is used for growth [36].

Mersmann (1995) and Bramley et al. (1996) have argued that under supersaturation conditions particles grow before they agglomerate. Mersmann (2001) reports that particle growth can be considered to be diffusion-controlled at high supersaturation. Schwarzer et al. (2004), however, reported that particle growth could be considered to be transport-controlled at high supersaturation, though it may not be purely diffusional due to electrostatic attraction/repulsion and the transport of the ionic species through particle charging [39].

Aggregation (or agglomeration) and breakage are defined as secondary processes since they are characterized by slower rates and, as a consequence, usually occur after particle formation; moreover, they do not consume solute molecules, leaving unchanged the total particle mass [32]. Bramley et al. (1996) and Mersmann (1995) have reported that agglomeration during a precipitation reaction in a supersaturated environment involves particle growth and bridge formation which occur simultaneously. Schwarzer and Peukert (2005) stated that agglomeration occurs after solid formation.

Mersmann (1995) has argued that for agglomeration of particles, particles need to be brought close together by diffusion and/or convection, collide, stay together for a sufficiently long time (contact time) and then successfully stick together. It is to be noted that growth and bridging may be extremely fast processes and may be happening simultaneously. Both rates are dictated by the local supersaturation and significant particle agglomeration has been observed by Baldyga et al. (2002) at large reactant concentration. In a turbulent flow, turbulence brings about collisions, with fluid viscosity, particle-number density, particle size, and supersaturation determining the time of contact and successful 'sticking' of particles. "Under turbulent flow conditions, where the shear forces are very high, the weaker or incompletely

bridged particles/aggregates may break giving smaller agglomerates (Mersmann, 2001). Particles would agglomerate if they were in contact for a time longer than the time required to form material bridges." [39]

At low supersaturation the effects of agglomeration are usually negligible, and the crystal size distribution is mainly affected by competition between creation and consumption of supersaturation. At higher super-saturation the process is dominated by agglomeration [34,44].

The turbulent agglomeration (collision) frequency increases with particle sizes and is significantly large for micron size or bigger particles. Siddiqui et al., 2009, found that agglomeration is largely turbulence-induced at the scale of the hard agglomerates [39].

From an understanding of mixing, nucleation theory, diffusional growth of particles and its effect on supersaturation, one can infer that both mixing and reactant concentration will have a significant effect on the agglomeration of primary particles which in turn depends on their size, and that a close interrelationship exists between the various steps in the process.

Turbulent mixing is of great importance in process engineering because it can considerably influence product properties [18,19]. When the chemical time scales t_R are in a similar range or faster than the turbulent time scales, the turbulent mixing determines the reaction rate and thus has a dominating influence on all subsequent steps as e.g. nucleation, growth, agglomeration, and aggregation in a precipitation process. "Controlling the mixing process is therefore the key technology in process engineering of a wide class of products." [21]

In recent years there has been a growing interest in production of particles with size in the sub-micron range (40-200 nm) on an industrial scale. This can be done by controlling particle formation in order to nucleate very small particles and produce stable suspensions. [32]

1.6 Jet Mixers and Confined Impinging Jet Reactor (CIJR)

Since precipitation at high supersaturation is often very fast, rapid mixing is very important. The role of mixing is very complex and usually it is difficult to predict it a priori, however, it has been shown that submicron particles with narrow particle size distribution can be obtained only working under extremely high mixing rates [32]. In fact, it is only under these operating conditions that nucleation is favored over molecular growth.

Although precipitation reactions have traditionally been carried out in stirred tanks, impinging jets have caught attention in recent years. Impinging jets offer a better choice over stirred tanks due to their fast, efficient, intense and continuous mixing characteristics [45]. The high mixing rates required by precipitation reactions can be readily achieved in confined impinging jet reactors that consist of a small cylindrical chamber, where an impinging plane is originated by the collision of two inlet streams, creating a region characterized by fast production and dissipation (ε) of turbulent kinetic energy where the scale of segregation decreases rapidly [38].

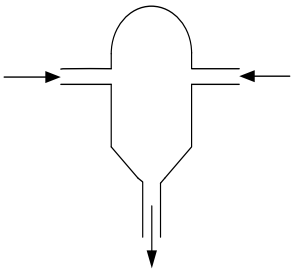

Figure 1-3- Schematic of a CIJR

When the chemical time scales are small, confined impinging jet reactors (CIJR) are often used as they are capable of achieving rapid mixing. This configuration usually consists of two opposing feeding pipes or ducts opening in a main duct under different angles, leading to two impinging jets

in a confined space. Speed and efficiency of the mixing in such a device are determined by the characteristics of the flow, e.g. the Reynolds number, the inflow conditions and the mixer geometry. By changing these process parameters the product properties might be adjusted to the desired values, e.g. the size and size distribution of particles in a precipitation process [46].

Impinging jets consist of two high velocity linear jets of fluid that collide to rapidly reduce the scale of segregation between the fluid streams. They have been shown to be successful at the production scale for several processes [24,48,49,50]. In confined impinging jets, the chamber size affects the process performance of the mixer. Impinging jets can deliver mixing times less than the characteristic process time for fast precipitation processes [28]. The key to rapid mixing is twofold: (1) produce a region of high turbulent energy dissipation; (2) ensure that the process streams for mixing pass through the high intensity region without bypassing. The first criterion ensures the proper scale of mixedness and the second ensures that the desired molar flow ratios are preserved during the rapid mixing process. High energy dissipation occurs for impinging jets because the kinetic energy of each jet stream is converted into a turbulent-like motion through a collision and redirection of the flow in a very small volume [31].

The essential rapid mixing of reagents is brought about by high local energy dissipation in the CIJR [45]. Mixing facilitates built-up of local supersaturation which is discharged by rapid precipitate formation in a fast chemical precipitation reaction. The faster the mixing is, the smaller the particles [35,45]. Post nucleation, the remaining supersaturation is consumed in particle growth and subsequent agglomeration of the precipitated nanoparticles. This aggregational growth transforms nanoparticles into submicron particles [45].

Recently CIJR's have found many interesting applications. The ability of these jet mixers to provide very efficient mixing performances is of paramount

importance in the production of very fine particles. “In fact, in many particle precipitation processes mixing plays a crucial role in determining the final particle size distribution and therefore the final product quality.” [51]

1.6.1 The CIJR used in this research

The undesired side-reaction in manufacturing MDI, which is the reaction of interest in this research project, is a precipitation reaction that produces micron size aminehydrochloride particles. As discussed in the above literature review, CIJRs can provide practical features such as high mixing intensity for the study of precipitation reactions because mixing facilitates a rapid build-up of local supersaturation that is discharged through precipitation of nuclei from the liquid phase. Mixing can thus have a significant effect on particle size and morphology, which was one of the main aims of investigation in this research project.

Siddiqui et al., 2009, in a doctorate research conducted in this research group, fully characterized an identical CIJR to the one used in this work over a wide range of flow rates (50x variation) by measuring the dissipation, and the yield of a homogeneous reaction. Operational limits were evaluated by performing experiments at equal flow rates for all three performance tests and unequal flow rates (up to a 30% difference) for the dissipation and the product yield [39]. Although different reaction and operating conditions such as pressure are used in this project, the previous work provides key data for experimental design analysis.

2 Experimental

2.1 Introduction

The experimental part of the project required strict safety considerations because of the nature of the reagents. A Safe Work Procedure for this project was submitted on the website of Department of Chemical and Material Engineering, University of Alberta, and is available in the Appendices.

In the next sections, after an overview of the reaction, the Confined Impinging Jet Reactor and schematic of the process are described. Analysis of the solid product aminehydrochloride, AHC particles, was done using different qualitative and quantitative techniques including elemental analysis, FTIR spectroscopy and differential scanning calorimetry (DSC) to define the components present in and the composition of the particles, followed by scanning electron microscopy (SEM) and optical microscopy studies to understand the morphology and average particle sizes of AHC particles.

Section 2.6 provides the experimental design description where experimental validation is covered in Section 2.7 in summary referred to the detailed calculations in Appendices. A concise description of the considered and selected analysis techniques is subject of the last section of this chapter, Section 2.8.

2.2 Overview of the Reaction

As described in Chapter 1, in polyurethane synthesis there is a series of undesired side reactions causing loss of the starting materials and very expensive reprocessing. The side reaction involving MDA and gaseous HCl which produces the AHC particles is the main focus of this project.

$$R - NH_2 \ + \ HCl \ \rightarrow R - NH_2.xHCl$$

In this reaction *R* is ½ of the MDA amine group and *x* is between 0.5 and 1.

The reaction was studied in a CIJR reactor with the MDA/MCB blend and HCl/MCB reactant streams entering from opposite sides of the CIJR. The product was analyzed using a range of analysis techniques.

2.3 CIJR Design and Specifications

Figure 2-1 gives an isometric view and full dimensions of the CIJR. This CIJR is made of plastic (KEL-F and Lucite) with stainless steel plates and screws on the sides. The total volume of the CIJR is 0.125 ml and the residence time varies with flowrate from around 50 to 152 ms (for flowrate of 300ml/min down to 100ml/min).

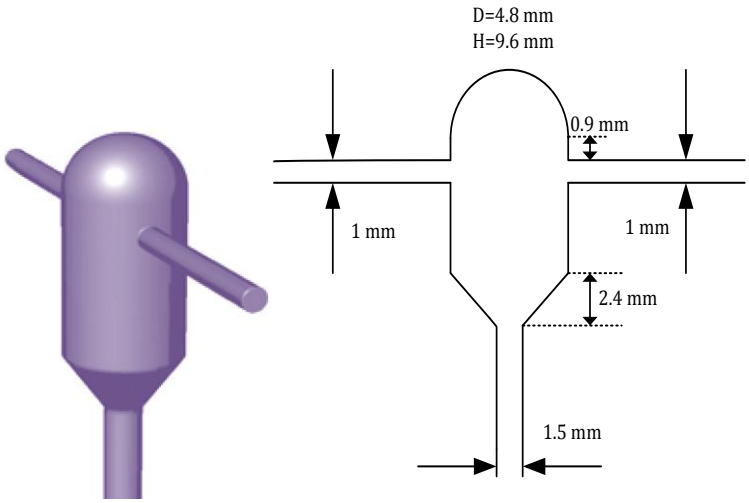

Figure 2-1-CIJR isometric and dimensions

A Confined Impinging Jet Reactor identical in size and design was characterized and simulated by two former students in the group [39,45,52], with parameters such as the local velocity in CFD simulations and the energy

dissipation fully covered in these publications. One of the flowrates which is used in the CIJR as the highest range, 300 ml/min produces the simulation results in Figure 2-2. Reynolds number is calculated by the following equation:

$$Re = \frac{\rho v_{jet} d}{\mu}$$

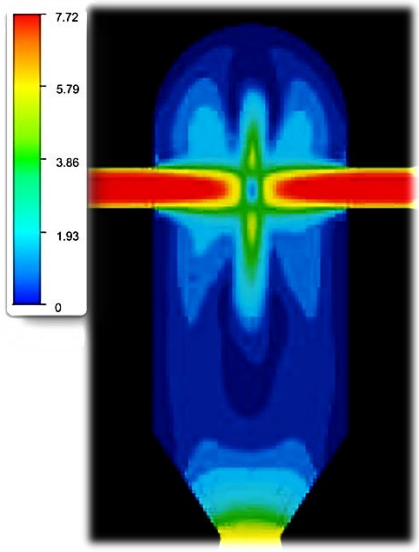

Figure 2-2-Mean velocity contours (m/s) in the CIJR simulation for 300ml/min flowrate from [45]

Table 2-1-Simulation and Experimental data of CIJR characterization from [45]

Parameter	***Value for flowrate of 300 ml/min***
Energy Dissipation Rate, ε (W/kg)	*Experimental: 1490*
	1 time step simulation: 1360
	3 time step simulation: 1365
Maximum Velocity, u_{max} (m/s)	*7.72*
Simulated residence time peak, τ_{res} (ms)	*56*

2.4 Experimental and Analysis Plan

Two major components of the experimental chapter are the experiment set-up and the plan of the experiments which are needed to define the most important process variables. Each variable has restrictions that define the practical range. Most of the restrictions originate from the physics and stoichiometry of the problem, and the equipment used in the set-up. A schematic of set-up is shown in Figure 2-3 (with the full detailed set-up given in Section 2.6).

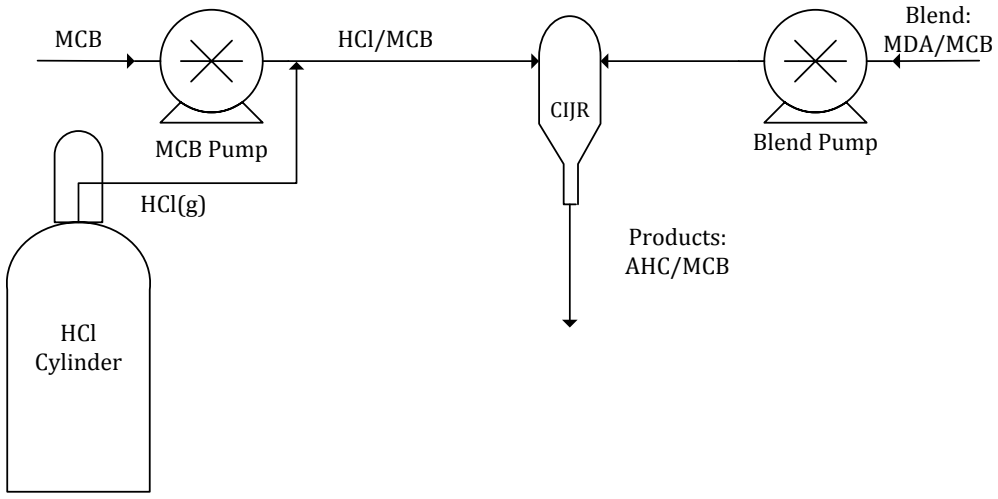

Figure 2-3- Schematic of the process

Initially, four different variables were identified: pressure, temperature, reactant concentration and mixing intensity, which in this case is the flowrate of the streams entering the CIJR. Simplified experiments and optical microscopy images from the first set of products showed that temperature in 25-65°C range has no major effect on the precipitated particles.

Difficulties in changing the variables such as the system pressure narrowed the process variables down to three; concentration of the two feed streams and flowrate of the feed streams. The pressure had to be maintained at 4 bar to ensure that the HCl is fully dissolved in the MCB (see Appendix 2).

The first set of experiments showed that the MDA concentration dominates the structure of the products. The solubility of MDA in MCB has an upper limit of 6.5 wt% in standard condition (1 atm and 25°C). The HCl concentration was set in terms of the percent excess HCl from 0% (no excess gaseous HCl) up to 700% (8 times the stoichiometric requirement of HCl).

$$\%\ HCl\ excess = \frac{Actual\ injected\ HCl - Required\ HCl(Stoichiometric)}{Required\ HCl(Stoichiometric)} \times 100$$

The range of flowrates was based on past work from this research group on the same size CIJR [39]. To stay in the turbulent regime a flowrate of 100 ml/min is required. At the maximum flowrate, 300 ml/min, the sample container capacity allowed a one minute run. The flowrates were kept approximately equal for both sides of the CIJR. Table 2-2 provides a summary of the variables and experimental plan.

Table 2-2- Overview of Process Variables

Experimental Variables	***Blend Strength (wt %)***	***Flowrate (ml/min)***	***HCl Amount (% excess)***
Values	*0.5* *1* *2* *3.5* *5*	*100* *200* *300*	*0* *100* *300* *700*

Note that not all of the possible runs and analysis were done, i.e. out of 60 possible AHC formation runs, 46 runs were completed and 33 of these plus precipitated pure MDA particles were fully analyzed.

2.5 Reagents and Safety

2.5.1 Monochlorobenzene (MCB)

MCB is an aromatic solvent which forms the reaction environment in the process. MCB is used in the lab to prepare solutions and to flush the equipment before and after running the experiments. For these experiments, the MCB was provided by Huntsman Polyurethane as a sample of the MCB used in the plant.

Monochlorobenzene must be handled under the fume hood because it is very toxic and long-term exposure can cause kidney and liver damage. MCB is water-white, volatile, flammable, and liquid at ordinary handling temperatures, and has a boiling point of 131°C.

2.5.2 4,4'-Methylene dianiline (MDA)

As a model for the industrial polymeric amine, 4,4'-methylene dianiline, also known as 4,4′-Diaminodiphenylmethane (DADPM), reacts with anhydrous hydrogen chloride to form amine hydrochloride under different conditions. MDA at ordinary temperatures has a light yellow crystalline form and a melting range of 88-92°C.

MDA is a carcinogen and it damages liver in case of excessive or chronic exposure. Therefore, MDA must be handled with care and any skin contact must be avoided.

2.5.3 Anhydrous Gaseous Hydrogen Chloride (HCl)

An HCl gas cylinder with commercial name of hydrogen chloride HC 2.0 (purity >99%) was provided by Praxair Canada. The gas dissolved in MCB to react with the MDA in MCB blend.

HCl gas is toxic, corrosive, and may cause liver and kidney damage. It can cause eye, skin, and respiratory tract burns. Under ambient conditions, this colorless gas has a pungent, suffocating odor with less than 1 ppm odour threshold. The occupational safety and health administration permissible exposure level (OSHA PEL) for gaseous HCl is 5 ppm and the immediately dangerous to life and health (IDLH) limit HCl (g) is 50 ppm.

A gas detector with a calibrated HCl censor was used to monitor the HCl concentration in the lab to prevent over exposure of HCl and to ensure that the allowable time-weighted average concentration (TWA) for a normal 8-hour workday or 40-hour week of 2 ppm was not exceeded.

2.6 Synthesis of Amine Hydrochloride (AHC) Salts

2.6.1 Supply lines

A. HCl line

As illustrated in Figure 2-4, anhydrous HCl gas from a Praxair K size cylinder, containing 85 kg of 99% HCl at 42 bar, passed through 3 valves and a stainless steel regulator where its pressure was reduced to 4 bar.

In the gas line from the HCl cylinder to the flowmeter, 3 valves and a regulator were used in the following order: cylinder head valve, regulator, needle valve and a 3-way valve which can switch between Air and HCl. Air from the Chemical and Materials Engineering utility compressor has pressure up to around 7 bar and can be used for purging the gas line from the needle valve to the sample container in situations such as shut-down, unclogging or emergencies.

Based on the calculated stoichiometric required HCl for complete reaction to MDA.2HCl and excess HCl, the high resolution flowmeter was adjusted to

maintain the HCl flowrate at a fixed percent excess feed. A venturi feed throat was used to improve the dissolution of HCl in the MCB stream. The MCB was pumped from the MCB container using a positive displacement pump. Constant pulse-free flows to the CIJR were provided by micropump-heads (Series GB, external gear pump, max flow rate 4L/min), which were fitted onto pump drives (MCP-Z standard, IDEX corporation). This stream entered the CIJR on one side to react with the MDA component in the other stream. The flowrates of the two feed streams were set to be equal, although the CIJR can tolerate up to a 30% difference in flows [39].

B. Amine line

On this side, a pump identical to the MCB pump was calibrated for the mid-strength blend (2 wt% MDA) of MDA dissolved in MCB. This was used to maintain an approximately equal flowrate and pressure to the HCl and MCB side. The amine blend enters from the opposite side of the CIJR and reacts with the dissolved HCl.

C. Product Line

Figure 2-4 shows a detailed schematic of the set-up. A back pressure regulator (BPR) just after the CIJR was used to maintain the system pressure at 4 bar gauge. This ensures solubility of the HCl in MCB. The products leaving the CIJR and passing through the BPR were collected in an Erlenmeyer flask packed with 1/8" glass spherical packing to allow the excess HCl to degas and separate from the liquid. The degassed HCl passed thru the flask of 1M NaOH solution and was neutralized. After each run the change of the NaOH pH was recorded by titration. This helps in the mass balance calculation and validation of the run (see Appendix 1). The reaction freezes by dropping the system pressure from 4 bar to atmospheric pressure just passing the back pressure regulator where dissolved HCl degased.

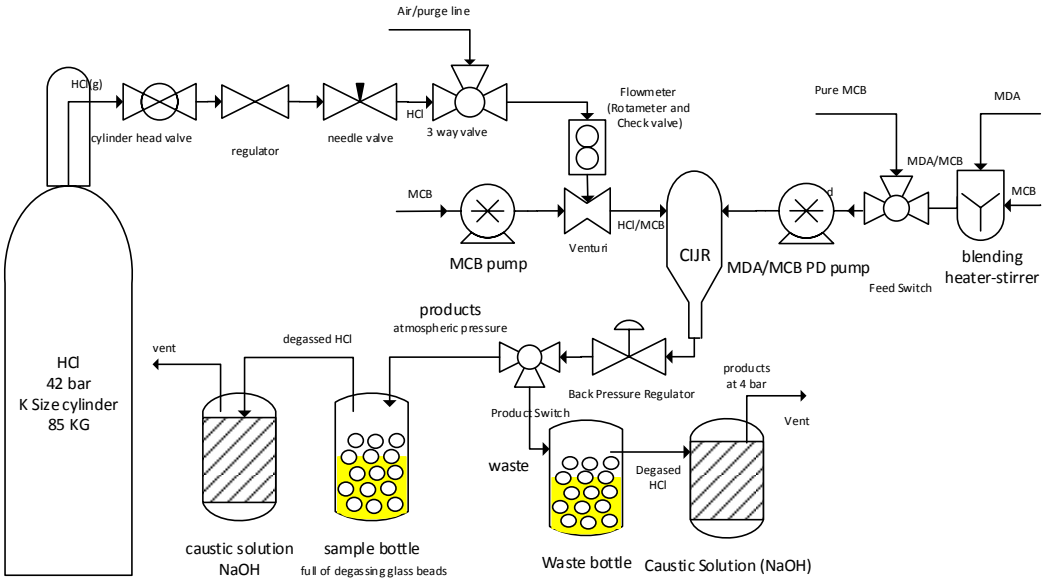

Figure 2-4- Detailed schematic of the experimental set-up

2.6.2 Equipment, Apparatus and Details of Run

On the amine-side, the blend was prepared in a batch process and stored in a beaker connected to a 3-way valve. The valve switched between the pure MCB and the blend. The pure MCB stream was used to flush the line and fill the tubing with MCB before starting the reaction. Also adjusting the HCl flowrate according to calculated amount for the reaction takes time as it must be stabilized before starting the reaction- which is simply switch from MCB to the blend. A magnetic heater-stirrer was used to blending the MDA in MCB in a batch process that takes 15 minutes stirring at 200 rpm at 65°C.

More details can be found in the safe work procedures (SWP) submitted for this project and also available in Appendix 3.

2.6.3 Synthesis of AHC Procedure

As mentioned in Section 2.6 safety is very important because of the nature of the materials used in the process. The procedure of synthesis of the AHC salts followed a checklist for preparation, start-up, production and shutdown. A full description is given in Appendix 3.

Each run took 1 to 3 minutes depending on flowrate of the reagents. During the runs the HCl gas detector was kept close to the set-up in the fumehood. Checking for HCl leaks outside the fumehood was done before and after the run using the same monitor. In case of an alarm exceeding the limit (2ppm), the main valve must be shut off quickly, following by closing all other valves.

2.7 Experimental Validation

A. Process Validation:

Three check valves are used to make sure there is no backflow of the reactants, especially after the flowmeter and before the venturi. The other two check valves were placed just after the pumps to prevent any damage due to backflow of the streams.

The pumps were calibrated under the same operating conditions with the same check valves and the system pressure as the runs with HCl. The first pump calibrations were done using air and water instead of risky materials; then the pumps were re-calibrated for MCB and the blend.

B. Reaction Validation:

MDA is to be completely dissolved in MCB in the experiments. Under standard conditions (25°C, 1 atm) there is a limit for dissolution of pure 4,4'-MDA in MCB which is slightly higher than 6.5 wt%. No more than 5 wt% MDA was used in the experiments; the blend is pumped to the CIJR from an open blend container stored in the fume hood.

HCl is also to be fully dissolved in MCB in the experiments. Data acquired from the plant and from simulations in VMGSim showed that at 4 bar pressure (gauge) the solubility limit of HCl in MCB is 9 mol% which is 10 times the HCl needed for reaction with 5 wt% blend. The HCl concentration was limited to 700% excess at a maximum MDA blend strength of 5 wt%. Details are presented in Appendices.

The material balance for the starting amine was closed with less than 9% error in first experiments. Later more accurate sets of experiments took into account the dissolved HCl in filtrated product stream and remaining blend in the set-up tubing, giving less than 6% error.

The remaining errors could be caused by residual unreacted amines dissolved in the MCB, recording the run times exactly, switching the 3-way valves, or the filtration and drying techniques.

2.8 Analysis Techniques

The product from the CIJR contains AHC particles and MCB in slurry form which needs to be prepared for further analysis. A range of qualitative and quantitative analysis techniques were used to study the morphology, thermal properties, average particle size, as well as determining the components present and the compositions of the solids.

2.8.1 Preparation of Particles for Analysis

The product was filtered using gravity filtration with a Buchner funnel and Whatman cellulose Grade 1 filter papers. After filtering, the particles were dried in the fumehood, weighed and stored in sample bottles. This procedure transforms the slurry first to a wet paste, and then to fine powder. Samples of dried solids were used for each of the six analysis techniques.

2.8.2 Elemental Analysis

Elemental analysis includes identification and quantification of elements and elemental compounds of the bulk of a sample. Samples were tested for trace elements including organic and non-organic, aqueous and non-aqueous materials.

Goal: To identify the elemental composition of a sample. The results include the mass fractions of carbon, hydrogen, nitrogen, and heteroatoms (X) (halogens, sulfur) of a sample- CHNX analysis. This information is used to determine the structure of an unknown compound.

Description: The most common method for elemental analysis, CHN analysis, is accomplished by combustion. In this technique, a sample is burned in an excess of oxygen, and various traps collect the combustion products: carbon dioxide, water, and nitric oxide. The masses of these combustion products can be used to calculate the composition of the unknown sample [53].

In this work, CHN data was obtained from combustion by the Schöniger method and the chlorine content was obtained from titration with $Hg(NO_3)_2$ in presence of Sodium nitroprusside as an indicator.

2.8.3. X-ray diffraction (XRD):

Goal: To determine the average crystal size, polydispersity, and the proportion of solid formed which is crystalline/amorphous which has already been studied in past work sponsored by Huntsman Polyurethanes [12].

Description: X-ray crystallography use the diffraction pattern caused by the scattering of monochromatic X-rays to determine the structure of a crystal based on the electron density in the crystal sample. For the crystal structure

to be fully determined, the crystal must be completely within the diameter of the X-ray beam. The optimum size of the crystal is a few tenths of a millimeter. The diffraction pattern contains information on the amplitude of the scattered waves (F) from the intensity of the diffraction spots, but no information on the phase of the waves [54].

An analysis of the diffraction pattern yields the geometry and symmetry of the unit cell. Mathematical analysis of the intensities of the diffraction pattern is difficult, and takes a lot of computational time, but gives the full molecular structure through refinement of a predicted model structure. As the absorption of X-rays also depends on the path length of the X-rays, it will change with the orientation of the crystal in the X-ray beam, which will in turn affect the diffracted X-rays. If the crystal has a needle-like shape, absorption will be greater through the length than through the thin width of the crystal. In general, providing crystals of sufficient size and quality can be grown, X-ray diffraction provides an excellent description of the molecular structure [54].

2.8.4 Scanning Electron Microscopy (SEM)

Goal: To visualise the structures formed and perform elemental analysis on small regions of the sample. Some SEM techniques such as energy-dispersive X-ray analysis (EDX) can be applied simultaneously with SEM allowing the elemental analysis of small regions of the sample under study. This method can be used to look for differences between apparently crystalline and amorphous regions of a given sample [55].

Description: The scanning electron microscope uses a focused beam of high-energy electrons to generate a variety of signals at the surface of solid specimens. The signals that derive from electron-sample interactions reveal information about the sample including external morphology (texture), chemical composition, crystalline structure and orientation of materials

making up the sample. In most applications, data are collected over a selected area of the surface of the sample, and a 2-dimensional image is generated that displays spatial variations in these properties [55].

Below is the method used to do EDX in this work:

1- SE image (Secondary Electron) taken from an area in which a good disparity of different shapes was available. In SE imaging, low-energy (<50 eV) secondary electrons that are ejected from the k-orbitals of the specimen atoms by inelastic scattering interactions with beam electrons are collected. In practice on AHC salts 2kV and 5kV are used as charge accelerated voltage.

2- BSE image (Back-Scattered Electron) taken to show the points and areas of interest for running EDX. BSE will show a diversity of heavier and lighter atoms in particles which brighter spots represent denser areas of heavier atoms, and darker areas have much lighter atoms in them. BSE consists of high-energy electrons originating in the electron beam that are reflected or back-scattered out of the specimen interaction volume by scattering interactions with specimen atoms.

3- Some spots (3-5) were selected to do spot scanning of the chlorine and carbon elements.

4- A line between two selected points was analyzed using line-scan function, the outcome graph shows areas in which Chlorine and Carbon are higher or lower.

2.8.5 Thermogravimetric Analysis (TGA) and Differential Scanning Calorimetry (DSC)

Goal: TGA provides information about the thermal stability of solid materials and measuring the change in mass during the reaction or vaporization. DSC can report the temperature range and heat of crystallization and melting

processes. Multiple peaks in DSC can also report different compounds existing in a sample.

Description: TGA measures the change in mass of a sample against time or temperature. There are three main parts of a thermobalance, the electrobalance, the furnace and the PC which controls the thermobalance and acquires the data. The balance is protected from corrosive or oxidizing gasses by purging with an inert gas. A few milligrams of the solid sample are placed on the pan of an electrobalance in a furnace. The mass of the sample is then continually measured during either an isothermal experiment or a temperature ramp. A graph of mass loss against temperature or time is produced [56,57].

DSC is a technique in which the solid sample is placed in the oven in a sealed pan alongside an empty reference pan. The heat flow in or out of the sample is measured by taking the difference between the temperatures of the sample and the reference as the temperature of the oven is ramped linearly. During a melting process, the sample will not change temperature as it is using the energy to change phase, but the reference pan will continue to increase in temperature, and the difference is measured. If there is no phase transition, the heat flow is the heat capacity of the material. Crystallization is exothermic and so a positive heat flow would be recorded, melting is endothermic and gives a negative heat flow [56,57].

2.8.6 Fourier Transform Infra-Red Spectroscopy

Goal: The method of Infrared spectroscopy can identify unknown materials. It also can determine the quality or consistency of a sample, and the amount of a component in a mixture. FTIR KBr pellet is the best spectroscopy analysis technique to define components available in the AHC products [58].

FTIR spectroscopy can be used as a diagnostic tool for the extent of hydrochlorination of prepared samples of the amine hydrochlorides. [12].

Description: In infrared spectroscopy, IR radiation is passed through a sample. Some of the infrared radiation is absorbed by the sample and some of it is passed through (transmitted). The resulting spectrum represents the molecular absorption and transmission, creating a molecular fingerprint of the sample [59]

2.8.7 Optical Microscopy

Goal: To study morphology, shape and size of the particles. It can be used in both qualitative and quantitative studies.

Description: Optical microscopy was the first analysis technique used in analysis of the formed products. It has helped understanding the sensitivity of the particles to each process variable in order to plan the experiments. Carl Ziess Axio Lab.A1 microscope was used to take images from the samples made under different process variables in the CIJR.

Microscopy images were later processed to measure the average particle size of the samples. The protocol of detecting single particles was based on the threshold and contrast in images. After detecting the single particles, the surface area was measured and reported as an equivalent diameter of the particles. By increasing in the number of images taken from each sample, errors could be minimized. The procedure is explained in Section 4.5 in detail.

2.8.8 Summary of Analysis Techniques Used

Among all of analysis techniques available for the solid particles, only some techniques were used to study particles. There is a lack of essential reference data for AHCs for some of the methods, which limits our analysis to five techniques.

Table 2-3- Summary of Selected and Considered Analysis Techniques

Method	*Elemental Analysis*	*FTIR KBr Pellet*	*TGA*	*DSC*	*SEM (SE and BSE imaging, EDX)*	*Optical Microscopy*	*XRD*
Considered?	✓	✓	✓	✓	✓	✓	✓
Selected?	✓	✓	✗	✓	✓	✓	✗

Elemental analysis and EDX of a sample provide a list of existing components and compositions which can be validated by FTIR and DSC. The morphology and qualitative studies of the growth and aggregation in molecular structure are shown in the SEM images, while the optical microscopy image processing can provide the average particle size.

3 Characterization of Aminehydrochloride Salts

3.1 Introduction

In this work, a number of analytical techniques were used to characterize particles made in the CIJR. These results were used to quantify the effects of reaction variables such as local concentrations and mixing intensity on the AHC particles.

Chapter 3 contains characterization of high concentration AHC salts and MDA using the most successful analytical techniques. This provides reference data for each of three high concentration salts (MDA, MDA.HCl and MDA.2HCl). Once the best practical qualitative and quantitative techniques are selected, it is possible to compare samples made under the effect of different reaction variables in Chapter 4 with the high concentration salts as reference data from Chapter 3.

Five samples are characterized in this chapter:

1&2) two high concentration MDA.2HCl samples (above 99% based on elemental analysis results) made in the CIJR with the following two sets of reaction conditions:

0.5% MDA, 100 ml/min flowrate, 100% excess HCl (sample 1)

0.5% MDA, 200 ml/min flowrate, 300% excess HCl (sample 2)

3&4) two high concentration MDA.HCl samples (above 99% based on elemental analysis results) made in the CIJR with the following two sets of reaction conditions:

5% MDA, 100 ml/min flowrate, 100% excess HCl (sample 3)

5% MDA, 200 ml/min flowrate, 300% excess HCl (sample 4)

5) 97% MDA as supplied by Sigma-Aldrich, precipitated from a super-saturated solution of MDA dissolved in MCB as it was cooled down from 65°C to room temperature.

3.2 Identifying Compounds and Compositions Using FTIR and Elemental Analysis

Elemental analysis provided some of the best analysis of MDA and AHC salts. It gives C H N and Cl elemental compositions for all of the samples. These results can be compared with the theoretical the C/Cl ratio for MDA.HCl and MDA.2HCl.

FTIR is used to confirm and distinguish the sample compounds. The peak assignments are available from the past work by Emma Gibson et al. [11,12,14]. The FTIR results verified consistently the compounds predicted by the elemental analysis data.

3.2.1 Elemental Analysis of High-Concentration AHC Salts and Comparison with Theory

In Table 3-1, CHN data from combustion by the Schöniger method and Cl from titration by $Hg(NO_3)_2$ in presence of sodium nitroprusside as indicator are compared with the C/Cl ratio for pure salts. The C/Cl ratio is used to calculate the percentage purity for each sample.

The experimental results are in very close agreement with the theoretical values. From here on, higher than 98% MDA.HCl and MDA.2HCl based on elemental analysis are called pure salts. Two samples of each AHC salt are characterized in this chapter and then used as reference data for Chapter 4.

Table 3-1- Elemental analysis of high concentration AHC salts

Titles / Salts	Reaction Conditions			C	H	N	Cl	C/Cl	Compound and Purity
	MDA conc. (%)	Flowrate (ml/min)	HCl excess (%)						
Salts Made in CIJR	0.5	100	100	57.5	5.9	10.2	26.3	2.19	99% MDA.2HCl
	0.5	200	300	57.5	6.0	10.0	26.3	2.19	99% MDA.2HCl
	5	100	100	66.5	6.5	11.8	15.0	4.43	99% MDA.HCl
	5	200	300	66.5	6.6	11.7	15.1	4.40	100% MDA.HCl
Sigma Aldrich	97	-	-	78.8	7.1	14.1	0.0	-	Pure MDA
MDA in Theory	100	-	-	78.9	7.0	14.1	0.0	-	MDA in Theory
MDA.HCl in Theory	-	-	-	66.5	6.4	11.9	15.1	4.4	MDA.HCl in Theory
MDA.2HCl in Theory	-	-	-	57.6	5.9	10.3	26.2	2.2	MDA.2HCl in Theory

3.2.2 FTIR Data from High Concentration Salts and Comparison with Past Work

The FTIR KBR Pellet method is the best available method for detecting amine groups. Spectra of 5 pure samples, one for MDA, two for MDA.HCl and two samples of MDA.2HCl are presented in Figure 3-1, along with a copy of three pure salts' spectra from Emma Gibson's thesis [12] to illustrate the similarity in trends and peak assignments.

Table 3-2 contains the most distinguishable peaks on FTIR spectra for pure samples from past work on similar materials. The peak assignments and relative peaks' frequencies were verified with the 5 pure samples made in the CIJR in order to investigate whether FTIR can successfully distinguish the

compounds present in these samples. The verification of results is given in Table 3-3 for MDA.2HCl, Table 3-4 for MDA.HCl and in Table 3-5 for MDA.

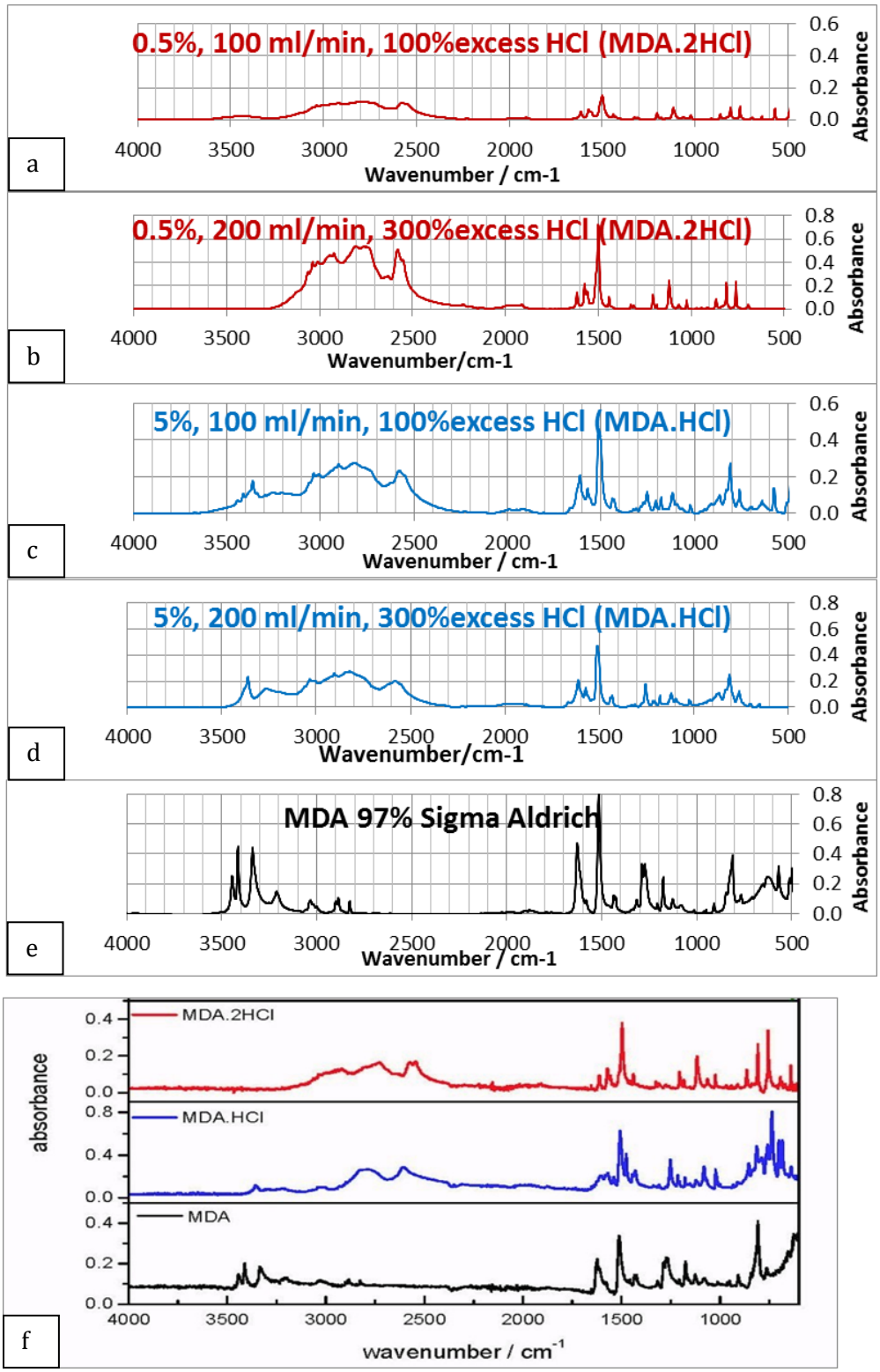

Figure 3-1- FTIR spectra of MDA.2HCl (a: Sample 1 and b: Sample2), MDA.HCl (c: Sample 3 and d: Sample 4), and MDA (e); compared with Emma Gibson's FTIR Spectra (f).

Table 3-2- The most distinguishable peak assignments and frequencies for MDA, MDA.HCl and MDA.2HCl-selected from [12]

Assignment		Peak Frequency (cm^{-1})		
		MDA	MDA.HCl	MDA.2HCl
1	$\vartheta(N-H)NH_2$	3472-3435 3329	3360 3215	- -
2	$\vartheta(N-H)NH_3$	-	2794 One peak	3240-2610 2 broad bands
3	NH_3 Femi resonance	-	2600	2560
4	$\delta(NH_3)$asymm	-	1570	1571 Weak band
5	$\delta(C-H)$	1274	1248	-
6	$\rho(NH_2)+CH_2$ twist $+\delta(C-C-C)$	1075	1083 Not sure which it is most similar to.	-
7	$\rho(NH_3)$	-	1083 Not sure which it is most similar to.	1061
8	$\delta(C-C-C)$	-	1022	1018
9	?		740 Sharp	-
10	$\delta(C_6-C_1-C_2)$	-	699 Strong	695 Weak
11	?	-	641 Weak	639 Strong

Table 3-3- Verification of the quality of the selected assignments in distinguishing the samples-FTIR spectra of the two pure MDA.2HCl samples

Assignment	Frequency (cm^{-1}) Sample 1 (Top Spectra)	Frequency (cm^{-1}) Sample 2 (Bottom Spectra)	Quality Check
1	-	-	OK
2	3200-2580: two broad bands	3200-2580: two broad bands	OK
3	2556	2554	OK
4	1570 weak	1568 sharp	OK
5	-	-	OK
6	-	-	OK
7	1060	1057	OK
8	1020	1020	OK
9	-	-	-
10	696	690	OK
11	-	635	Not Distinguishable

Table 3-4- Verification of the quality of the selected assignments in distinguishing the samples-FTIR spectra of the two pure MDA.HCl samples

Assignment	*Frequency (cm^{-1})* Sample 3 (Top Spectra)	*Frequency (cm^{-1})* Sample 4 (Top Spectra)	*Quality Check*
1	*3358, 3218*	*3360, 3219*	*OK*
2	*2787*	*2790*	*OK*
3	*2585*	*2591*	*OK*
4	*1568*	*1570*	*OK*
5	*1247*	*1247*	*OK*
6	*1087*	*1086*	*Not Distinguishable*
7	*1087*	*1086*	*Not Distinguishable*
8	*1018*	*1019*	*OK*
9	*751*	*748*	*OK*
10	*700*	*700*	*OK*
11	*639 weak*	*640 weak*	*OK*

Table 3-5-Verification of the quality of the selected assignments in distinguishing the samples-FTIR spectra of the 97% pure MDA

Assignment	*Frequency on MDA 97% pure (Sigma Aldrich)*	*Quality Check*
1	*3427, 3343*	*OK*
2	-	*OK*
3	-	*OK*
4	-	*OK*
5	*1269, 1273*	*OK*
6	*1072*	*OK*
7	-	*OK*
8	-	*OK*
9	-	*OK*
10	-	*OK*
11	-	*OK*

As it is shown in the above tables, the suggested 11 assignments have a number of specific peak frequencies for each component, which can be used to confirm elemental analysis data and later compare with the DSC data.

3.3 Thermal Properties of High Concentration MDA and AHC Salts

Thermal gravimetric analysis (TGA) and differential scanning calorimetry (DSC) of the samples provide phase change temperature ranges. The TGA, dTGA and DSC results for each pure salt are presented. The most important information obtained from DSC of the 5 pure samples is summarized in Table 3-6 followed by conclusions and comparison with thermal properties reported in the literature for MDA and AHC salts.

As inert gas is selected as the environment gas, it is unlikely that a chemical reaction occurs during the analysis.

3.3.1 TGA and DSC Graphs of MDA, MDA.HCl and MDA.2HCl

Figures 3-2 to 3-6 show the TGA/DSC results for each high concentration sample, MDA.2HCl (Samples 1 and 2), MDA.HCl (Samples 3 and 4), and MDA (Sample 5), all obtained using a programmed heating ramp of 10°C/min. The purities in the caption are based on the elemental analysis data, Table 3-1.

The TGA graph shows the thermal stability of solids and change in mass during the vaporization or reaction. As inert gas is used for the TGA runs, the no-reaction assumption is reasonable. In Figure 3-6, the MDA has a very clear trace on the TGA graph with a sharp fall of weight as the sample pan was heated gradually from 150 to 280°C where more than 94% of the initial sample has been evaporated and left the pan. At 500°C the remaining weight of sample is just 1%. The DSC graph of MDA reveals a very clean sharp peak at 94°C, related to phase change that must be for the melting, with a range of 92-94°C.

The thermal stability of MDA.2HCl and MDA.HCl is a more complicated case than MDA. In theory for MDA.2HCl, a mass loss of 13% would be consistent with the loss of one mole of HCl, resulting in MDA.HCl. A further loss of 16 % would be consistent with the further loss of HCl to form MDA. The total mass

loss expected for the dissociation of 2 moles of HCl from MDA.2HCl would be 27% shown in the following route: $MDA.2HCl \xrightarrow{13\%} MDA.HCl \xrightarrow{16\%} MDA$

The percentage weight loss of 79-83% shown in Figures 3-2 and 3-3 shows wider drops in the TGA graphs for MDA.2HCl salts than the MDA TGA graph, which start at 150°C just like the MDA, but continue to around 550°C. At this high temperature there is still more than 10% of the starting sample weight remaining. These large steps (79-83%) mean that there must be a gradual loss of MDA.2HCl units or dissociation of MDA.2HCl and the subsequent loss of MDA.HCl/MDA units.

For the MDA.HCl salt, there was a similar in thermal stability; perhaps at lower temperatures, below 100°C, there is a very small mass loss because of vaporization of the residual MCB solvent. At 550°C the remaining percentage of sample mass is just more than 10%.

The distinguishable data in studying thermal properties of the AHC salts are the DSC temperature ranges identified for phase changes and the related peak temperatures. MDA, as described above, has a very sharp peak with a range of 92-94, whereas MDA.HCl has two wide peaks. One of them is expected between 87 and 105°C, and the other appears in the 186-190°C range (two selected salts and the peaks are shown in Figures 3-4 and 3-5). The other AHC salt, MDA.2HCl, has one peak shown between 247-267°C in Figures 3-2 and 3-3. The next section reports the most important data extracted from the TGA/DSC data. As the TGA data could not reveal any outstanding characteristics of AHC salts independently, it was used to check the sample thermal stability and to pick the DSC heating program ranges.

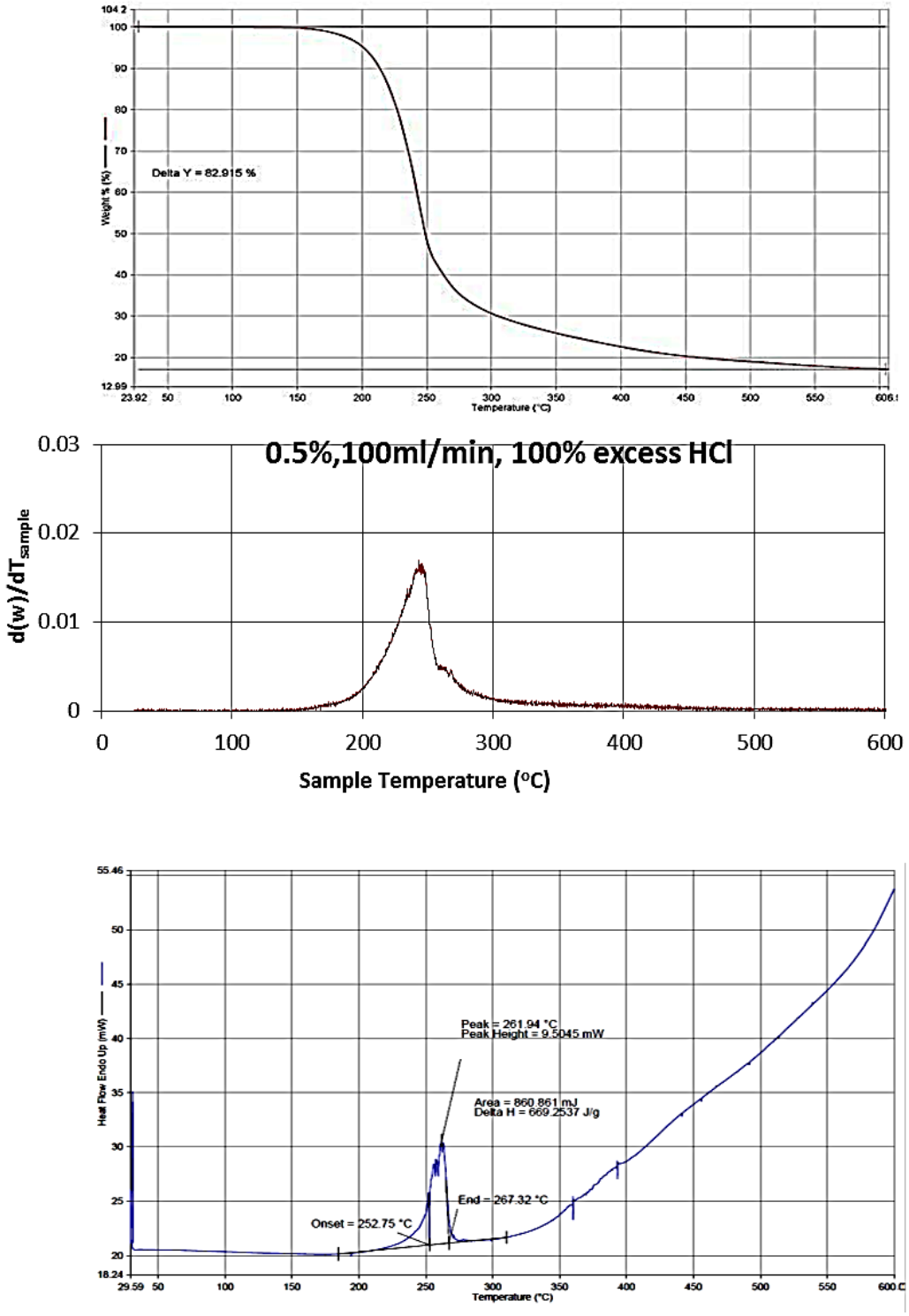

Figure 3-2- TGA, dTGA and DSC of Sample 1, 99% MDA.2HCl

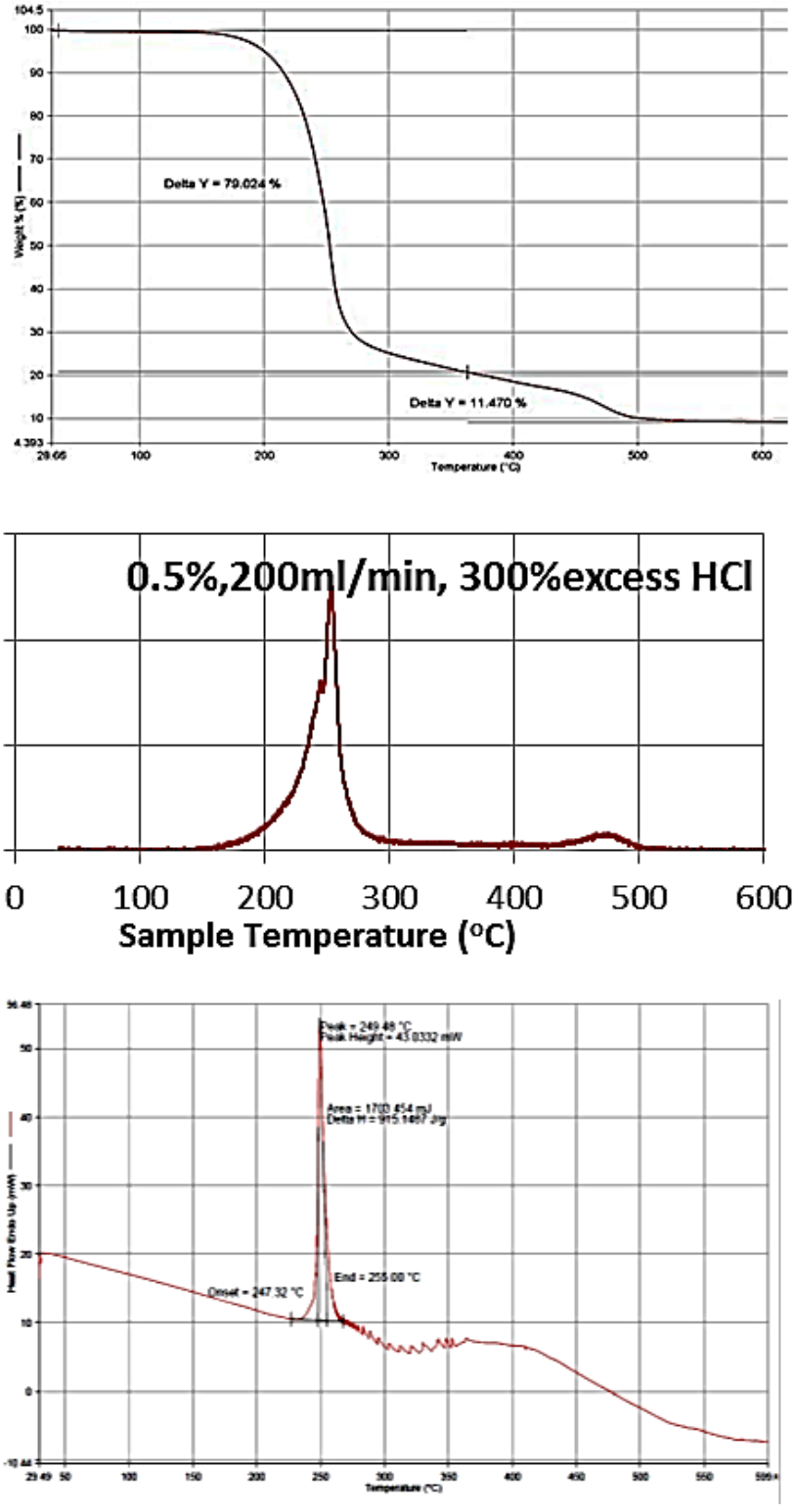

Figure 3-3-TGA, dTGA and DSC of Sample 2, 99% MDA.2HCl

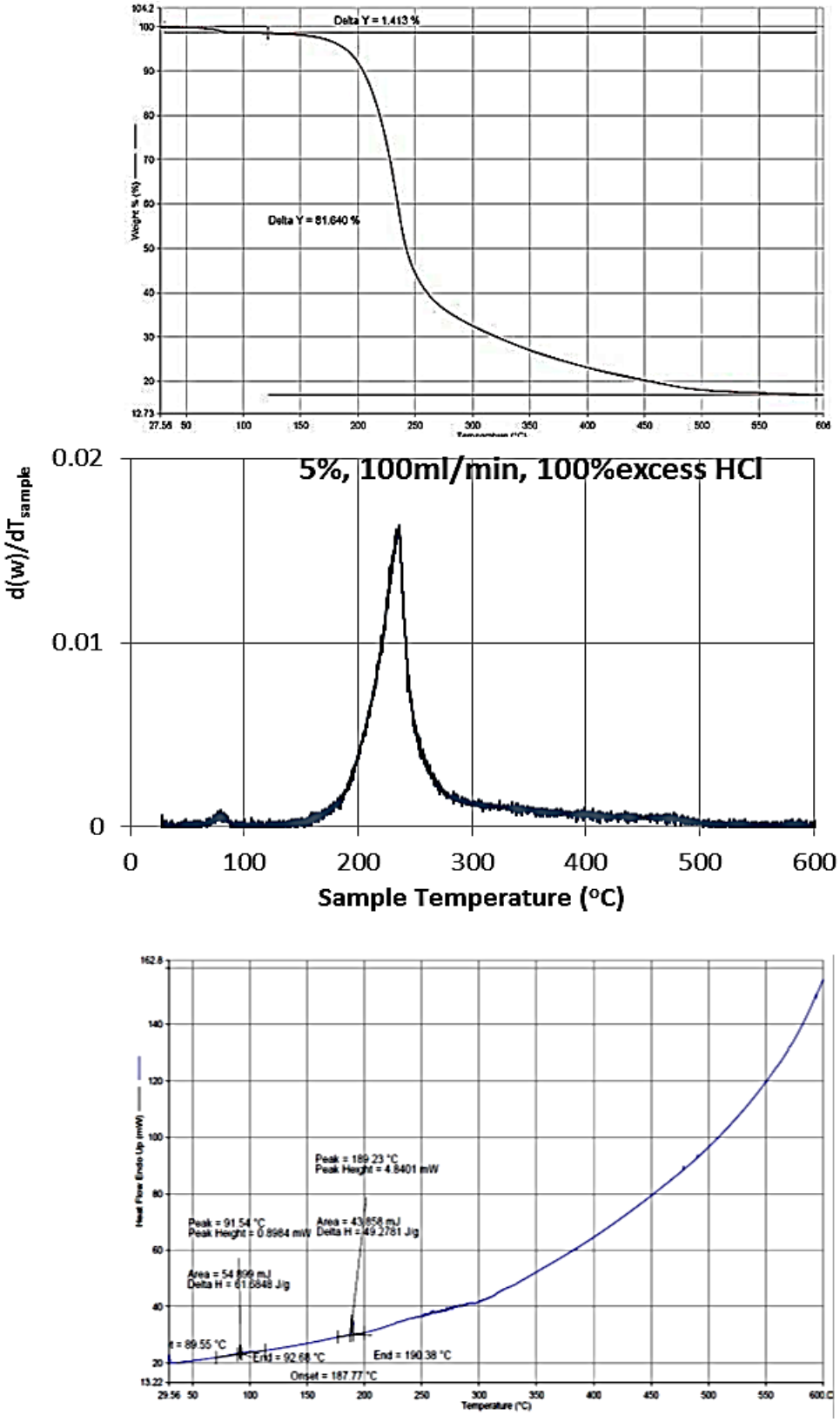

Figure 3-4-TGA, dTGA and DSC of Sample 3, 99% MDA.HCl

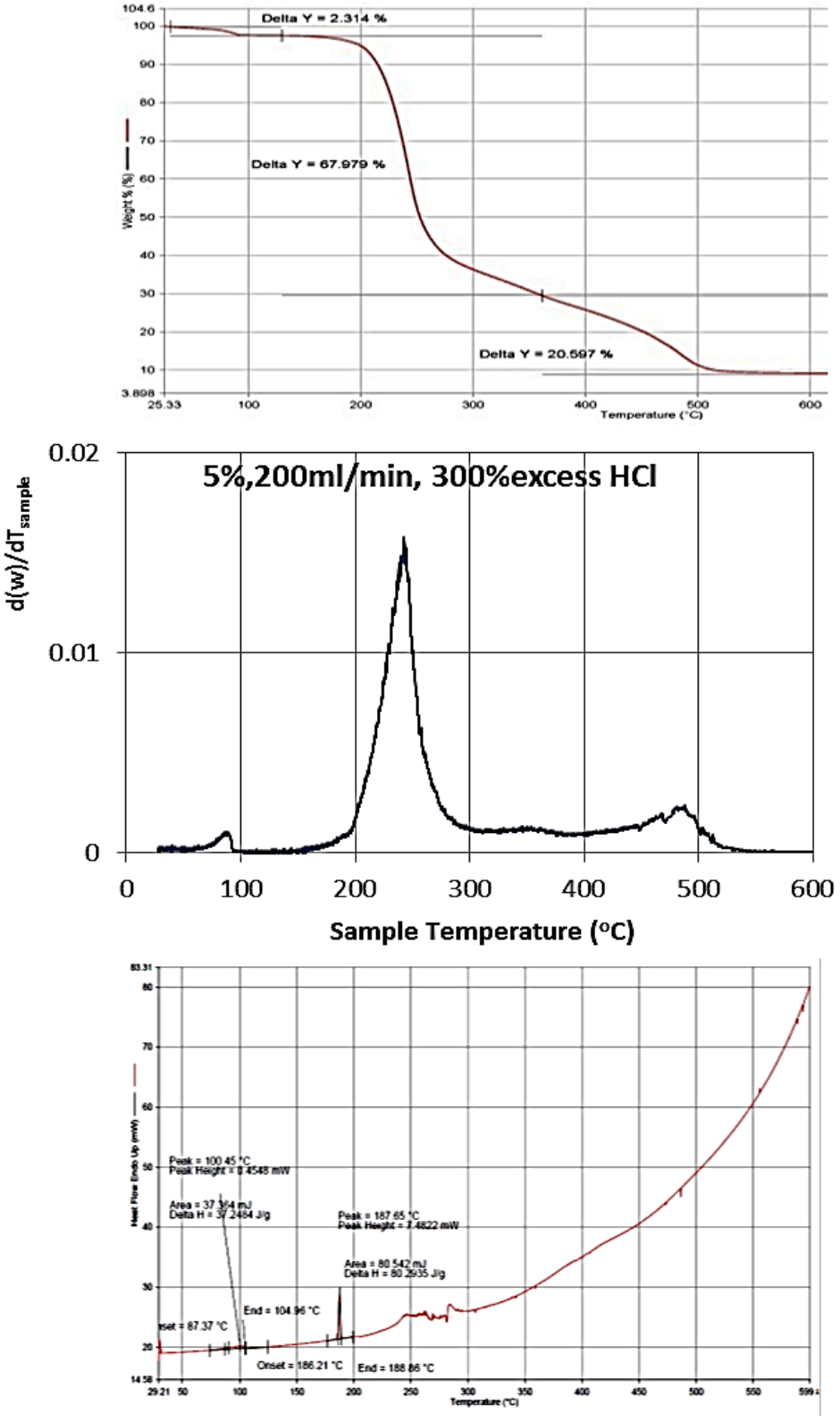

Figure 3-5- TGA, dTGA and DSC of Sample 4, 100% MDA.HCl

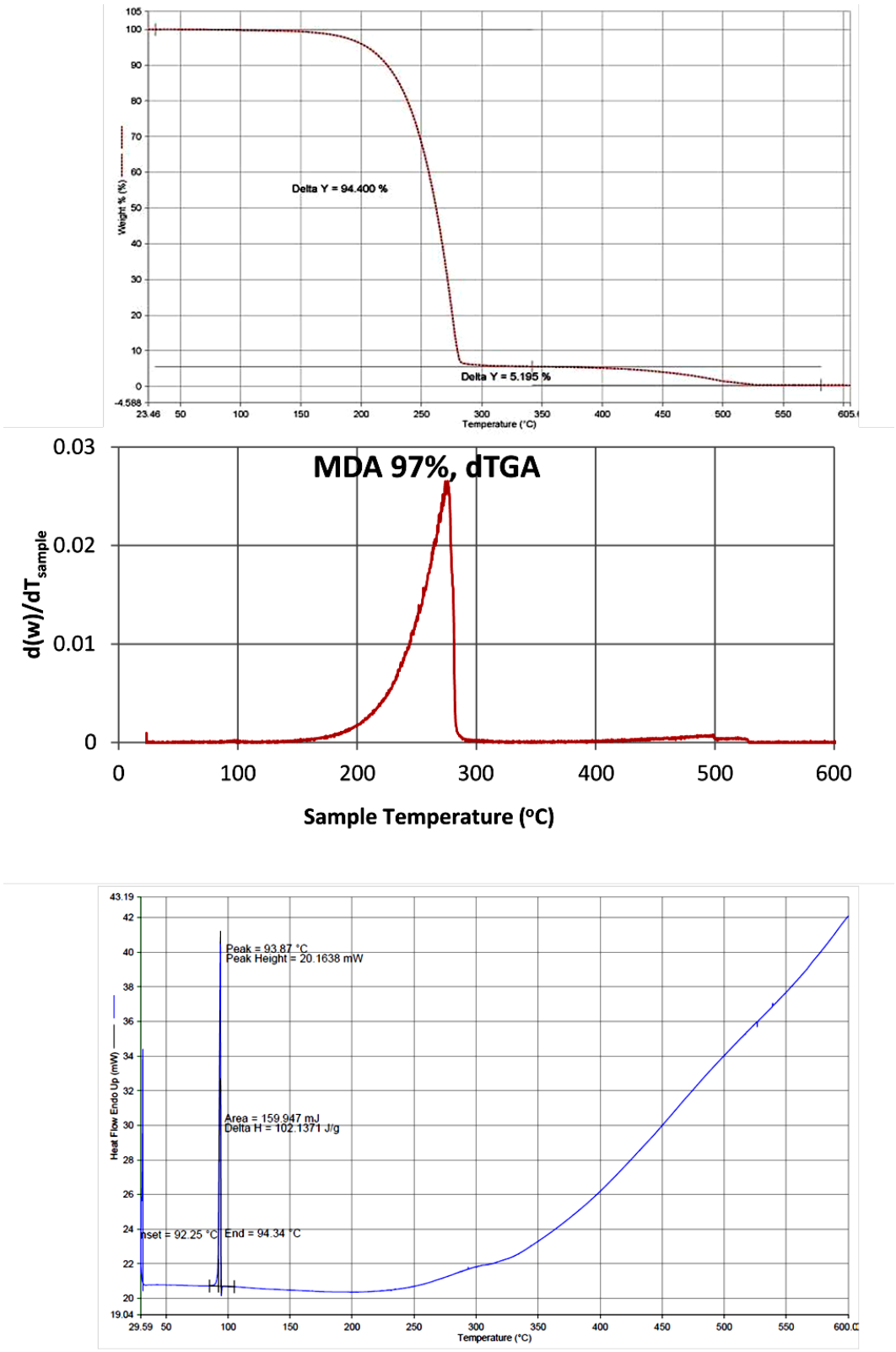

Figure 3-6- TGA, dTGA and DSC of Sample 5, Precipitated MDA

3.3.2 Summary of the Most Important Thermal Properties and Comparison of Conclusions with Past Work

Table 3-6 contains the most important information obtained from the TGA and DSC data. The peaks in DSC data normally show the range of phase transition or any physical or chemical change such as crystallization or chemical reaction. As described in Section 3.3.1 the DSC temperature ranges are used to distinguish between the AHC salts in Chapter 4.

Table 3-6-Summary of TGA/DSC data for AHC salts- Samples 1-5

Reaction Conditions			*Purity based on E.A*	*TGA T_{Peak} in dTGA (°C)*	*DSC Data T (°C), ΔH (J/g)*
MDA Conc. %	*HCl Excess %*	*Flow rate (ml/min)*			
0.5	*100*	*100*	*99% pure in MDA.2HCl*	*241*	*Peak T=262, ΔH=669 T_{Peak} range=252-267*
0.5	*300*	*200*	*99% pure in MDA.2HCl*	*243*	*Peak T= 249, ΔH=915 T_{Peak} range=247-255*
5	*100*	*100*	*99% pure in MDA.HCl*	*232*	*Peak1 T=92, ΔH=62, T_{Peak} range=90-93 Peak2 T=189, ΔH=49 T_{Peak} range=187-190*
5	*300*	*200*	*100% pure in MDA.HCl*	*233*	*Peak1 T=100, ΔH=37 T_{Peak} range=87-105 Peak2 T=188, ΔH=80 T_{Peak} range=186-189*
97	*-*	*-*	*MDA Pure*	*270*	*Peak T= 94, ΔH=102 T_{Peak} range= 92-94*

Table 3-7 has a comparison between the DSC peaks and melting temperatures found in Emma Gibson's work [12] and in melting point tables in literature [60,61]. Table 3-7 has a wider range than the data in Table 3-6 because samples with a slightly lower concentration of MDA.HCl and MDA.2HCl are included in Table 3-7.

Table 3-7-Melting Temperature obtained from DSC in comparison with Literature and past work

Source	*MDA Melting range (°C)*	*MDA.HCl Melting range (°C)*	*MDA.2HCl Melting range (°C)*
Literature [60,61]	*92*	*N/A*	*N/A*
Emma Gibson's Work [12]	*89-91*	*188-235*	*261 Decomposed*
This Research	*92-94*	*186-190*	*247-272*

For the boiling temperature range, there was not enough data in the literature for comparison. The DSC data shows weak and wide peak areas in this range that the software could not resolve. The MDA.HCl and MDA.2HCl are nearly insoluble in MCB [11].

3.4 Morphology of High Concentration MDA and AHC Salts

This section shows the microscopic structures and morphologies of the 5 samples. After filtering and drying the samples, the particles in powder form are ready to be analyzed; SEM, SE and BSE imaging all need powders to be scattered evenly on a sticky carbon tape layer. The prepared samples are imaged using SEM at various magnifications.

Energy-dispersive X-ray spectroscopy (EDX) analysis with spot-scan and line-scan showing the carbon and chlorine elemental concentration on the surface of the particles is another useful function that can be done using SEM. The data from EDX is compared with the elemental analysis data for the bulk sample.

3.4.1 Imaging of Samples

SEM images can be studied simultaneously with optical microscopy images, as shown in Figure 3-7, to estimate particle size. The average sizing of the

particles is the subject of study in the next chapter. AHC particles are sticky powders which make working with them a little difficult. One of the most practical ways to make an even surface on the SEM pans is to pour the powders on the pans with a pipette and then spray air parallel with the surface. After blowing air with moderate speed, a fine layer of particles can be seen on the SEM pan and it is ready for imaging.

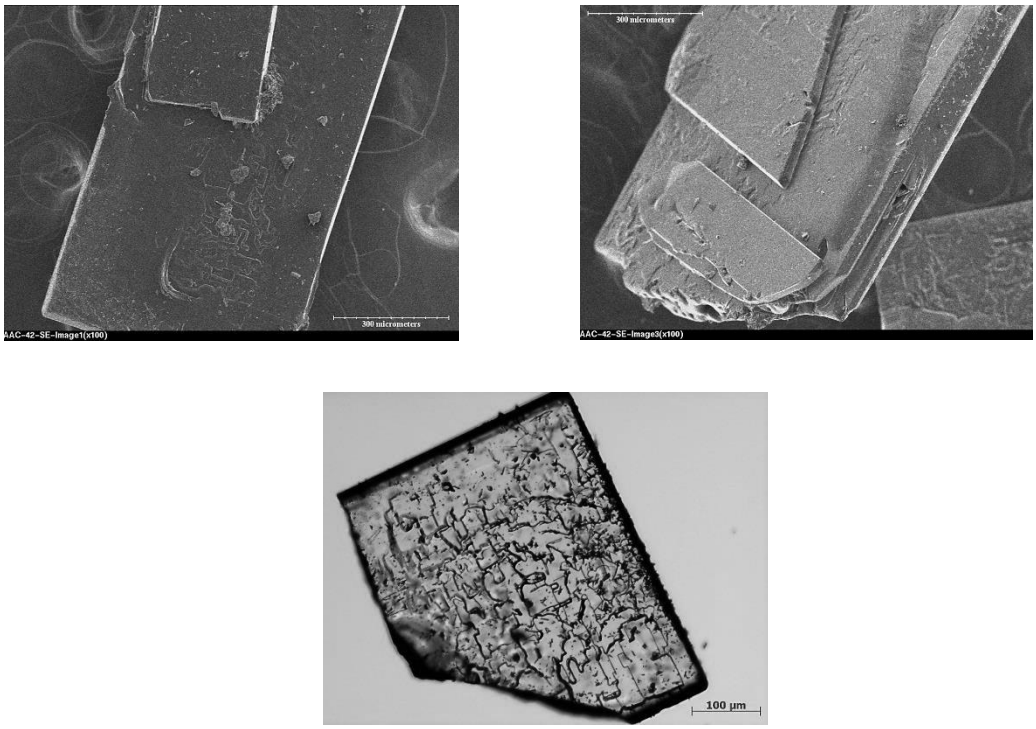

Figure 3-7- Precipitated MDA from MDA/MCB solution (Sample 5) Top images 100X SEM images (scale bar shows 300µm); Bottom image 100X optical microscopy (scale bar shows 100µm)

Two samples of MDA.HCl and MDA.2HCl are presented in Figures 3-8 and 3-9. Although elemental analysis shows very similar elemental compositions, the images show differences in morphology especially on the surface. Process variables such as flowrate and HCl concentration affect the shape of particles made in the CIJR, as shown in Figures 3-8 and 3-9.

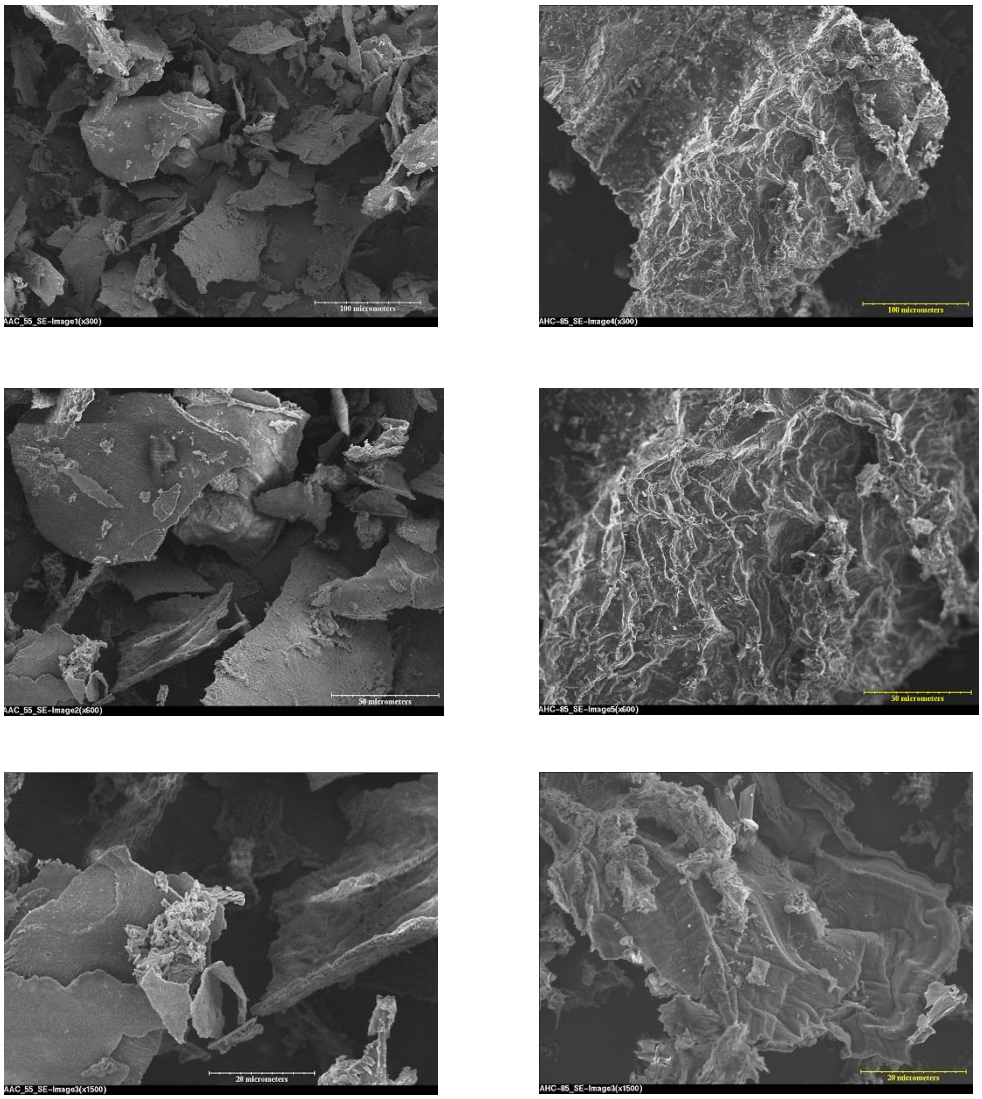

Figure 3-8- MDA.HCl, from top to bottom 300X, 600X, and 1500X Left side: sample 3; 5% blend, 100% excess HCl and 100ml/min; Right side: sample 4; of 5% blend, 300% excess HCl and 200ml/min

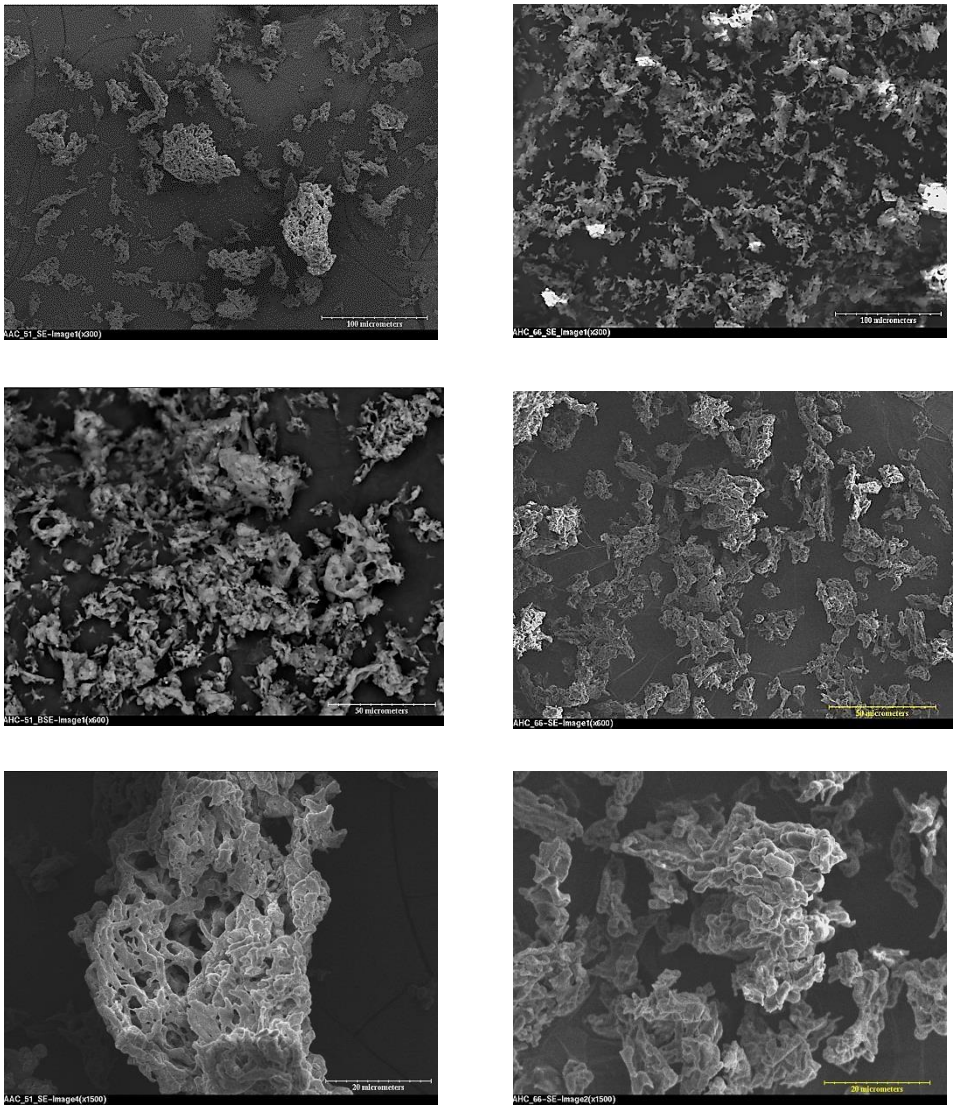

Figure 3-9-MDA.2HCl, from top to bottom 300X, 600X, and 1500X Left side: sample 1; 0.5% Blend, 100%excess HCl and 100ml/min. Right side: sample 2; 0.5% Blend, 300%excess HCl and 200ml/min

While there are some obvious differences in the two samples shown in Figures 3-8 and 3-9, images show similar morphology. A detailed comparison between these two cannot tell how a change in HCl concentration or flowrate affects particles, because more than one variable is changing; this question is the subject of the next chapter.

MDA.2HCl particles are soft, spongy and fluffy in comparison with the MDA.HCl particles that are hard and rocky shaped on the surface. MDA.2HCl

has higher porosity particles and it is easy to see that single particles are bonded together to form small masses of particles. This story is different for MDA.HCl where fine powders formed very large masses where it is more difficult to find single and primary particles.

In the next section, some additional images from the same samples are combined with EDX studies to give a better idea of the morphology and local composition of the samples.

3.4.2 EDX Studies; Composition on Surface vs. the Bulk for Pure Salts

During SEM studies, salts are looked at under X-ray beams using back scattered electron microscopy (BSE) technique and EDX analysis. The high energy charge voltage, 20kV, damages unstable particles; and after about 5 minutes running EDX analysis and BSE imaging, there were obvious changes in the particles such as shifting and shrinking under X-ray beams. In spite of this difficulty, EDX analysis was attempted for most of the samples and the most stable sets of data are presented in this section.

BSE images were taken to show the points and areas of interest for EDX. BSE images show a diversity of heavier and lighter atoms on the surface of the particles where the brighter spots represent denser areas of heavier atoms, and the darker areas contain much lighter atoms. Some spots are selected to do spot-scanning and also a line crossing interesting particles is used for line-scanning. Table 3-12 provides a summary of EDX vs. elemental analysis results and Tables 3-8 to 3-11 shows how compositions in the bulk are different from EDX results which measure composition of elements on the surface of the particles.

As EDX can detect only Cl and C from the existing elements in AHCs, running EDX on pure MDA will not show any interesting data as there is no Cl in MDA. The 4 samples of MDA.HCl and MDA.2HCl are studied in this section.

In the following figures, EDX points are indicated with arrows and the related plots show the C and Cl peaks. The values must be normalized using atomic number before doing any comparison. In the line scanning, a line in the middle of the BSE image is subjected to EDX, and the plot is adjusted to show an upper red line which relates to chlorine and a black (or blue) line which shows the carbon on the surface. In the line scanning plots in Figures 3-10 to 3-13 the Cl shows sharper fluctuation, where the C has steadier spectra and it is basically because of the background tape and lower amplitude of the detected C.

MDA.2HCl 99%; 0.5 wt% Blend, 100ml/min FR, 100% Excess HCl

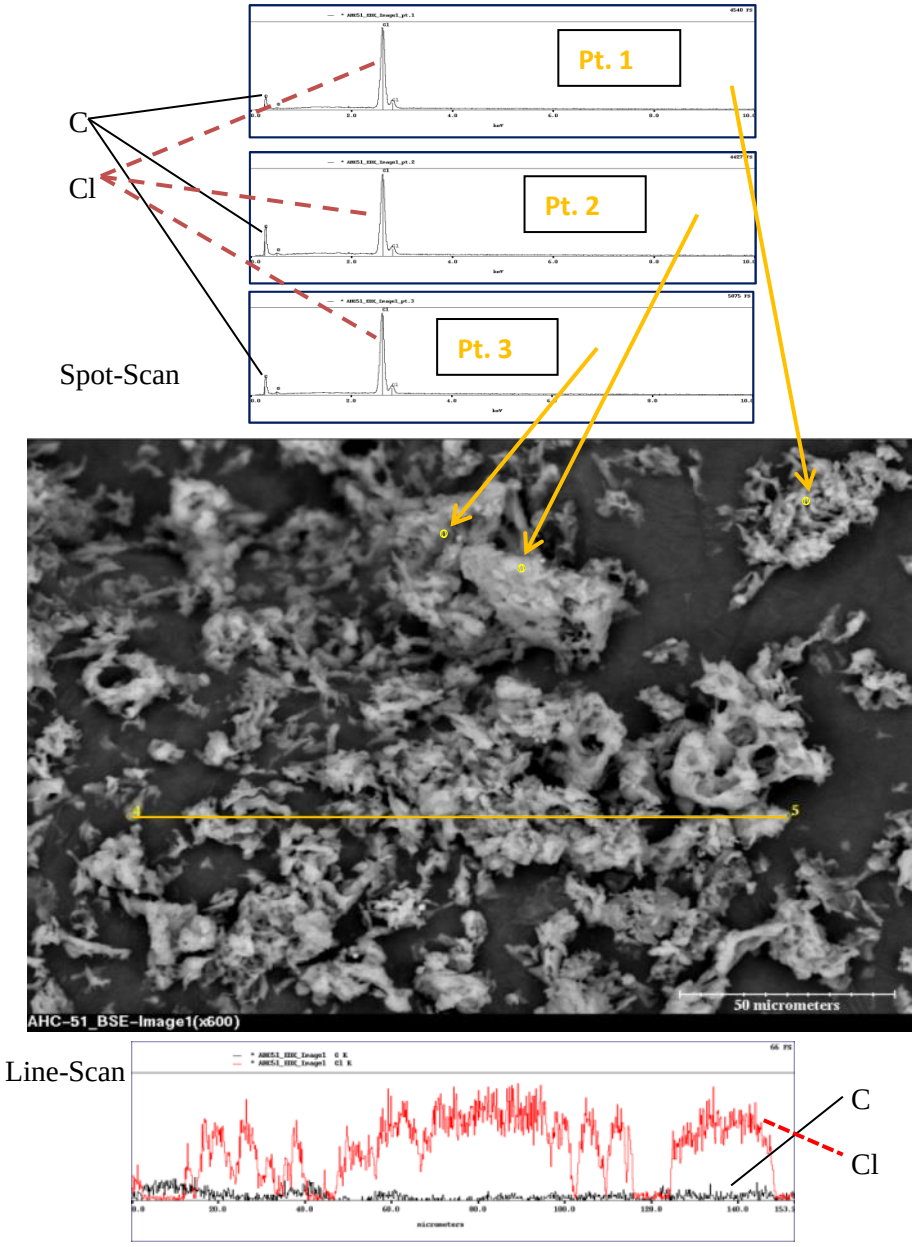

Figure 3-10- SEM and EDX semi-quantitative analysis for Sample 1(MDA.2HCl) - Magnification: 600X

MDA.2HCl 99%; 0.5 wt% Blend, 200ml/min FR, 300% Excess HCl

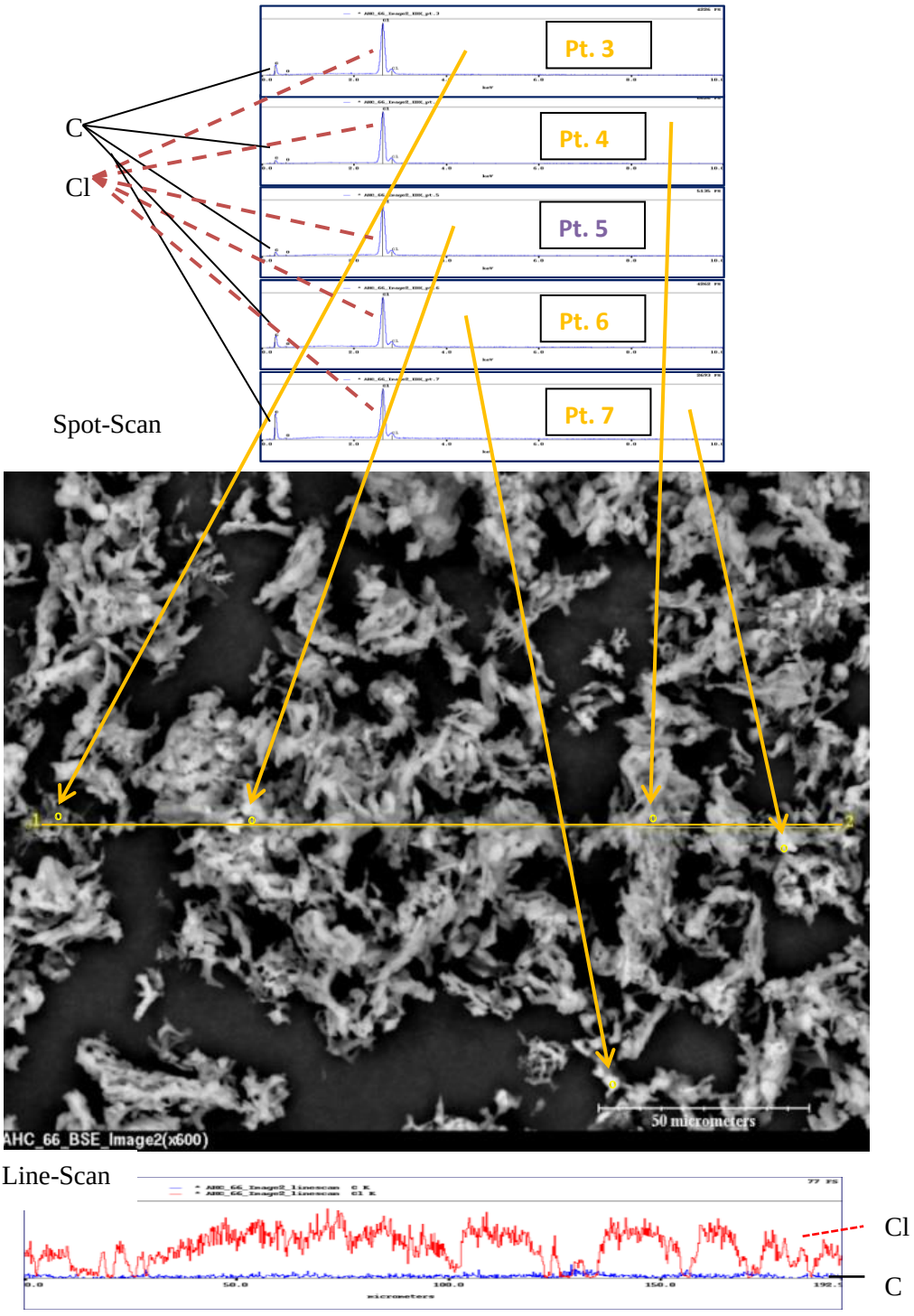

Figure 3-11- SEM and EDX semi-quantitative analysis for Sample 2(MDA.2HCl) - Magnification: 600X

MDA.HCl 99%; 5 wt% Blend, 100ml/min FR, 100% Excess HCl

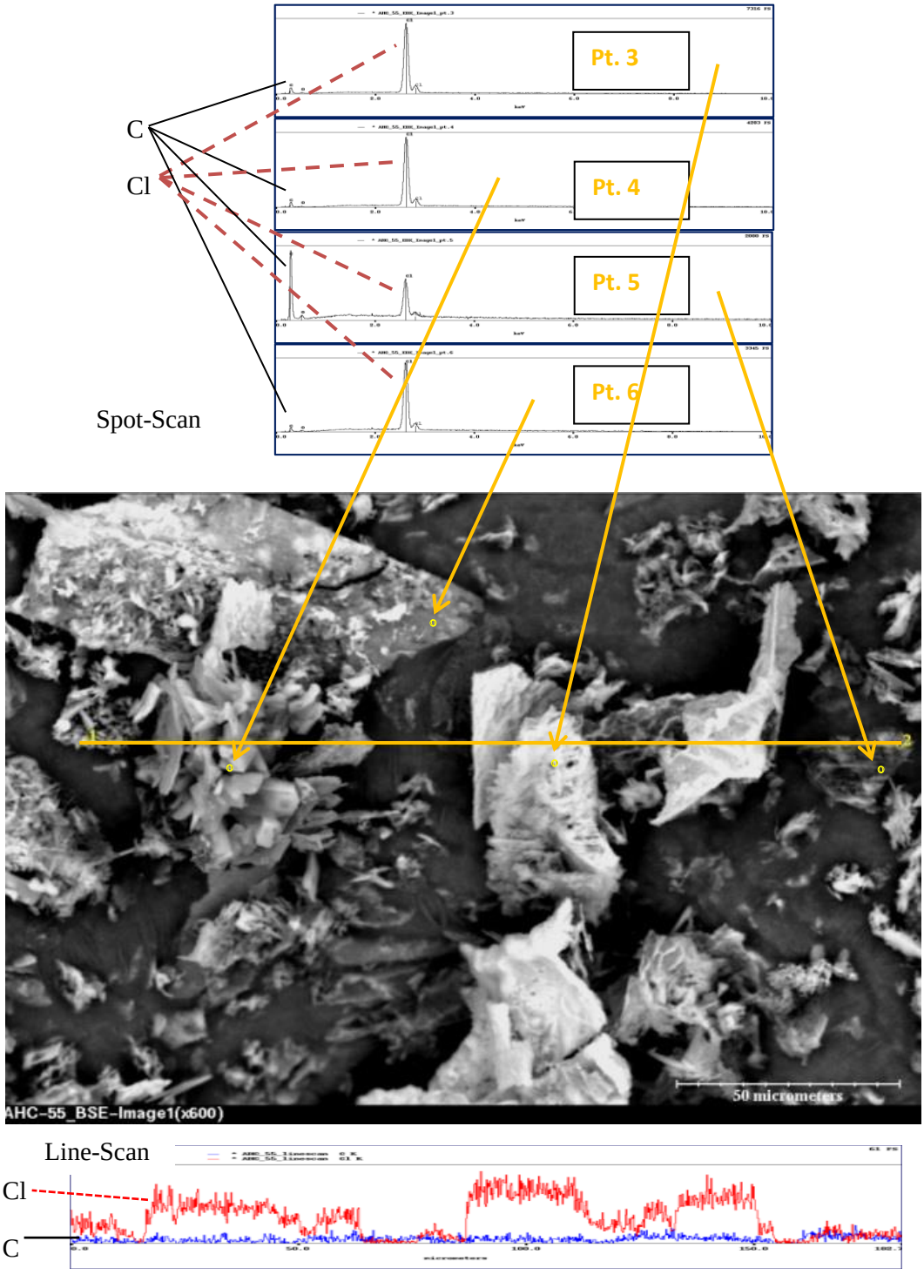

Figure 3-12- SEM and EDX semi-quantitative analysis for Sample 3(MDA.HCl) - Magnification: 600X

MDA.HCl 100%; 5 wt% Blend, 200ml/min FR, 300% Excess HCl

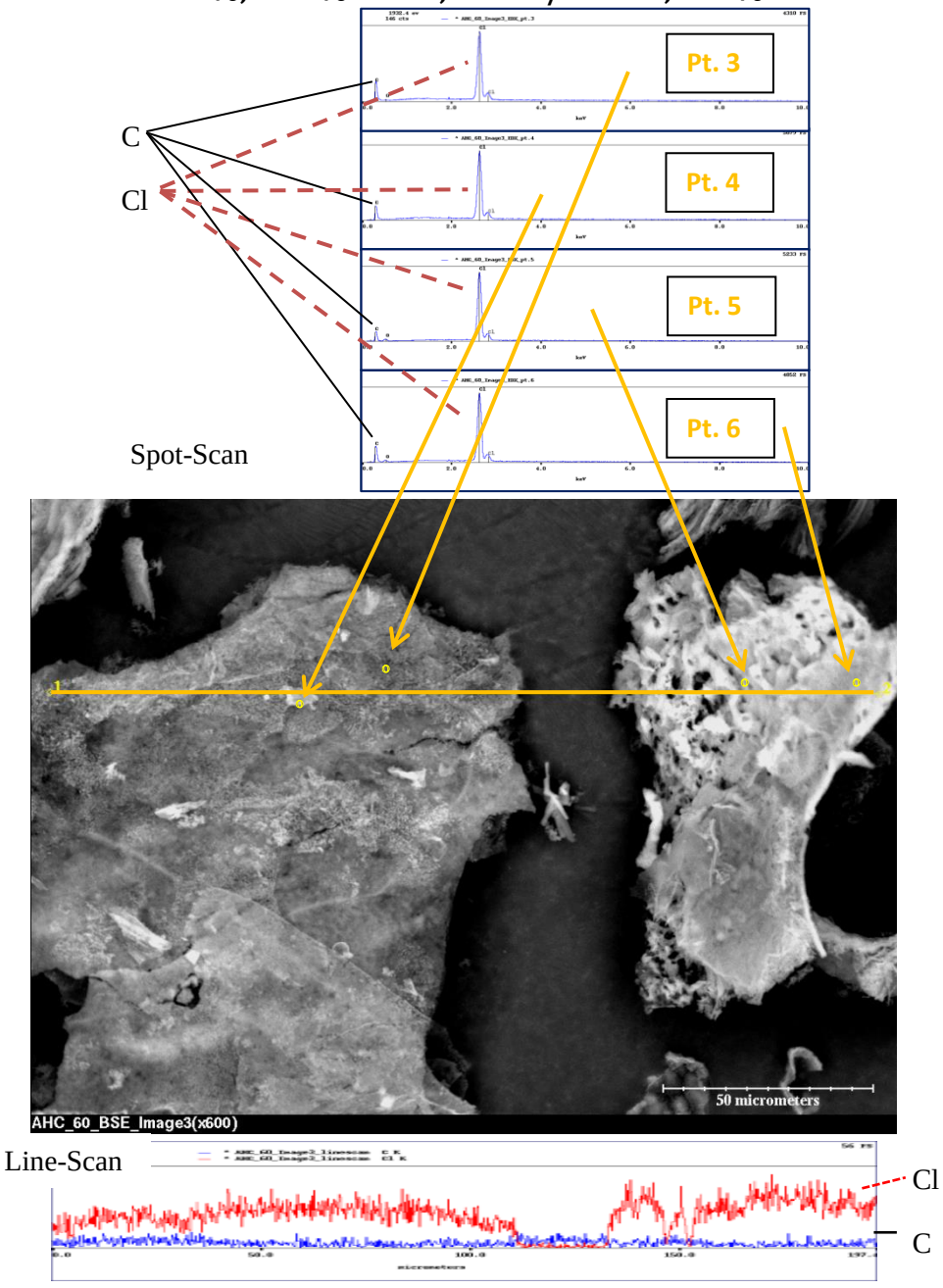

Figure 3-13- SEM and EDX semi-quantitative analysis for Sample 4(MDA.HCl) - Magnification: 600X

Table 3-8- SEM and EDX summary data for Sample 1(MDA.2HCl)

Method	*Points*	*Component*	*C/Cl*
EDX Results	*Pt 1*	*MDA.2HCl*	*2.5*
	Pt 2	*MDA.2HCl*	*2.1*
	Pt 3	*-*	*2.9*
Elemental Analysis	*-*	*MDA.2HCl 99%*	*2.2*
In Theory	*-*	*MDA.HCl*	*4.4*
	-	*MDA.2HCl*	*2.2*

Table 3-9- SEM and EDX summary data for Sample 2(MDA.2HCl)

Method	*Points*	*Component*	*C/Cl*
EDX Results	*Pt 3*	*MDA.2HCl*	*1.9*
	Pt 4	*MDA.2HCl*	*2.2*
	Pt 5	*MDA.2HCl*	*2.2*
	Pt 6	*MDA.2HCl*	*2.4*
	Pt 7	*-*	*3.0*
Elemental Analysis	*-*	*MDA.2HCl99%*	*2.2*
In Theory	*-*	*MDA.HCl*	*4.4*
	-	*MDA.2HCl*	*2.2*

Table 3-10- SEM and EDX summary data for Sample 3(MDA.HCl)

Method	*Points*	*Component*	*C/Cl*
EDX Results	*Pt 3*	*MDA.HCl*	*4.3*
	Pt 4	*MDA.HCl*	*4.6*
	Pt 5	*-*	*6.9*
	Pt 6	*MDA.HCl*	*4.0*
Elemental Analysis	*-*	*MDA.HCl 99%*	*4.4*
In Theory	*-*	*MDA.HCl*	*4.4*
	-	*MDA.2HCl*	*2.2*

Table 3-11- SEM and EDX summary data for Sample 4(MDA.HCl)

Method	*Points*	*Component*	*C/Cl*
EDX Results	*Pt 3*	*MDA.HCl*	*4.1*
	Pt 4	*MDA.HCl*	*4.6*
	Pt 5	*-*	*5.2*
	Pt 6	*MDA.HCl*	*4.5*
Elemental Analysis	*-*	*MDA.HCl 100%*	*4.4*
In Theory	*-*	*MDA.HCl*	*4.4*
	-	*MDA.2HCl*	*2.2*

In Figure 3-12 and Figure 3-13 point 5 is unstable which got darker after 5 minutes and later vanished; therefore carbon tape which was in the background of the particles had a significant effect in the EDX data and resulted a very high value of the C/Cl ratio.

Although the mentioned unstable points are excluded from Table 3-12 (point 5 in Figure 3-12, Samples 3, and in Figure 3-13, Sample 4), the range of EDX does not show an exact match with elemental analysis. If the points were selected from ordinary areas, i.e. all spots other than ends or edges of the particles, the error could be lowered and the results can show a better consistency with the elemental analysis data. Extreme light or dark areas are also the spots that make more deviation in the C/Cl ratio from what is expected for the value of this ratio in MDA.HCl or MDA.2HCl (in Theory and elemental analysis).

However, picking spots from different parts of particles and to analyze using EDX provides interesting information about non-homogeneous distribution of AHC salts formed in the CIJR. The brighter areas on the surface and the edge of agglomerated particles, versus the darker areas of the particles in BSE images have the different C/Cl ratio, which means gaseous HCl could not penetrate the bulk of particles; and it is perhaps because of very fast growth and agglomeration rate of the primary formed particles.

In Table 3-12, the maximum relative error column is defined by the following equation: $\frac{\text{Maximum difference between the } {}^{C}/_{Cl} \text{ ratio from EDX data and elemental analysis}}{{}^{C}/_{Cl} \text{ ratio calculated from elemental analysis}} \times 100$

Table 3-12-EDX vs. elemental analysis quantitative results

Reaction Conditions			*Purity based on E.A*	*EDX points' Range of C/Cl**	*Elemental Analysis C/Cl*	*Maximum Relative Error*
MDA Conc %	*HCl Excess %*	*Flow rate (ml/min)*				
0.5	*100*	*100*	*99% pure in MDA.2HCl*	*2.1-3.9*	*2.2*	*32%*
0.5	*300*	*200*	*99% pure in MDA.2HCl*	*1.9-3.0*	*2.2*	*36%*
5	*100*	*100*	*99% pure in MDA.HCl*	*4.0-4.6*	*4.4*	*9%*
5	*300*	*200*	*100% pure in MDA.HCl*	*4.1-4.5*	*4.4*	*7%*
In Theory			*MDA.2HCl*	*2.2*		-
			MDA.2HCl	*4.4*		-

3.5 Conclusion

From the analysis, we conclude that MDA.HCl and MDA.2HCl are the two stable structures of hydrochlorination of 4-4 Methylenedianiline produced in this reactor. The specific peaks in FTIR spectra, melting ranges in DSC, and elemental composition studies with elemental analysis and EDX match literature values. Microscopy images show that the shape and size vary and, that there are differences in the surface structure.

Elemental analysis and FTIR were the most useful analytical techniques for detecting compounds and compositions, and were the most promising to start with in characterization of the AHCs. DSC was useful for detecting melting peaks and ranges. DSC does not give the exact melting point but it detects phase transitions and the enthalpy changes of phase transitions.

The SEM images taken from the AHC particles show a more porous morphology and spongy solids in MDA.2HCl samples. The MDA.HCl particles

have a harder and smoother surface; particles stick together and form aggregated masses in the case of MDA.HCl more than for the other AHC salt.

Looking at the microscopy images to make statements about the particles qualitatively helps deeper understanding of AHC salts. “Semi-quantitative” EDX, in Section 3.4.2, could not give us very reliable elemental compositions compared with elemental analysis data, as the X-ray beams penetrate no more than 0.5 μm in the depth of particles; while the average particle size of the AHC salts is more than 2 μm, but it revealed very interesting facts about differences in elemental composition on the surface of AHC particles by line scanning thru a mass of aggregated particles or picking points from different parts of the BSE images; which had more chlorine at the ends or on the edges than the ordinary areas.

4 Effects of Local Concentration and Flowrate on the Production of AHC Salts

4.1 Introduction

This chapter contains a report of the analysis of samples made in the CIJR under various reaction conditions: local concentration of reagents (MDA and HCl) and mixing intensity. In Sections 4-2 to 4-4 two cases are studied for each variable in a way that the effects of each variable alone on the AHC salts can be investigated.

As described in Chapter 1, the hydrochlorination of MDA is a precipitation reaction that produces unwelcome solid particles, loss of starting amines, and high reprocessing costs. Local concentration is dominant factor in precipitation reactions which usually take place very fast; therefore, studying the effects of these process variables on the products will be very interesting. The ranges selected for each process variable were discussed in Chapter 2, Experimental.

The procedure starts with detecting compounds and compositions using elemental analysis and FTIR, continues with the thermal properties data acquired from DSC plots, and at the end looks at the microscopy images and EDX analysis of the particle surfaces. This approach provides data on the formation of the two different types of the AHC salts. As was shown in the previous chapter, MDA.2HCl forms at low blend strength (0.5 wt% MDA) whereas a high blend strength (5 wt% MDA) a different AHC salt, MDA.HCl, forms.

At the end of the chapter, the average particle size of the samples based on image processing from optical microscope images of the samples is reported.

4.2 Effect of MDA Concentration on the Formation of AHC salts

By keeping the other two variables- HCl excess and flowrate of the reactants entering the CIJR- constant, the effect of MDA concentration on product particles can be isolated. The range of MDA concentration in the MDA/MCB blend was chosen in the range of 0.5-5 wt%, because above 5% all of the MDA cannot dissolve in the MCB at room temperature and atmospheric pressure. Decreasing blend strength to less than 0.5% is not realistic for the industrial scale synthesis of polyurethane.

Case 1- Low Flowrate and Low HCl Concentration

Reaction Conditions: 100ml/min flowrate and 100% excess HCl

This case studies 5 samples that all have the same flowrate of 100 ml/min at the outlet of the CIJR and the same HCl concentration, set at 100% excess HCl. The MDA concentration (blend strength) varies from 0.5 to 5 wt% with the following intervals: 0.5, 1, 2, 3.5 and 5%.

Case 2- High Flowrate and High HCl Concentration

Reaction Conditions: 200ml/min flowrate and 300% excess HCl

Case 2 studies a very similar trend to Case 1 but with different reaction variables. A flowrate of 200 ml/min is set at the outlet of the CIJR and the HCl concentration is set at 300% excess HCl. The MDA concentration (blend strength) varies from 0.5 to 5 wt% at the same values as for Case 1.

Tables 4-1 and 4-2 provide the compounds and compositions of the samples made for Case 1 and Case 2 based on FTIR and elemental analysis. The rows of FTIR assignments are the same assignments as in Tables 3-2 to 3-4. The cells in bold are the data from the previous chapter, the MDA.HCl and MDA.2HCl characterized in Chapter 3.

The summary of the results is that the AHC salts produced in the CIJR change from MDA.2HCl to MDA.HCl with increase in entering MDA concentration, similar to the conclusions in Chapter 3.

Studying these two cases shows that increasing in the MDA concentration above 1 wt%, eliminates the presence of MDA.2HCl in the products. In other words, the production of AHC salts is very sensitive to the blend strength and changes dramatically as the MDA concentration increases from 1% to 2%. The trend was similar in Cases 1 and 2, regardless of the percent of excess HCl and flowrate.

Table 4-1- Components and Compositions for Case Study 1

Assignment	***Frequency for each Compound(cm^{-1})*** *(for all samples: 100% excess HCl and 100 ml/min flowrate)*				
	0.5% MDA	*1% MDA*	*2% MDA*	*3.5% MDA*	***5% MDA***
1	**-**	*3220*	*3360, 3221*	*3358,3219*	***3358, 3218***
2	***3200-2580***	*3200-2600*	*2793*	*2790*	***2787***
3	***2556***	*2556*	*2554, 2585*	*2556, 2591*	***2585***
4	***1570***	*1569*	*1568*	*1568*	***1568***
5	**-**	*1247*	*1246*	*1247*	***1247***
6	**-**	-	-	*1084*	***1087***
7	***1060***	*1060*	*1060*	*1084*	***1087***
8	***1020***	*1021*	*1016*	*1017*	***1018***
9	**-**	*751*	*751*	*750*	***751***
10	***696***	*696*	*703*	*701*	***700***
11	**-**	-	*639*	*640*	***639***
Components based on FTIR	***MDA.2HCl***	*MDA.HCl MDA.2HCl*	*MDA.HCl MDA.2HCl*	*MDA.HCl MDA.2HCl*	***MDA.HCl***
Compositions based on Elemental Analysis	***99% MDA.2HCl***	*91% MDA.2HCl*	*86% MDA.HCl*	*94% MDA.HCl*	***99% MDA.HCl***

Table 4-2-Components and Compositions for Case Study 2

Assignment	*Frequency for each Compound(cm^{-1})* *(for all samples: 300% excess HCl and 200 ml/min flowrate)*				
	0.5% MDA	*1% MDA*	*2% MDA*	*3.5% MDA*	***5% MDA***
1	***-***	*-*	*-*	*3358, 3218*	***3360, 3219***
2	***3200-2580***	*3205-2577*	*2795*	*2790*	***2790***
3	***2554***	*2555*	*2556, 2591*	*2555, 2589*	***2591***
4	***1568***	*1568*	*1566*	*1571*	***1570***
5	***-***	*1244*	*1247*	*1248*	***1247***
6	***-***	*-*	*-*	*-*	***1086***
7	***1057***	*1055*	*1058*	*-*	***1086***
8	***1020***	*1023*	*1018*	*1019*	***1019***
9	***-***	*782*	*783*	*785*	***784***
10	***690***	*690*	*701*	*699*	***700***
11	***635***	*-*	*646*	*642*	***640***
Components based on FTIR	***MDA.2HCl***	*MDA.HCl MDA.2HCl*	*MDA.HCl MDA.2HCl*	*MDA.HCl MDA.2HCl*	***MDA.HCl***
Compositions based on Elemental Analysis	***99% MDA.2HCl***	*95% MDA.2HCl*	*76% MDA.HCl*	*91% MDA.HCl*	***100% MDA.HCl***

The peaks and temperature ranges obtained from DSC data in Table 4-3 confirm the components existing in each sample. For example, at 2% MDA in Case 2 both MDA.HCl and MDA.2HCl are expected, based on the FTIR and elemental analysis data. This is confirmed by the temperature ranges and peaks detected on the DSC plot; both the MDA.HCl and MDA.2HCl peaks and ranges are present (shown in bold).

Now that the components in each sample in Case 1 and 2 are confirmed, the morphology of the samples can be studied and compared with the reference particles. In these two cases samples made from 0.5 and 5% MDA in MCB blends are the references and the other 8 samples (4 samples in each case), are shown in Figure 4-1 in order to investigate the way morphology changes as a result of varying the MDA concentration.

Table 4-3- Thermal Properties of Cases 1 and 2

Cases	MDA Conc %	Purity based on E.A	DSC Data T(°C), ΔH(J/g)	Compounds based on DSC
Case 1 100% excess HCl and 100 ml/min	**0.5**	**99% MDA.2HCl**	**Peak T=262, ΔH=669 T_{Peak} range=252-267**	**MDA.2HCl**
	1	91% MDA.2HCl	Peak T=263, ΔH=589 T_{Peak} range=250-269	MDA.2HCl
	2	86% MDA.HCl	Peak1 T=97, ΔH=44, T_{Peak} range=86-101 Peak2 T=187, ΔH=73 T_{Peak} range=185-189 Peak3 T=263, ΔH=N/A >450	MDA.HCl MDA.2HCl
	3.5	94% MDA.HCl	Peak1 T=91, ΔH=58, T_{Peak} range=90-93 Peak2 T=188 ΔH=38 T_{Peak} range=179-191	MDA.HCl
	5	**99% MDA.HCl**	**Peak1 T=92, ΔH=62, T_{Peak} range=90-93 Peak2 T=189, ΔH=49 T_{Peak} range=187-190**	**MDA.HCl**
Case 2 300% excess HCl and 200 ml/min	**0.5**	**99% MDA.2HCl**	**Peak T= 249, ΔH=915 T_{Peak} range=247-255**	**MDA.2HCl**
	1	95% MDA.2HCl	Peak T= 247, ΔH=797 T_{Peak} range=243-255	MDA.2HCl
	2	76% MDA.HCl	Peak1 T=96, ΔH=32, T_{Peak} range=88-100 Peak2 T=187, ΔH=67 T_{Peak} range=183-188 Peak3 T=260, ΔH=N/A >560	MDA.HCl MDA.2HCl
	3.5	91% MDA.HCl	Peak1 T=99, ΔH=37, T_{Peak} range=87-102 Peak2 T=186, ΔH=67 T_{Peak} range=176-187 Peak3 T=257, ΔH=N/A >430	MDA.HCl MDA.2HCl
	5	**100% MDA.HCl**	**Peak1 T=100, ΔH=37 T_{Peak} range=87-105 Peak2 T=188, ΔH=80 T_{Peak} range=186-189**	**MDA.HCl**

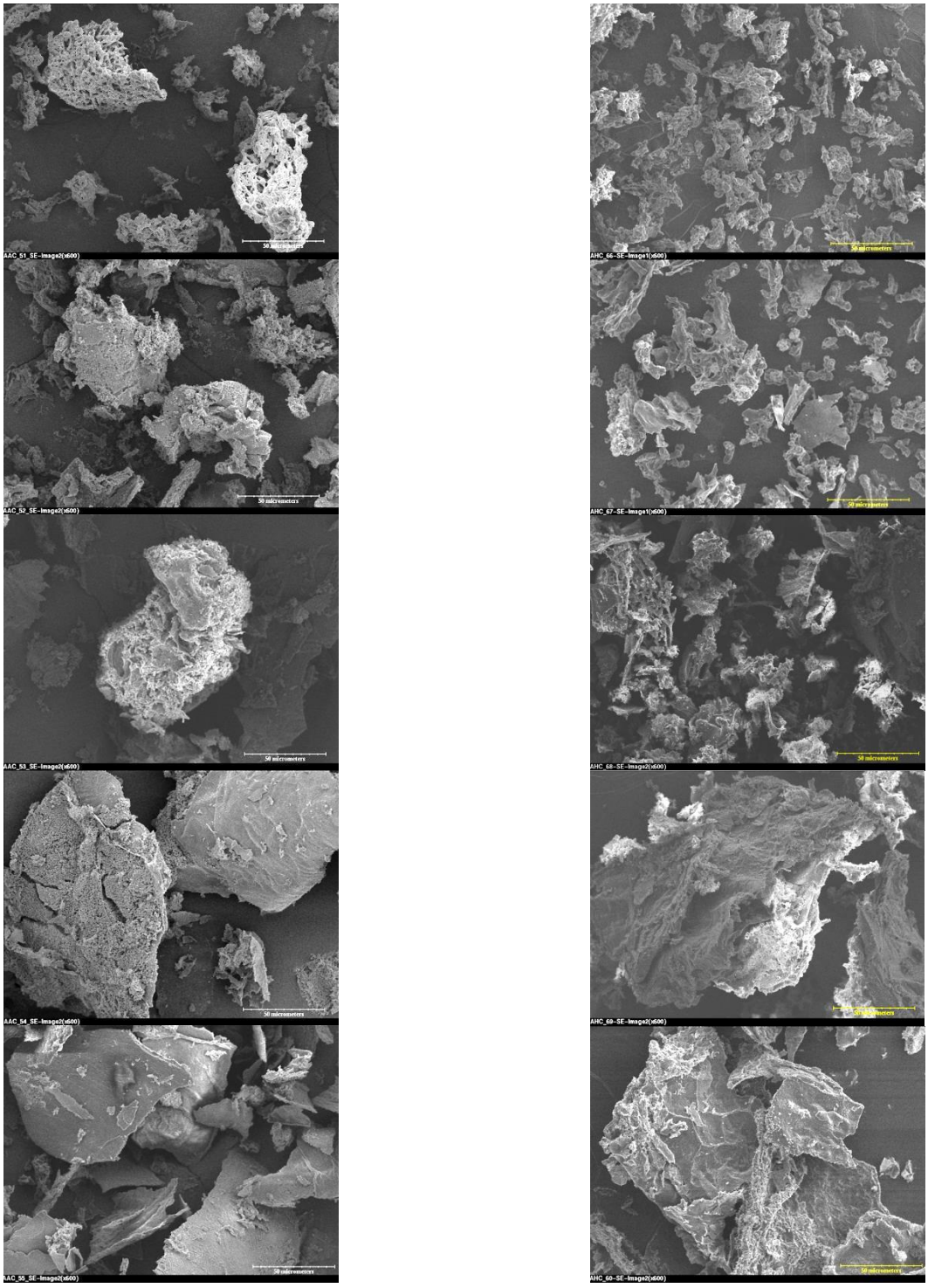

Figure 4-1- Effect of increase in MDA concentration from top (0.5%) to bottom (5%) on Case 1 (left) and Case 2(right) product particles. SEM images with Magnification of 600(Scale bar is 50 µm)

A direct comparison cannot be made between left hand side and right hand side images, since two variables are varying at the same time; but from top to bottom the composition of MDA.2HCl is decreasing, from 99% to 0 and the purity of MDA.HCl is increasing from less than 1% to 99 or 100%.

MDA.2HCl particles have much more holes and caves on the surface, whereas in MDA.HCl particles there are rocky-shapes and smoother surfaces. Therefore MDA.2HCl is more porous than the other type of AHC. Another obvious point is that the particle size increases in the transition from MDA.2HCl to MDA.HCl. This result is verified in Section 4.5.

Unfortunately the EDX analysis could not be done for all of the samples in these two cases because of instability under the beams, as discussed in 3.4.2. For those samples where EDX analysis was successful, the maximum relative percent difference from elemental analysis data, defined in Chapter 3, ranged from 8-23%.

The degree of chlorination (%Cl) is a factor reported in organic products which contain chlorine in their structure. MDA.HCl and MDA.2HCl in pure salts have respectively 15.1 and 26.2 %Cl in the molecules. Figure 4-2 shows the trend of change in %Cl of AHC salts as a function of MDA blend strength for Case 1 and 2, and also two other cases not discussed here.

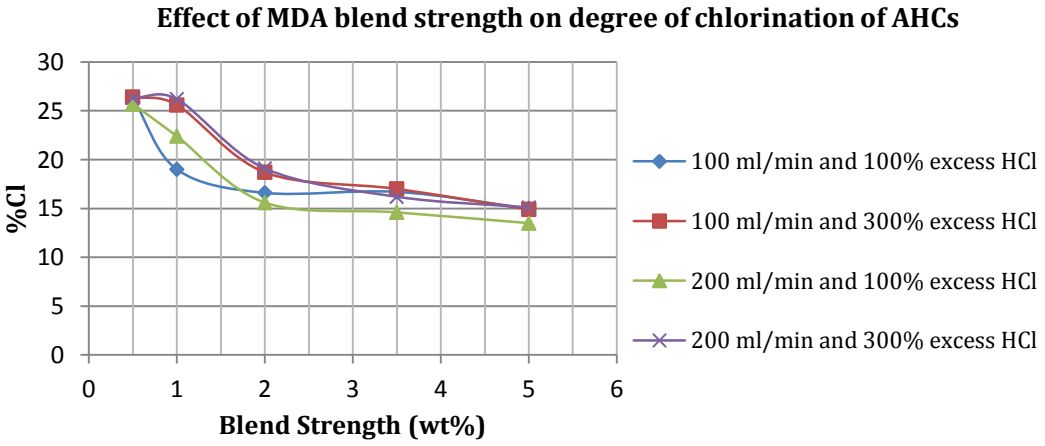

Figure 4-2- Degree of chlorination vs. MDA blend strength

4.3 Effect of HCl Concentration on the Formation of AHC salts

The approach for this set of runs is the same as the previous section, confirming the compounds and compositions existing in the samples, and then studying morphology. The cases considered here have EDX results available for all of the samples with different HCl concentrations. For the HCl concentration, the HCl percent excess was varied as discussed in Chapter 2. Values selected for HCl excess were 0%, 100%, 300% and 700%.

In this section, the range selected can show how the HCl excess affects completion of the reaction, i.e. can any concentration of MDA, even high MDA blend strength, form MDA.2HCl if the HCl availability is higher than the stoichiometric requirement? Does the lack of the hydrogen chloride prevent formation of MDA.2HCl in case of low blend strength? Is the HCl concentration dominant or is the most important reaction condition in formation of the AHC salts the MDA concentration?

Case 3- Low Blend Strength

Reaction Conditions: 0.5%wt MDA concentration and 200 ml/min flowrate

This case studies 4 samples that all have the same flowrate and 0.5 wt% blend strength which should result in high purity MDA.2HCl. A flowrate of 200 ml/min was the optimum flowrate set for the pumps (lower flowrates caused back-flow on the discharge line of the MCB pump for high HCl flowrates, and higher flowrates were harder to operate). Values for the HCl percent excess were chosen in a consistent pattern. The flowrate of HCl is doubled each time, i.e. 300% excess HCl is equal to 4 times the required stoichiometric HCl and 700% has a flowrate of 8 times that much.

Case 4- High Blend Strength

Reaction Conditions: 5%wt MDA concentration and 200 ml/min flowrate

Case 4 has a very similar trend to Case 3 with a blend strength of 5 wt%. According to studies in Chapter 3, the products are expected to be rich in MDA.HCl unless a very high concentration of HCl has a dominant effect on the reaction. The flowrate was again set to 200 ml/min.

Studying these two cases together reveals more interesting behaviour in the formation of the AHC salts. In both cases, the HCl concentration varies from 0% excess HCl, which means stoichiometric HCl moles, to 700% excess, that is 8 times the required stoichiometric HCl to react with the amines. The tables and figures in this section provide FTIR, Elemental Analysis, DSC, SEM and EDX data obtained from analysis of the samples.

Table 4-4- Compounds and Compositions for Case Study 3

Assignment	***Frequency for each Compound(cm^{-1})*** *(for all samples: 0.5% MDA conc. and 200 ml/min flowrate)*			
	0% ex HCl	*100% ex HCl*	***300% ex HCl***	*700% ex HCl*
1	*3358, 3219*	*3219*	**-**	*-*
2	*3205-2576*	*3206-2583*	***3200-2580***	*3201-2583*
3	*2592, 2554*	*2553*	***2554***	*2553*
4	*1570*	*1570*	***1568***	*1567*
5	*1248*	*-*	**-**	*-*
6	*-*	*-*	**-**	*-*
7	*1057*	*1055*	***1057***	*1058*
8	*1022*	*1020*	***1020***	*1020*
9	*-*	*-*	**-**	*-*
10	*690*	*677*	***690***	*690*
11	*638*	*-*	***635***	*-*
Components based on FTIR	*MDA.2HCl MDA.HCl*	*MDA.2HCl MDA.HCl*	***MDA.2HCl***	*MDA.2HCl*
Compositions based on Elemental Analysis	*92% MDA.2HCl*	*96% MDA.2HCl*	***99% MDA.2HCl***	*98% MDA.2HCl*

Table 4-5- Compounds and Compositions for Case Study 4

Assignment	*Frequency for each Compound* (for all samples: 5% MDA conc. and 200 ml/min flowrate)			
	0% ex HCl	*100% ex HCl*	***300% ex HCl***	*700% ex HCl*
1	*3470-3436, 3329, 3360*	*3329, 3360, 3215*	***3360, 3219***	*3362, 3220*
2	*2787*	*2790*	***2790***	*2788*
3	*-*	*2592*	***2591***	*2591*
4	*1569*	*1569*	***1570***	*1572*
5	*1274*	*1276, 1248*	***1247***	*1250*
6	*1073*	*1086*	***1086***	*1088*
7	*-*	*1086*	***1086***	*1088*
8	*1018*	*1017*	***1019***	*1020*
9	*784*	*784*	***784***	*786*
10	*699*	*699*	***700***	*669*
11	*639*	*643*	***640***	*638*
Components based on FTIR	*MDA MDA.HCl*	*MDA MDA.HCl*	***MDA.HCl***	*MDA.HCl ?*
Compositions based on Elemental Analysis	*79% MDA.HCl*	*93% MDA.HCl*	***100% MDA.HCl***	*97% MDA.HCl*

Table 4-4 contains interesting information about MDA.2HCl salts all made from 0.5% MDA blend and with the same flowrate, but varying HCl concentrations, where it can be seen that the best HCl excess percent to make the highest concentration of MDA.2HCl is 300% excess HCl. This was also the optimum percent excess HCl for making MDA.HCl from 5% blends. There is an increase in MDA.HCl concentration when the HCl excess is changed from 0-700 in Case 4.

Interestingly, MDA does not fully react to MDA.HCl unless there is excess HCl, as shown in Table 4-5. Another important point concluded from Table 4-4 is that without excess HCl, MDA.HCl appears as an impurity in the MDA.2HCl particles.

Just as in the previous section, DSC data can verify the components existing in these samples. Figure 4-3 shows the DSC plot for one sample from Case 3. An

obvious sharp peak and peak distinguishable range can be extracted to compare with the other samples studied in Case 1.

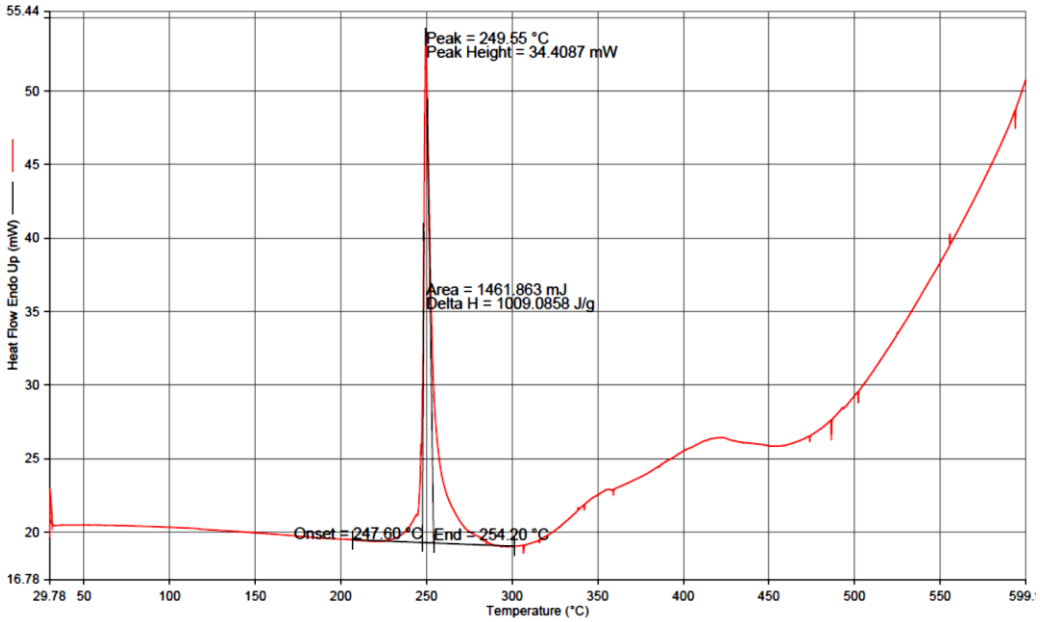

Figure 4-3- DSC plot of the sample made from 0.5% MDA reacted with 700% excess HCl with 200ml/min flowrate in the CIJR

Table 4-6, has a summary of the thermal properties of the samples studied in this section, similar to Table 4-3. The cells in bold were characterized as pure AHC salts in Chapter 3, and are used as references to compare with the other samples in this table. Impurities in the samples such as in the last row can be detected by processing the Table 4-6 data. For instance the sample made from 5% MDA exposed to 700% excess HCl and flowrate of 200 ml/min, has MDA.2HCl as the impurity in MDA.HCl, because the Peak 3 has a temperature range that is expected to be detected in presence of MDA.2HCl compound, as discussed in Chapter 3. This is a fact that FTIR could not identify, perhaps because of a poor spectra or being negligible- less than 3% of the sample bulk. There is no conflict between what was expected from the FTIR and elemental analysis data: the thermal properties verify the FTIR completely.

Table 4-6- Thermal Properties of Cases 3 and 4

Cases	*HCl Excess %*	*Purity based on E.A*	*DSC Data T(°C), ΔH(J/g)*	*Compounds based on DSC*
Case 1 *0.5% MDA Conc. and 200 ml/min*	***0***	*92% MDA.2HCl*	*Peak1 T=184, ΔH=8* T_{Peak1} *range=181-186* *Peak2 T=242, ΔH=317* T_{Peak2} *range=240-245*	*MDA.HCl MDA.2HCl*
	100	*96% MDA.2HCl*	*Peak T=270, ΔH=593* T_{Peak} *range=241-272*	*MDA.2HCl*
	300	***99% MDA.2HCl***	***Peak T= 249, ΔH=915*** T_{Peak} ***range=247-255***	***MDA.2HCl***
	700	*98% MDA.HCl*	*Peak T=250, ΔH=1009* T_{Peak} *range=248-254*	*MDA.2HCl*
Case 2 *5% MDA Conc. and 200 ml/min*	***0***	*79% MDA.HCl*	*Peak T= 93, ΔH=27* T_{Peak} *range=90-95* *Peak2 T=186, ΔH=59* T_{Peak} *range=178-188*	*MDA MDA.HCl*
	100	*93% MDA.HCl*	*Peak T= 97, ΔH=28* T_{Peak} *range=88-105* *Peak2 T=188, ΔH=62* T_{Peak} *range=182-191*	*MDA.HCl*
	300	***100% MDA.HCl***	***Peak1 T=100, ΔH=37*** T_{Peak} ***range=87-105*** ***Peak2 T=188, ΔH=80*** T_{Peak} ***range=186-189***	***MDA.HCl***
	700	*97% MDA.HCl*	*Peak1 T=99, ΔH=36,* T_{Peak} *range=89-102* *Peak2 T=188, ΔH=65* T_{Peak} *range=180-189* *Peak3 T=258, ΔH=N/A*	*MDA.HCl*

The SEM images for these two cases are shown in Figure 4-4 and in general, the effect of change in HCl concentration on the samples is not dramatic, in contrast with the case for MDA concentration. In this figure it is apparent that evenness in the particle shape and size increases as a result of an increase in HCl concentration. This statement will be verified in Section 4-5 where the average particle size is reported.

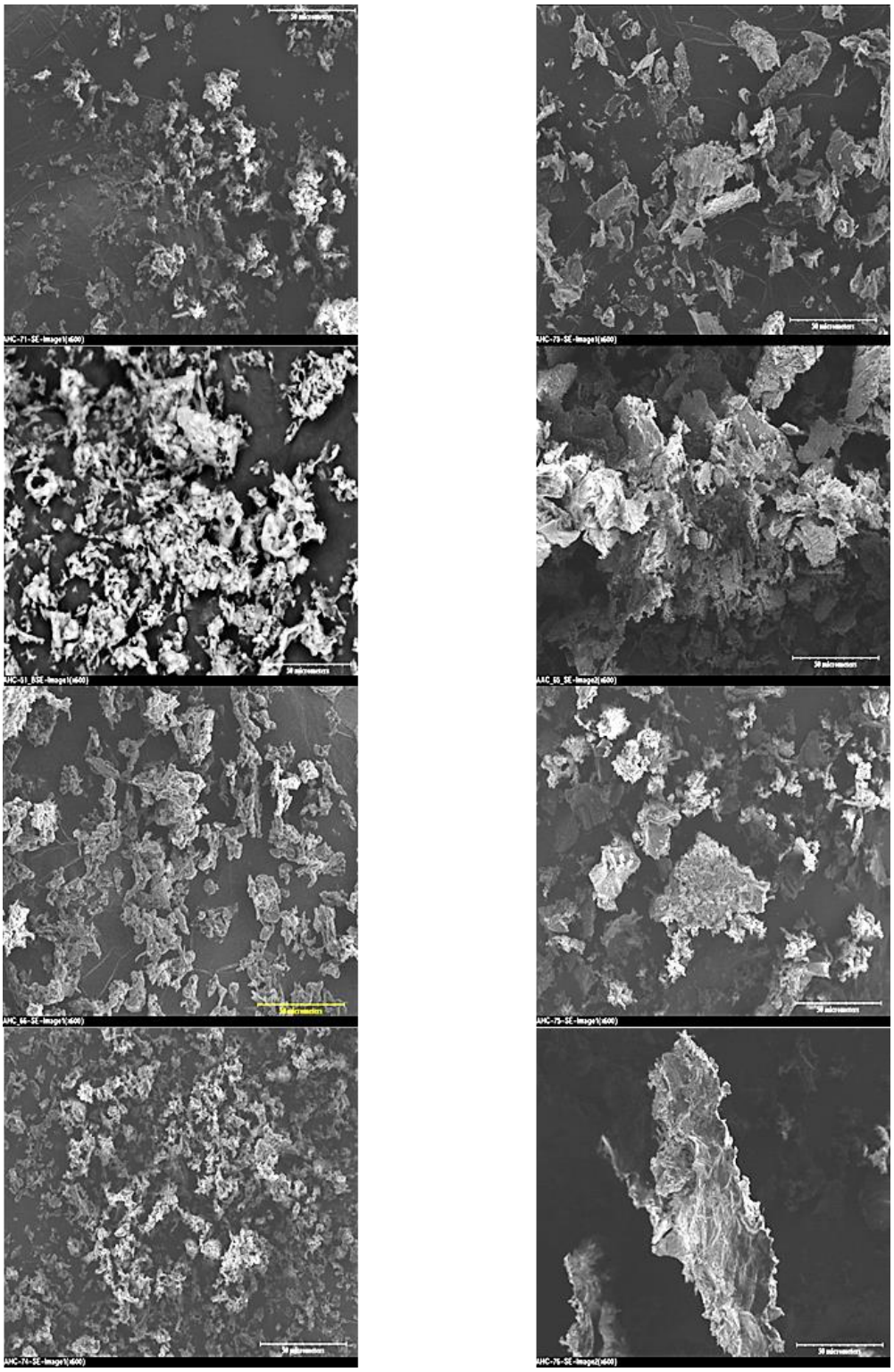

Figure 4-4- Effect of increase in the HCl concentration from top (0%) to bottom (700%) on Case 3(left) and Case 4(right) product particles. SEM images with Magnification of 600(Scale bar is 50µm)

In processing EDX data, Table 4-7, the maximum relative error is high for some of the analyzed salts and it shows that EDX, which represents elemental compositions on the surface, detects different compositions from elemental analysis of the bulk as discussed in Chapter 3.

Table 4-7-EDX results vs. Elemental Analysis of Cases 3 and 4

Reaction Conditions			*Purity Based on E.A*	*EDX Points' Range of C/Cl*	*Elemental Analysis C/Cl ratio*	*Maximum Relative Error*
MDA Conc %	*Flow rate (ml/min)*	*HCl excess %*				
0.5	*200*	*0*	*92% MDA.2HCl*	*2.0-3.1*	*2.4*	*29%*
0.5	*200*	*100*	*96% MDA.2HCl*	*1.9-2.8*	*2.3*	*22%*
0.5	*200*	*300*	*99% MDA.2HCl*	*1.9-3.0*	*2.2*	*36%*
0.5	*200*	*700*	*98% MDA.2HCl*	*1.8-2.9*	*2.2*	*32%*
5	*200*	*0*	*79% MDA.HCl*	*4.4-6.1*	*5.3*	*15%*
5	*200*	*100*	*93% MDA.HCl*	*4.3-5.0*	*4.7*	*7%*
5	*200*	*300*	*100% MDA.HCl*	*4.1-4.5*	*4.4*	*2%*
5	*200*	*700*	*97% MDA.HCl*	*3.8-4.4*	*4.3*	*12%*
In Theory			*MDA.2HCl*	*2.2*		*-*
			MDA.HCl	*4.4*		*-*

Figure 4-5 shows effect of percent excess HCl on degree of chlorination which is expected to have a slightly growing trend in 3 cases including 3 and 4.

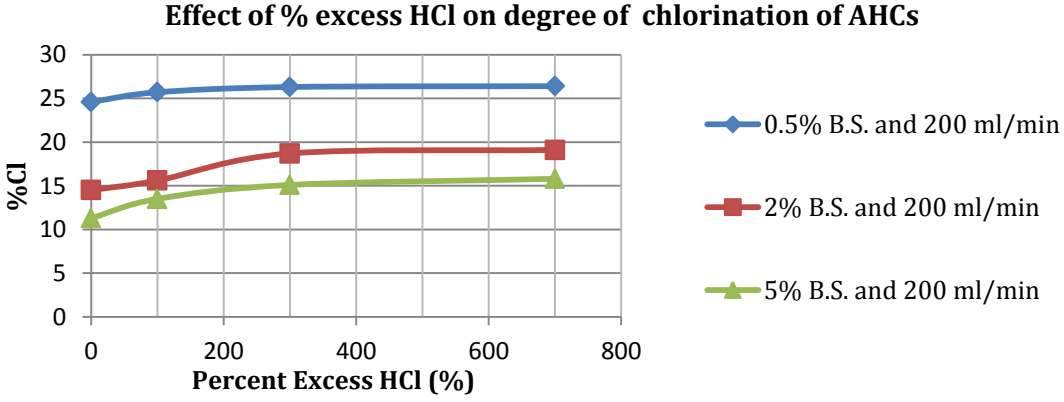

Figure 4-5- Degree of chlorination vs. percent excess HCl

4.4 Effect of Flowrate on the Formation of AHC salts

The last process variable discussed here, flowrate, is the most interesting variable to work with, since the reaction takes place in a Confined Impinging Jet Reactor, and the turbulence intensity determines the rate of mixing at the smallest scales. There were a number of process limitations that made the achievable range of flowrate narrow: the CIJR dimensions, the HCl flow meter range, the pumps, the sample container and tubing. In order to keep the flow in the turbulent regime, the flowrate must not drop to less than 100ml/min for this CIJR, and for very high flowrates, the process handling gets more difficult. Similar to the previous sections there are two full case studies provided here both having 100% excess HCl. There were two other cases with 300% excess HCl not reported in this section because of very unstable particles under X-ray beam; however the particle sizes of all of the cases are analyzed in the next section. The flowrate values are the total flowrate for the outlet stream of the CIJR and the two inlet flows are always equal.

Case 5- Low Blend Strength

Reaction Conditions: 0.5%wt MDA Concentration and 100% excess HCl

In this case study, 3 samples with different flowrates are fully analyzed: 100, 200, and 300 ml/min. The HCl concentration for all of the samples was two times the required stoichiometric amount (100% excess HCl). Because a low blend strength is picked (0.5 wt% MDA) a high concentration of MDA.2HCl is expected in the product particles. The purity and morphology of each sample, and later in Section 4.5 the average particle size of the solids will show how mixing intensity affects the formation of AHC salts.

Case 6- High Blend Strength

Reaction Conditions: 5%wt MDA Concentration and 100% excess HCl

This case is identical to Case 5 in terms of varying the flowrate, but here high blend strength (5 wt% MDA concentration) was picked.

The same approach is taken here as for the other variables, starting with compounds and compositions, thermal properties, and later on looking at the morphologies and basic conclusions. More data about the effect of this variable is available in Section 4.5, studying the average particles size.

Table 4-8-Compounds and Compositions for Case Study 5

Assignment	***Frequency for each Compound(cm^{-1})*** *(for all samples: 0.5 wt% MDA conc. and 100% excess HCl)*		
	100 ml/min	*200 ml/min*	*300 ml/min*
1	**-**	-	*3219*
2	***3200-2580***	*3199-2580*	*3194-2586*
3	***2556***	*2558*	*2557, 2586*
4	***1570***	*1570*	*1568*
5	**-**	-	*1248*
6	**-**	-	-
7	***1060***	*1057*	*1057*
8	***1020***	*1018*	*1020*
9	**-**	-	*750*
10	***696***	*670*	*698*
11	**-**	-	*640*
Components based on FTIR	***MDA.2HCl***	*MDA.2HCl ?*	*MDA.HCl MDA.2HCl*
Compositions based on Elemental Analysis	***99% MDA.2HCl***	*96% MDA.2HCl*	*91% MDA.2HCl*

Table 4-9- Components and Compositions for Case Study 6

Assignment	*Frequency for each Compound(cm^{-1})* (*for all samples: 5 wt% MDA conc. and 100% excess HCl)*		
	100 ml/min	*200 ml/min*	*300 ml/min*
1	*3358, 3218*	*3330, 3361, 3216*	*3470-3436, 3329, 3359*
2	*2787*	*2790*	*2788*
3	*2585*	*2587*	*-*
4	*1568*	*1569*	*1570*
5	*1247*	*1276, 1248*	*1276*
6	*1087*	*1086*	*1070*
7	*1087*	*1086*	*-*
8	*1018*	*1018*	*1019*
9	*751*	*784*	*785*
10	*700*	*700*	*699*
11	*639*	*641*	*640*
Components based on FTIR	*MDA.HCl*	*MDA MDA.HCl*	*MDA MDA.HCl*
Compositions based on Elemental Analysis	*99% MDA.HCl*	*86% MDA.HCl*	*72% MDA.HCl*

Table 4-8 to 4-9 have some cells in **bold** which are data from Chapter 3, used here as the reference particles. Similar to the one sample in Section 4-3, FTIR could not determine the impurity in one of the samples, the column containing question mark, but the thermal properties in Table 4-10 can provide that piece of information- the sample made with 0.5 wt% MDA reacted with 100% excess HCl at 200ml/min flow. Two impurities in Table 4-10 could not be identified, which is perhaps because of the very close peak temperature ranges of MDA and MDA.HCl, as described in Chapter 3.

Studying the effects of flowrate on the AHC is more complicated than local concentration. Tables 4-8 to 4-10 show that at very high flows neither reaction went to completing and the particles precipitated with a lower degree of chlorination, or an explanation for this influence (dropping the %Cl) can be reduction in residence time (τ_{res}): at higher flows, the feed concentration will persist for a higher portion of the residence time.

Table 4-2-Thermal Properties of Cases 5 and 6

Cases	*Flowrate (ml/min)*	*Purity based on E.A*	*DSC Data T(°C), ΔH(J/g)*	*Compounds based on DSC*
Case 5 *0.5% MDA Conc. and 100% excess HCl*	***100***	***99% MDA.2HCl***	***Peak T=262, ΔH=669 T_{Peak} range=252-267***	***MDA.2HCl***
	200	*96% MDA.2HCl*	*Peak1 T= 185, ΔH=11 T_{Peak1} range=182-186 Peak2 T= 270, ΔH=593 T_{Peak2} range=241-272*	*MDA.2HCl MDA.HCl*
	300	*92% MDA.2HCl*	*Peak1 T= 184, ΔH=14 T_{Peak1} range=181-186 Peak2 T= 272, ΔH=487 T_{Peak2} range=270-275*	*MDA.2HCl MDA. HCl*
Case 6 *5% MDA Conc. and 100% excess HCl*	***100***	***99% MDA.HCl***	***Peak1 T=92, ΔH=62, T_{Peak1} range=90-93 Peak2 T=189, ΔH=49 T_{Peak2} range=187-190***	***MDA.HCl***
	200	*86% MDA. HCl*	*Peak1 T= 92, ΔH=62 T_{Peak1} range=89-93 Peak2 T= 189, ΔH=49 T_{Peak2} range=187-190*	*MDA.HCl ?*
	300	*72% MDA.HCl*	*Peak1 T= 91, ΔH=21 T_{Peak1} range=90-92 Peak2 T= 188, ΔH=42 T_{Peak2} range=187-189*	*MDA.HCl ?*

Figure 4-6 shows the SEM images taken with the same magnification for Case 5 and 6. Looking at the images from top to bottom shows that evenness in shape and size are increased, but perhaps an incomplete reaction (in the right hand side, Case 6), or the combination of the two reactions (in the left hand side, Case 5) is the cause of less purity in the two cases as the flowrate is increased.

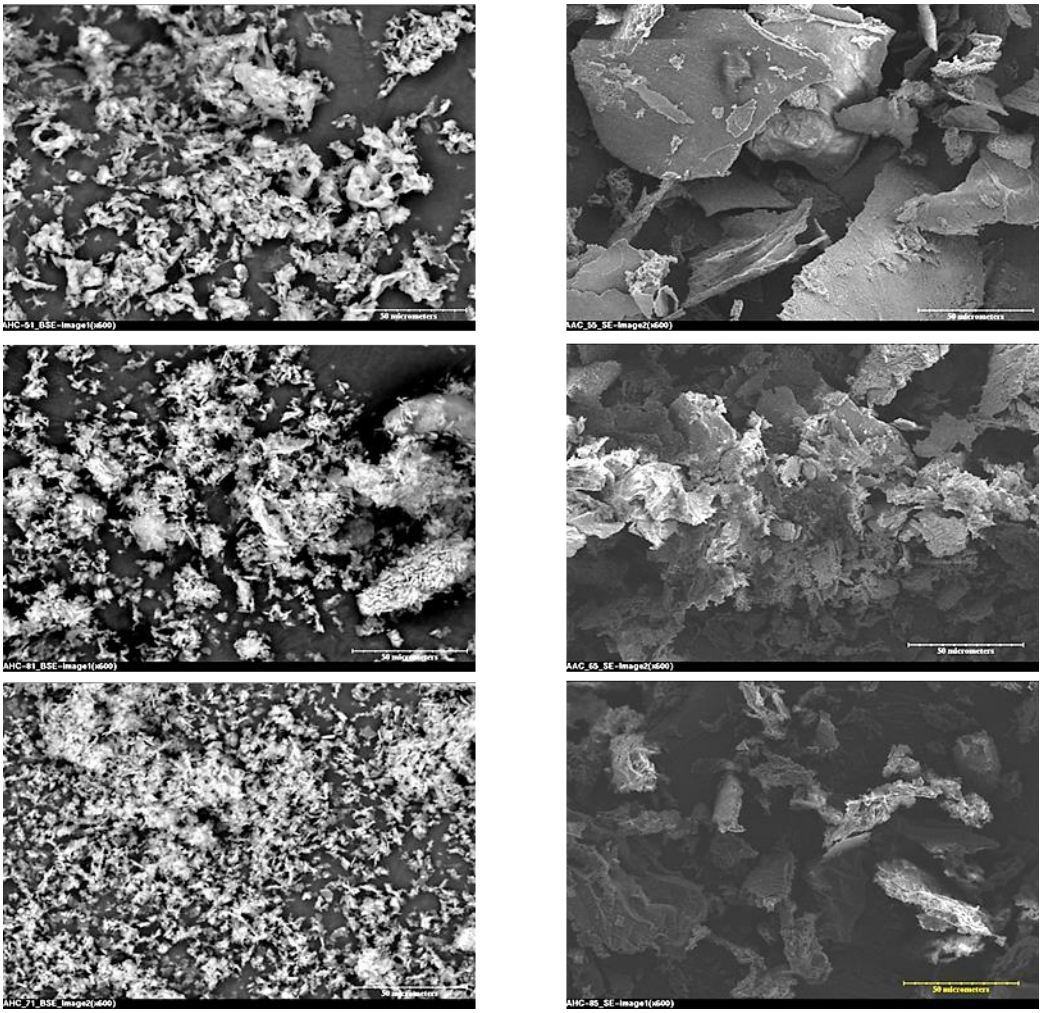

Figure 4-6- Effects of increase in flowrate from top (100) to bottom (300 ml/min) on the samples of Case5 (left) and Case 6 (right). SEM images with Magnification of 600(Scale bar is 50μm)

Trends of change in degree of chlorination as a function of flowrate for 5 different cases are shown in Figure 4-7. Only two of them, Cases 5 and 6 were fully analyzed with all of discussed analytical techniques and reported in this Chapter.

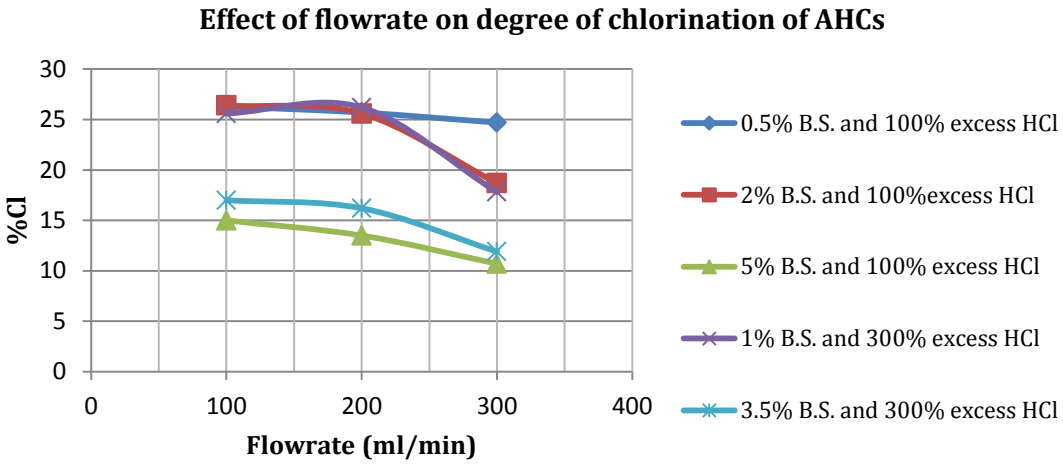

Figure 4-7- Degree of Chlorination vs. flowrate

4.5 Average Particle Sizing of AHC Salts

This section contains supplementary analysis of the average particle sizing (d_P) that can help in justifying the effects of each variable on aminehydrochloride (AHC) particles made in the CIJR.

First the protocol used in determining the average size of particles is explained in detail. Second, the quantitative data acquired from 800 images is illustrated and summarized in tables.

There is a way to do average sizing, using the surface of particles under optical microscopy, and calculate respective diameter for each sample. This would show average size of the single particles, excluding the large masses of particles.

The MDA used in making blends was 97% pure Sigma-Aldrich and came in white granular form. Sizing of the precipitated colorless bar shape MDA particles cannot make much sense and be useful to compare with the AHC solids, since the AHC particles were formed in turbulence but the MDA was

precipitated from a stagnant blend. Therefore, AHC samples are the only subjects of study in this section.

4.5.1 The Procedure Used in Processing the Optical Microscopy Images

AHC particles are sticky powders and it makes working with them a little difficult. One of the most practical ways to make an even surface on the microscope slides is to pour particles on the slides with a pipette and then spray air parallel with slide surface. After blowing air with moderate speed, a fine film of fine particles can be seen on the slide and it is ready to take images with the optical microscope.

Images taken at 100X magnification are scaled and saved using "AxioVision" software that operates the camera on the microscope. Images need to be adjusted with post processing software packages. Adobe Photoshop is used to adjust brightness and colors of images.

AxioVision itself can manually measure particles by drawing a circle around the selected particles, but this is not very accurate and is also very time-consuming. There is a free image processing software package called "ImageJ" that can detect particles based on a threshold. This is used in analyzing particle size of the small, single particles in this work. To illustrate described procedure, two different cases are presented in following pages in detail.

Case 7 provides images taken with the optical microscope from the particles made of 0.5% MDA blend reacted with 100% excess HCl in the CIJR and 100ml/min flowrate, and Case 8 has the images taken with the optical microscope from the particles made of 3.5% MDA reacted with 300% excess HCl in the CIJR with 200ml/min flowrate. All images have the same magnification, 100X and original dimension of 1386x1036 pixels (487x651 μm).

Figures 4-8 and 4-9 show the post processing procedure on two selected images of Cases 7 and 8 step-by-step. Tables 4-11 and 4-12 provide a summary of the obtained quantitative data from all microscope images taken from Cases 7 and 8.

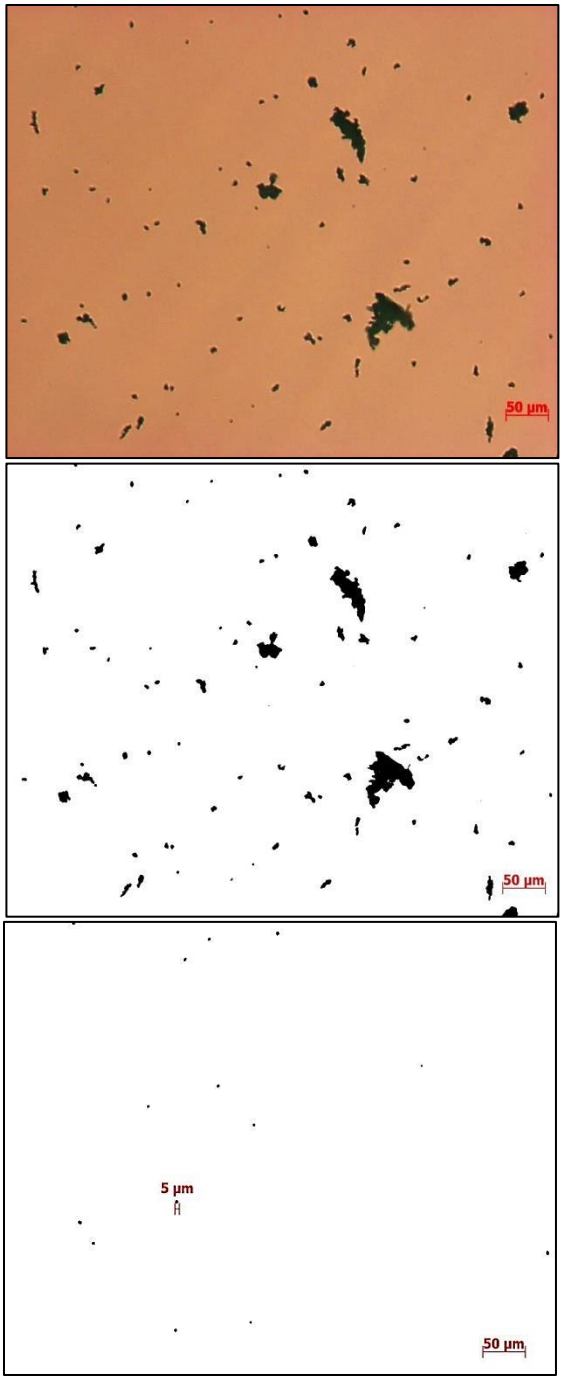

Figure 4-8- Post image processing of an image of Case 7; <u>Top:</u> original image. <u>Middle:</u> threshold adjusted image. <u>Bottom:</u> large agglomerated particles filtered. (100X magnification for all images)

Table 4-11-Data from analysis of the images taken from Case 7

Titles		*Area(μm²)*	*Circularity[1]*	*Solidity[2]*	*Diameter(μm)[3]*
Figure 4-5 14 Particles	*Mean*	*6.62*	*0.97*	*0.88*	*2.90*
	Min	*2.43*	*0.75*	*0.78*	*1.76*
	Max	*12.6*	*1*	*1*	*4.01*
Total of 8 Images 185 particles	*Mean*	*6.74*	*0.97*	*0.88*	*2.93*
	Min	*2.21*	*0.7*	*0.77*	*1.68*
	Max	*14.59*	*1*	*1*	*4.31*

1: Circularity calculated from the following formula: $4\pi \times \frac{\text{Area}}{\text{Perimeter}^2}$ with a value of 1.0 indicating a perfect circle.

2: Solidity for each particle calculated from: $\frac{Area}{Convex\ Area}$.

3: Area based particle size equals the diameter of a sphere that has the same surface area as the particle.

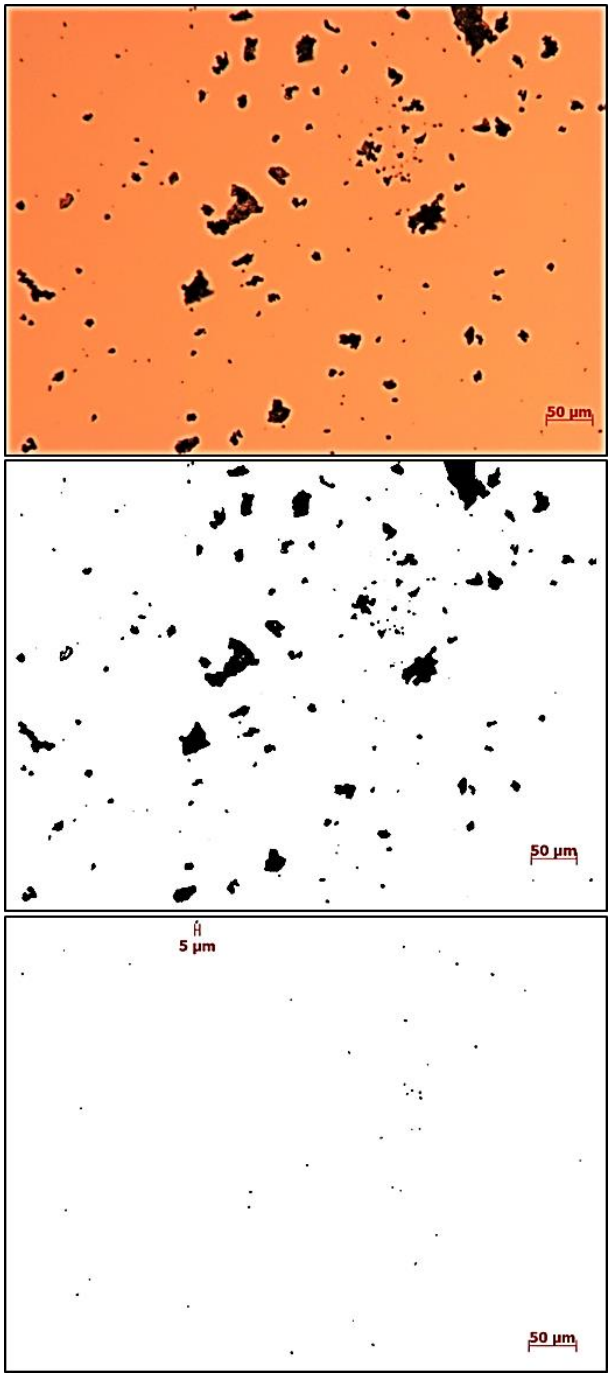

Figure 4-9-Post image processing of an image of Case 8; <u>Top:</u> original image. <u>Middle:</u> threshold adjusted image. <u>Bottom:</u> large agglomerated particles filtered. (100X magnification for all images)

Table 4-12- Data from analysis of the images taken from Case 8

Titles		*Area(μm²)*	*Circularity*	*Solidity*	*Diameter(μm)*
Figure 4-6 86 Particles	*Mean*	*9.02*	*0.94*	*0.9*	*3.39*
	Min	*3.92*	*0.89*	*0.84*	*2.49*
	Max	*14.0*	*0.99*	*0.95*	*8.92*
Total of 9 Images 1016 particles	*Mean*	*9.13*	*0.95*	*0.89*	*3. 41*
	Min	*2.86*	*0.88*	*0.74*	*2.46*
	Max	*14.12*	*0.99*	*0.96*	*8.99*

4.5.2. Effect of MDA Concentration on the Average Particle Size

As expected, by increasing the MDA concentration, or blend strength, theaverage particle size (d_P) increased, as shown in Table 4-13. A lower degree of chlorination results in bigger particles.

Table 4-13- Average particle size vs. MDA concentration

MDA Concentration (wt%)	*100ml/min flowrate and 100% excess HCl*		*200ml/min flowrate and 300% excess HCl*	
	Average Diameter (μm)	*Standard Deviation*	*Average Diameter* (μm)	*Standard Deviation*
0.5	*2.93*	*2.1*	*2.77*	*2.2*
1	*3.14*	*2.4*	*3.07*	*2.3*
2	*3.39*	*2.5*	*3.31*	*2.4*
3.5	*3.78*	*2.9*	*3.39*	*2.4*
5	*3.94*	*2.5*	*3.70*	*2.2*

4.5.3 Effect of HCl Concentration on the Average Particle Size

HCl concentration affects the particle size in reverse order, where increasing HCl excess percent makes smaller particles. The standard deviation (σ) in Table 4-14 shows that the particles also have more even size distributions at higher HCl concentration. In this case, the HCl concentration increases the evenness in the size of the particles as was noted from the SEM images.

Table 4-3- Average particle size vs. HCl concentration- 3 Case studies (200ml/min flowrate)

HCl Excess (%)	*0.5% MDA*		*2% MDA*		*5% MDA*	
	Average Diameter(µm)	*σ*	*Average Diameter*(µm)	*σ*	*Average Diameter* (µm)	*σ*
0	*3.13*	*2.4*	*3.65*	*2.6*	*3.96*	*2.4*
100	*2.89*	*1.9*	*3.33*	*2.4*	*3.70*	*2.3*
300	*2.77*	*1.9*	*3.31*	*2.3*	*3.70*	*2.1*
700	*2.78*	*1.8*	*3.28*	*2.3*	*3.64*	*2.0*

4.5.4 Effect of Flowrate on the Average Particle size

As discussed in Section 4.5.3, the effect of the HCl concentration on the average d_P of AHC salts, an increase in the flowrate results in smaller average particle sizes in almost all of the cases. In Tables 4-15 and 4-16, standard deviation columns show more evenness in the size of the AHC salts for a higher mixing intensity, and flowrate (shorter residence time).

Table 4-15-Average particle size vs. flowrate-3 case studies (100% excess HCl)

Flowrate (ml/min)	*0.5% MDA*		*2% MDA*		*5% MDA*	
	Average Diameter(µm)	*σ*	*Average Diameter*(µm)	*σ*	*Average Diameter* (µm)	*σ*
100	*2.93*	*2.1*	*3.39*	*2.5*	*3.94*	*2.5*
200	*2.89*	*1.9*	*3.33*	*2.4*	*3.70*	*2.3*
300	*2.87*	*1.7*	*3.28*	*2.4*	*3.67*	*2.0*

Table 4-16-*Average particle size vs. flowrate- 2 case studies (300% excess HCl)*

Flowrate (ml/min)	*1% MDA*		*3.5% MDA*	
	Average Diameter (µm)	*σ*	*Average Diameter* (µm)	*σ*
100	*3.18*	*2.7*	*3.41*	*2.7*
200	*3.07*	*2.3*	*3.39*	*2.4*
300	*3.06*	*1.8*	*3.39*	*2.2*

4.5.5 Summary of Particle Sizing

From the data in Tables 4-13 to 4-16, it can be concluded that the average particle size increases as the MDA concentration of the blend increases, but there was no strong effect of flowrate or HCl concentration on particle size. Figures 4-10 to 4-12 show the trends for all cases studied in Section 4.5, confirming the above statement and demonstrating inverse effect of an increase in flowrate or HCl concentration on the average particle size of the AHC salts.

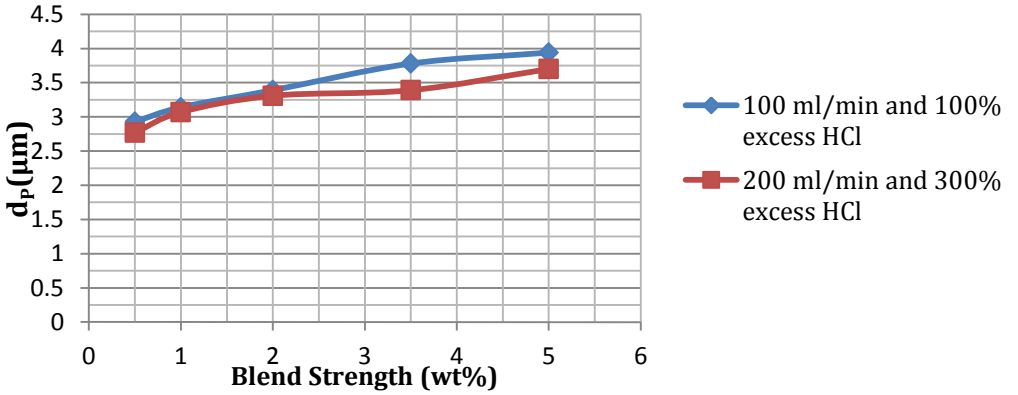

Figure 4-10- Effect of MDA blend strength on d_P of AHC salts

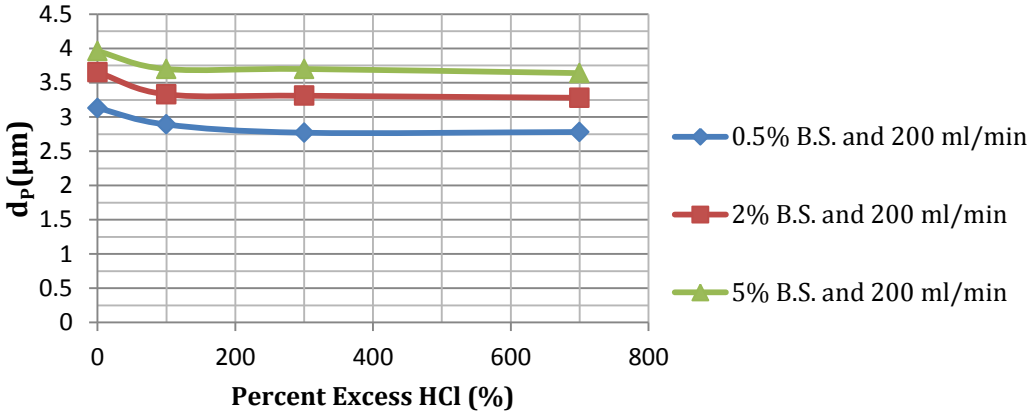

Figure 4-11-Effect of % excess HCl on d_P of AHC salts

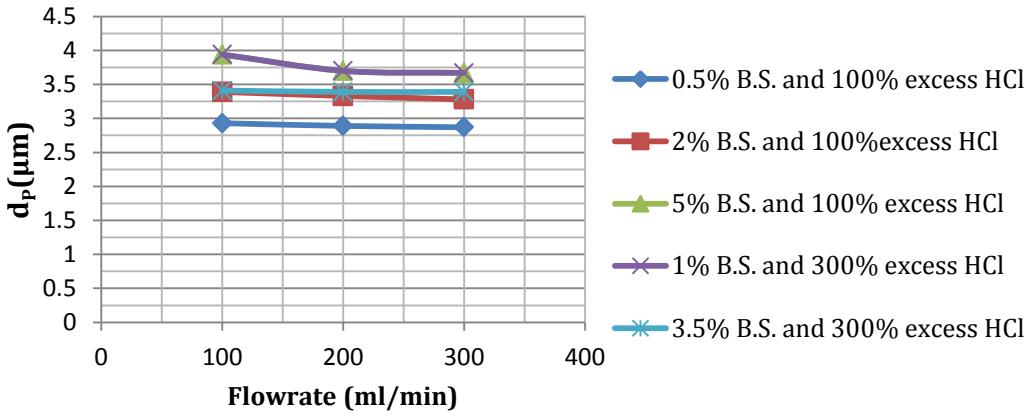

Figure 4-12- Effect of flowrate on d_P of AHC salts

4.5.6 Statistical Analysis of the Effect of Process Variables on the Particle Size

Two-way Analysis of Variance

A two-factor or two-way analysis of variance is used to examine how two variables (independent variables) affect the mean of a response variable (dependent variable). Therefore, there is interest in the effect of each factor, and combined effect of both factors. It is important to realize that a factor is considered controllable by the experimenter; that is, the values or levels, of the factor can be determined prior to the beginning of the test program. The objective of proposed experiment is to determine the effect of factors on the response. In general, suppose two factors A and B; factor A has r levels and factor B has c levels [62].

For two factors A and B, the level means from the total mean for factor A can be estimated by $\mu_i = \mu + \alpha_i$, where α_i denotes the effect of the i^{th} level for factor A (i.e. the departure of the i^{th} level mean μ_i for factor A from the total mean μ).

Similarly, the level means from the total mean for factor B, is estimated: $\mu_j = \mu + \beta_j$, where β_j denotes the effect of the j^{th} level for factor B (i.e. the departure of the j^{th} level mean μ_j for factor B from the total mean μ). Table 4-17 shows the relevant null hypothesis to the test for effect of each factor A and B.

Table 4-17- Null Hypothesis (H_0) in two-way ANOVA test

Test Desired	*Null Hypothesis (H_0)*	*Equivalent H_0*	*Statistical Test*
Effect of factor A	$\mu_{1.} = \mu_{2.} = \cdots = \mu_{r.}$	$\alpha_i = 0$ *for all* i	$\frac{MS_A}{MS_W} \sim F(df_A, df_E)$
Effect of factor B	$\mu_{.1} = \mu_{.2} = \cdots = \mu_{.c}$	$\beta_j = 0$ *for all* j	$\frac{MS_B}{MS_W} \sim F(df_B, df_E)$

It means there is no significant difference between the levels of Factor A or B and response variable will be the same in each one. In other words, this factor has no effect on the output. In statistical terms, *MS* is the mean square, *w* and *e* subscripts stand for within and error, and *df* is degrees of freedom.

In the following equations, Table 4-18, r is the sample size (at level r) of Factor A, c is sample size (at level c) of Factor B and N is the total sample size which is equal to $r \times c$.

Table4-18- The Analysis of Variance Table for Two-Factor, Fixed Effect Model.

Source of Variation	*Sum of Squares(SS)*	*Degree of freedom(df)*	*Mean Square (MS)*
Between Treatment A	$SS_A = c\sum_{i=1}^{r}(\bar{y}_i - \bar{\bar{y}})^2$	$df_A = r - 1$	$MS_A = SS_A/df_A$
Between Treatment B	$SS_B = r\sum_{j=1}^{c}(\bar{y}_i - \bar{\bar{y}})^2$	$df_B = c - 1$	$MS_B = SS_B/df_B$
Error (within Treatment)	$SS_E = \sum_{j=1}^{c}\sum_{i=1}^{r}(y_{ij} - \bar{y}_i - \bar{y}_j + \bar{\bar{y}})^2$	$df_E = (r-1)(c-1)$	$MS_E = SS_E/df_E$
Total	$SS_T = \sum_{j=1}^{c}\sum_{i=1}^{r}(y_{ij} - \bar{\bar{y}})^2$	$df_T = N - 1$	$MS_T = SS_T/df_T$

F value for each treatment (k: A and B) is equal to: $F_k = \frac{MS_k}{MS_E}$

F_k is compared to F_{crit} obtained from F-tables at the 5% significance level, and if $F>F_{crit}$, then the effect is significant. There is another method to check the whether the effect is significant or not that uses P-values for a specific α(0.05), significance level, from the two-way ANOVA tables. In this case the P-value must be less than 0.05.

A. Two-Way ANOVA Test for studying effect of Percent HCl Excess on Particle Size

The objective is to investigate how significant the MDA concentration of the blend affects the particle size. Simultaneously, studying the effect of % HCl excess on particle size can be done. The experiment will be analyzed using a two-way layout design with four levels (HCl concentration of the 0, 100, 300, and 700) on factor A (% HCl excess), and three levels (MDA concentration of the 0.5%, 2%, and 5%) on factor B (blend strength). The two-way layout model without replication considers the influence of the main factor effects.

Table 4-19-Two-way ANOVA test for effect of % HCl excess and blend strength on particle size

Source of Variation	*SS*	*df*	*MS*	*F*	*P-value*	F_{crit}
% HCl Excess	*0.229167*	*3*	*0.076389*	*79.25072*	*3.23E-05*	*4.757063*
Blend Strength	*1.48415*	*2*	*0.742075*	*769.8761*	*5.85E-08*	*5.143253*
Error	*0.005783*	*6*	*0.000964*			
Total	*1.7191*	*11*				

Table 4-19 confirmed the visual results and there are significant differences on average particle size values by increasing the HCl concentration and the MDA concentration of the blend. As shown in Figures 4-10 and 4-11, it could be concluded that the average particle size increases as the MDA

concentration of the blend increases, and there is an inverse effect of increase in HCl concentration on the average particle size of the AHC salts. Therefore, at the 95% level of confidence we conclude there is a significant difference in the particle size produced by the three blends and four HCl concentrations. This experiment is done for the standard deviation of particle size with similar results, as shown in Table 4-20. Both % HCl excess and blend strength were effective factors on the average particle size of the AHC salts and its standard deviation (can be interpreted here as uniformity).

Table 4-20-Two-way ANOVA test for effect of % HCl excess and blend strength on standard deviation of particle size

Source of Variation	*SS*	*df*	*MS*	*F*	*P-value*	F_{crit}
% HCl Excess	*0.066851*	*3*	*0.022284*	*9.992927*	*0.009488*	*4.757063*
Blend Strength	*0.070359*	*2*	*0.03518*	*15.77593*	*0.004079*	*5.143253*
Error	*0.01338*	*6*	*0.00223*			
Total	*0.15059*	*11*				

B. Two-Way ANOVA Test for studying effect of Flowrate on Particle Size

In this case a two-way layout design with three levels (flowrate of 100, 200, and 300) on factor A (flowrate) and three levels (MDA concentration of the 0.5%, 2%, and 5%) on factor B (blend strength) is applied. Objective of proposed experiment is to determine the effect of flowrate and blend on the particle size (response).

Table 4-21- Two-way ANOVA test for effect of flowrate and blend strength on particle size

Source of Variation	*SS*	*df*	*MS*	*F*	*P-value*	F_{crit}
Flowrate	*0.035467*	*2*	*0.017733*	*7.360656*	*0.009886*	*6.944272*
Blend Strength	*1.144067*	*2*	*0.572033*	*140.6639*	*0.000197*	*6.944272*
Error	*0.016267*	*4*	*0.004067*			
Total	*1.1958*	*8*				

As it is shown in Table 4-21, there is significant difference and no strong effect of flowrate on particle size (P-value for flowrate is lower than α=0.05 which alpha is the level of acceptable significance). Particle size slightly decreased as a result of increase in the flowrate, but not significantly (or effectively). Table 4-22 shows the results of ANOVA test on standard deviation of particle size, which verifies the previous conclusions on the effect of flowrate on the evenness in particle size.

Table 4-22- Two-way ANOVA test for effect of flowrate and blend strength on standard deviation of particle size

Source of Variation	*SS*	*df*	*MS*	*F*	*P-value*	*F crit*
Flowrate	*0.037687*	*2*	*0.018844*	*8.731999*	*0.04246*	*6.944272*
Blend Strength	*0.099556*	*2*	*0.049778*	*17.7834*	*0.01022*	*6.944272*
Error	*0.011196*	*4*	*0.002799*	-	-	-
Total	*0.148439*	*8*	-	-	-	-

4.6 Conclusions

The dominant process variable in the formation of aminehydrochloride particles is the local concentration of MDA. When the MDA concentration is lower than 1 wt%, the particles are mainly MDA.2HCl; for higher than 1% MDA blend, mostly MDA.HCl is formed. To be more precise, a local concentration of 0.5 wt% in the CIJR is the dominant boundary in formation of AHC salts, because the approximately equal flowrate for the opposite inlet stream to the reactor, MCB solvent and dissolved HCl, after mixing in the CIJR drops the MDA local concentration to half of the blend side.

An increase in flowrate or local concentration of HCl- taken into account in this work as the percent excess HCl- results in more even particle size and

shape. The degree of chlorination, or purity, decreased at higher mixing intensity and shorter residence time, whereas an increase in HCl concentration has just the opposite effect on the products; each AHC salt was purer when the MDA blend reacted with 4 times the required stoichiometric HCl. Incomplete hydrochlorination was observed with 0% excess or 100% excess HCl.

Table 4-17, has the summary conclusions of all the sections of this chapter, showing the effect of each variable when the other two are constant.

Table 4-23- Summary of Conclusions of Chapter 4

Variable studied	***Morphology***	***Components and Compositions***	***General Statements***
Effect of increase in Blend Strength (MDA conc.)	*-Bigger Particles* *-Less porosity* *-Smoother surface* *-Harder particles*	*Less degree of chlorination; transition from MDA.2HCl to MDA.HCl*	*Structure depends on* ***blend strength*** *more than any other parameters.*
Effect of Increase in HCl excess	***Increase*** *in evenness of shape and particle size.*	***Increase*** *in Purity of the AHC salts.*	*Evenness and reaction progress increases. Minor effect on the AHC salts formation.*
Effect of Increase in Flowrate	***Increase*** *in evenness of shape and particle size.*	***Decrease*** *in Purity of the AHC salts.*	*Evenness increases but causes more unreacted or incomplete reacted amines in products, because of shorter* τ_{res}.

5 Discussion and Conclusion

From a mixing point of view, slow chemical reactions can be successfully carried out in stirred tanks by increasing the residence time, but confined impinging jet reactors (CIJR) can be used for fast reactions that have a smaller reaction time than the residence time of ordinary reactors.

Mixing in the CIJR has been characterized through chemical means by Johnson and Prud'homme (2003), and a CIJR identical in size to the reactor used in this study has also been characterized by Shad W. Siddiqui a former student of this research group[31,39]. Siddiqui et al. (2009), reported that above flowrate of 165ml/min the flow in CIJR was found fully turbulent and the energy dissipation (ε) varied from 20-6800 W/kg with peak dissipation occurring at the impingement point and decaying away in both radial and axial directions [45].

The reaction studied in this project, hydrochlorination of 4,4'-methylene dianiline, is a precipitation reaction with a very small reaction time. This reaction is an undesired side-reaction in the manufacture of isocyanates which produces highly insoluble amine hydrochloride salts, causing very costly downstream digestion and loss of starting material. Gibson et al., 2010, investigated the solid state structure, thermal stability and solution phase behavior of the products in order to conclude a kinetic model for recovery of the valuable starting material from the unwanted amine hydrochloride salts. Gibson found very extensive and strong intermolecular bonding present in structure of MDA and MDA.2HCl, determined from the lattice energy calculation, and very limited solubility of MDA.2HCl ($<1\times10^{-5}$ mol/lit) in the process solvent (chlorobenzene), measured using H NMR spectroscopy, that did not allow her to investigate kinetic studies for these AHC salts [11]. However, kinetic study on another hydrochloride salt formed from

hydrochlorination of 4-benzylaniline (4-BA.HCl), which is another unwanted side-reaction during synthesis of isocyanate, was very successful [12,14].

Formation of the two AHC salts produced in this work, MDA.HCl and MDA.2HCl which are representative of structures of industrial waste material in this process, were investigated. First the salts were formed in the CIJR under different reaction conditions: Local concentration of the reagents (MDA blend strength and percent excess HCl) and mixing intensity. Then the solid particle products were analyzed and characterized using a range of analytical techniques such as: Elemental analysis (CHNCl), Fourier transform infrared spectroscopy (FTIR), thermogravimetric analysis (TGA), differential scanning calorimetry (DSC), scanning electron microscopy (SEM) and optical microscopy. The compounds and compositions, morphology and average particle size of AHC salts were reported with the following main conclusions:

1- The two different structures of MDA.HCl and MDA.2HCl were identified as the main structures of the produced aminehydrochloride salts in the CIJR.

2- These two different structures were characterized using qualitative and quantitative analysis with some outstanding key properties:

2-1- Degree of chlorination (%Cl) is above 26% for MDA.2HCl, and under 15.5% for MDA.HCl.

2-2- These AHC salts have specific peak assignment in FTIR spectra that can distinguish each of them from MDA.

2-3- The DSC data reveals specific temperature range(s) for phase change in each AHC salt and this can verify the elemental analysis and FTIR data.

2-4- MDA.2HCl has a porous and spongy structure, whereas in MDA.HCl particles are harder with a rocky shape surface.

2-5- MDA.HCl particles agglomerated to very large masses which makes finding single particles in microscopic images more difficult than the MDA.2HCl samples.

2-6- The average size of a single (or primary) particle found in MDA.HCl powder samples is around 30% bigger than the MDA.2HCl particles.

3- The MDA blend strength (local concentration of amine) dominates the structure of AHC salts; low blend strength (less than 1 wt% which is later lowered in the CIJR to 0.5% because of mixing with the MCB stream entering from the opposite side of the CIJR) results in MDA.2HCl, and high blend strength up to 5 wt% produces particles of MDA.HCl.

4- The effect of HCl local concentration (discussed in this work as percent excess HCl) is not as important as MDA blend strength, but this study concludes that MDA does not fully react to MDA.HCl unless there is excess HCl; 300% excess HCl was the optimum percent excess for making the purest AHC salts for both low and high MDA blend strengths. In other words, higher excess HCl causes a higher degree of chlorination.

5- An increase in excess HCl slightly decreased the average particle size of the salts, while increasing evenness in the product powder size and shape.

6- The effect of mixing intensity (flowrate) on the formation of AHC salts was more complicated than the local concentration of the reactants; the degree of completion of reaction and the %Cl of the produced salts decreases as a result of increase in flowrate (rapid mixing) and consequently decrease in residence time.

7- The average particle size of the particles declined steadily by increasing flowrate, but a clear rise is reported in evenness in the particle size. Microscope images also show that higher flowrate makes the AHC particles evener in shape.

References

(1) Sonnenschein M, Koonce W. Polyurethanes. Encyclopedia of Polymer Science and Technology: John Wiley & Sons; 2011.

(2) Randall D, Lee S. The polyurethane Book: John Wiley & Sons; 2002.

(3) Polyurethanes VI. Skeist Inc.; 2006; p7-21.

(4) Six C, Richter F. Isocyanates, Organic. Ullmann's Encyclopedia of Industrial Chemistry: Wiley-VCH Verlag GmbH & Co. KGaA; 2003.

(5) Yakabe Y, Henderson K, Thompson W, Pemberton D, Tury B, Bailey R. Fate of Methylenediphenyl Diisocyanate and Toluene Diisocyanate in the Aquatic Environment, Environ. Sci. Technol. 1999;33:2579-2583.

(6) Markovic V, Hicks D. Design for Chemical Recycling, Philosophical Transactions of the Royal Society of London. 1997;355:1415-1424.

(7) Botella P, Corma A, Mitchell C. Synthesis of Diamine Diphenyl Methane (DADPM) and its Higher Homologues on Delaminated Zeolites: a challenge for a nonpolluting process. Molecular Sieves: from Basic Research to Industrial Applications. 2005;158:1263-1270.

(8) Wegener G, Brandt M, Duda L, Hofmann J, Klesczewski B, Koch D, et al. Trends in Industrial Catalysis in the Polyurethane Industry. Applied Catalysis A-General 2001 NOV 30;221(1-2):303-335.

(9) Weissermel K, Arpe H. Industrial Organic Chemistry. 3rd ed.: Wiley-VCH; 2003.

(10) de Angelis A, Ingallina P, Perego C. Solid Acid Catalysts for Industrial Condensations of Ketones and Aldehydes with Aromatics. Ind Eng Chem Res 2004 MAR 3;43(5):1169-1178.

(11) Gibson E, Winfield JM, Muir KW, Carr RH, Eaglesham A, Gavezzotti A, et al. A Structural and Spectroscopic Investigation of the Hydrochlorination of 4,4 '-Methylenedianiline. Physical Chemistry Chemical Physics 2010;12(15):3824-3833.

(12) Gibson E, Amine hydrochloride salts: a problem in polyurethane synthesis. University of Glasgow; 2007.

(13) Li S, Doyle P, Metz S, Royce A, Serajuddin A. Effect of Chloride Ion on Dissolution of Different Salt Forms of Haloperidol, a Model Basic Drug. J Pharm Sci 2005 OCT;94(10):2224-2231.

(14) Gibson EK, Winfield JM, Muir KW, Carr RH, Eaglesham A, Gavezzotti A, et al. A Structural and Spectroscopic Investigation of the Hydrochlorination of 4-Benzylaniline: the interaction of anhydrous hydrogen chloride with chlorobenzene. Physical Chemistry Chemical Physics 2009;11(2):288-297.

(15) Bourne J. Mixing and the Selectivity of Chemical Reactions. Organic Process Research & Development 2003 JUL-AUG;7(4):471-508.

(16) Baldyga J, Bourne J, Hearn S. Interaction Between Chemical Reactions and Mixing on Various Scales. Chemical Engineering Science 1997 FEB;52(4):457-466.

(17) Baldyga J, Bourne J. A Fluid Mechanical Approach to Turbulent Mixing and Chemical Reaction. Chem Eng Commun 1984;28(4-6):231-241.

(18) Baldyga J, Bourne J. Turbulent Mixing and Chemical Reactions. West Sussex, England: Wiley; 1999.

(19) Fox R. Computational Models for Turbulent Reacting Flows: Cambridge University Press; 2003.

(20) Kolmogorov A. The Local Structure of Turbulence in Incompressible Viscous Fluid for Very Large Reynolds Numbers, Proceedings of the USSR Academy of Sciences. 1941;30:299-303.

(21) Schwertfirm F, Gradl J, Schwarzer HC, Peukert W, Manhart M. The low Reynolds Number Turbulent Flow and Mixing in a Confined Impinging Jet Reactor. Int J Heat Fluid Flow 2007 DEC;28(6):1429-1442.

(22) Baldyga J, Pohorecki R. Turbulent Micromixing in Chemical Reactors - a Review, Chemical Engineering Journal and the Biochemical Engineering Journal. 1995;85:183-195.

(23) Kolodziej P, Macosko C, Ranz W. The Influence of Impingement Mixing on Striation Thickness Distribution and Properties in Fast Polyurethane Polymerization. Polym Eng Sci 1982;22(6):388-392.

(24) Macosko C. Fundamentals of Reaction Injection Molding. NY, USA: Hanser; 1989.

(25) Pohorecki R, Baldyga J. New Model of Micromixing in Chemical Reactors. Industrial & Engineering Chemistry Fundamentals 1983;22(4):392-397.

(26) Garside J, Tavare N. Mixing, Reaction and Precipitation - Limits of Micromixing in an MSMPR Crystallizer. Chemical Engineering Science 1985;40(8):1485-1493.

(27) Marcant B, David R. Experimental-Evidence for and Prediction of Micromixing Effects in Precipitation. AICHE J 1991 NOV;37(11):1698-1710.

(28) Mahajan A, Kirwan D. Micromixing Effects in a Two-Impinging-Jets Precipitator. AICHE J 1996 JUL;42(7):1801-1814.

(29) Paul E, Treybal R. Mixing and Product Distribution for a Liquid-Phase, Second-Order, Competitive-Consecutive Reaction. AICHE J 1971;17(3):718-&.

(30) Bourne J, Yu S. Investigation of Micromixing in Stirred-Tank Reactors using Parallel Reactions. Ind Eng Chem Res 1994 JAN;33(1):41-55.

(31) Johnson B, Prud'homme R. Chemical Processing and Micromixing in Confined Impinging Jets. AICHE J 2003 SEP;49(9):2264-2282.

(32) Marchisio D, Rivautella L, Barresi A. Design and Scale-up of Chemical Reactors for Nanoparticle Precipitation. AICHE J 2006 MAY;52(5):1877-1887.

(33) Dirksen J, RING T. Fundamentals of Crystallization - Kinetic Effects on Particle-Size Distributions and Morphology. Chemical Engineering Science 1991;46(10):2389-2427.

(34) Baldyga J, Orciuch W. Barium Sulphate Precipitation in a Pipe - an experimental Study and CFD Modelling. Chemical Engineering Science 2001 APR;56(7):2435-2444.

(35) Mersmann A. Crystallization Technology Handbook. NY, USA: Marcel Dekker; 1995.

(36) Schwarzer H, Peukert W. Combined Experimental/Numerical Study on the Precipitation of Nanoparticles. AICHE J 2004 DEC;50(12):3234-3247.

(37) Roelands M, Derksen J, ter Horst J, Kramer H, Jansens P. An Analysis of Mixing in a Typical Experimental Setup to Measure Nucleation Rates of Precipitation Processes. Chem Eng Technol 2003;26(3):296-302.

(38) Gavi E, Marchisio DL, Barresi AA. CFD Modelling and Scale-up of Confined Impinging Jet Reactors. Chemical Engineering Science 2007 APR;62(8):2228-2241.

(39) Siddiqui S. Use of the Confined Impinging Jet Reactor for Production of Nanoscale Iron Oxide Particles. University of Alberta; 2009.

(40) Marchisio D, Soos M, Sefcik J, Morbidelli M. Role of Turbulent Shear Rate Distribution in Aggregation and Breakage Processes. AICHE J 2006 JAN;52(1):158-173.

(41) Bramley A, Hounslow M, Ryall R. Aggregation During Precipitation from Solution: A method for extracting rates from experimental data. J Colloid Interface Sci 1996 OCT 15;183(1):155-165.

(42) Baldyga J, Jasinska M, Orciuch W. Barium Sulfate Agglomeration in a Pipe – An Experimental Study and CFD Modelling. Proceedings of the 15th International Symposium on Industrial Crystallization Italy; 2002.

(43) Mersmann A. Crystallization Technology Handbook. 2nd ed. NY, USA: Marcel Dekker; 2001.

(44) Baldyga J, Jasinska M, Krasinski A, Rozen A. Effects of Fine Scale Turbulent Flow and Mixing in Agglomerative Precipitation. Chem Eng Technol 2004 MAR;27(3):315-323.

(45) Siddiqui SW, Unwin PJ, Xu Z, Kresta SM. The Effect of Stabilizer Addition and Sonication on Nanoparticle Agglomeration in a Confined Impinging Jet Reactor. Colloids and Surfaces A-Physicochemical and Engineering Aspects 2009 OCT 20;350(1-3):38-50.

(46) Schwarzer H, Peukert W. Experimental Investigation Into the Influence of Mixing on Nanoparticle Precipitation. Chem Eng Technol 2002 JUN;25(6):657-661.

(47) Johnson B, Prud'homme R. Flash Nanoprecipitation of Organic Actives and Block Copolymers Using a Confined Impinging Jets Mixer. Aust J Chem 2003;56(10):1021-1024.

(48) Demyanovich R. Production of Commercial Dyes Via Impingement-Sheet Mixing Chem Eng Process 1991 MAY;29(3):179-183.

(49) Midler M, Paul E, Whittington M, Futran P, Liu J, Pan S, inventors. AnonymousCrystallization Method to Improve Crystal Structure and Size. US Patent No. 5,314,506. 1994 .

(50) Tamir A, Huang B. Impinging stream reactors. Fundamentals and applications, Drying Technology. 1995;13:503.

(51) Marchisio D. Large Eddy simulation of mixing and reaction in a confined impinging jets reactor, Computers & Chemical Engineering. 2009;33:480-420.

(52) Siddiqui SW, Zhao Y, Kukukova A, Kresta SM. Characteristics of a Confined Impinging Jet Reactor: Energy Dissipation, Homogeneous and Heterogeneous Reaction Products, and Effect of Unequal Flow. Ind Eng Chem Res 2009 SEP 2;48(17):7945-7958.

(53) Hage D, Carr J. Analytical Chemistry and Quantitative Analysis: Pearson Education; 2011.

(54) Clegg W. Crystal Structure Determination: Oxford University Press; 1998.

(55) Williams D, Flemming I. Spectroscopic Methods in Organic Chemistry. 5th ed.: McGraw Hill; 1995.

(56) Trimm H. Analytical Chemistry Methods and Applications: Apple Academic Press; 2011.

(57) Atkins P. Physical Chemistry. 6th ed.: Oxford University Press; 1998.

(58) Griffiths P. Chemical Infrared Fourier Transform Spectroscopy: John Wiley; 1975.

(59) Colthup N, Daly L. Introduction to Infrared and Raman Spectroscopy: Academic Press, 1975.

(60) Weast R. Hand book of Chemistry and Physics. 46th ed. Ohio: The Chemical Rubber Co; 1964.

(61) Carnelley T. Physico-Chemical Constants: Melting and Boiling Point Tables: Harrison and Sons; 1885.

(62) Anscombe F. The Validity of Comparative Experiments. Journal of the Royal Statistical Society. 1948; Series A (General) 111 (3): 181–211

Appendices

Appendix 1. Mass Balance Calculations

The simplified reactions in the CIJR are as follows:

$MDA + HCl \rightarrow MDA.HCl$

$MDA + 2HCl \rightarrow MDA.2HCl$ Picked for calculation

Mass Balance calculation needs some physical properties of the reactants and products which can be found in Table A-1. Sample detailed calculation is done for one of the samples, and summary data of 2 different case studies in Chapter 4 is provided in Table A-2.

Table A-1- Required Physical properties of the Components for Mass Balance Calculation

Material Name	*Formula*	*Molar Mass (g/gmol)*	*Density*
4,4'-Methylene dianiline(MDA)	$C_{13}H_{14}N_2$	*198.26*	*1.15 g/cm³ at 25°C*
MCB	C_6H_5Cl	*112.56*	*1.11 g/cm³ at 25°C*
Hydrogen Chloride	*HCl*	*36.46*	*SpGr=1.26 (Air=1 at 1 atm and 20°C)*
Methylene dianiline monohydrochloride (MDA.HCl)	$C_{13}H_{15}N_2Cl$	*234.72*	-
Methylene dianiline dihydrochloride (MDA.2HCl)	$C_{13}H_{16}N_2Cl_2$	*271.19*	-

Sample Calculation for the solids made from 2 wt% MDA reacted with 100% excess HCl and flowrate of 100 ml/min (50 ml/min each side):

$MDA_{in} = MDA_{out}$; MDA_{in} = MDA existing in the solid products + Error in MDA Balance

$MDA\ in\ (g) = 1\ min \times 50\ (\frac{cm^3}{min}) \times \left(\frac{2}{100}\right)(mass\ fraction) \times \rho(\frac{g}{cm^3})$; where $\rho \approx 1.11$

Then, $MDA\ in = 1.11\ g$

Produced solid weight = 1.28 g

$$\text{MDA exsisting in the solid product} = \text{Mass of the solid} \times \frac{\text{Molar Mass of MDA}}{\text{Molar Mass of the solid}}$$
$$= \frac{1.28(\text{g}) \times 198.26}{(234.72 \times \text{MDA. HCl\%} + 271.19 \times \text{MDA. 2HCl\%}) \times \frac{1}{100}} = 1.058g$$

$$\text{Relative Error Percent} = \frac{\text{MDA}_{in} - \text{MDA existing in the solid product}}{\text{MDA}_{in}} \times 100 = 4.67\%$$

There are a range of error sources contributing in the error term, such as: experimental error in measuring weight and volume, recording the run time, switching of the valves, remaining MDA in the waste MCB, dissolved AHC in the waste MCB. Also blend preparation might add another source of error, i.e. making MDA concentration of 2 wt% MDA.

The HCl side of the CIJR can have even more uncertainty in calculation, because setting the HCl flow on the specific point and switching the 3-way valve from Air to HCl, and dissolved HCl in the waste MCB definitely add difficulties in closing mass balance over the system.

HCl is fed based on 100 percent excess HCl of reaction to make MDA.2HCl salt and ideal gas law equation. The HCl flowmeter set to a volumetric flow to allow the HCl mass flow be exact as it calculated.

$\text{HCl}_{\text{in}} = \text{HCl}_{\text{out}}$;

$\text{HCl}_{\text{in}} = \text{HCl}_{\text{existing in the solid products}} + \text{HCl}_{\text{dissolved in MCB}} + \text{HCl}_{\text{degased}} + \text{Error in HCl Balance.}$

$$\text{HCl}_{\text{in}}\ (\text{g}) = 2\left(\frac{\text{Stoichiometric Coefficient of HCl}}{\text{Stoichiometric Coefficient of MDA}}\right) \times \text{mol of MDA} \times \text{Molar Mass of HCl} = 0.82\ \text{g}$$

$$\text{HCl}_{\text{existing in the solid product}} = \text{Mass of the solid} \times \frac{\text{Molar Mass of HCl}}{\text{Molar Mass of the solid}}$$
$$= 1.28 \times \frac{36.46 \times ((0.86) + 2 \times (0.14))}{239.82} = 0.22\ \text{g}$$

As the products exit the CIJR at atmospheric pressure, the solubility of HCl in MCB decreases, and the HCl mole fraction in MCB cannot exceed 0.03 or in terms of mass is 1.09 g. Titration of the caustic solution shows no change in

pH which makes sense because the expected remaining HCl in the waste was 0.82-0.22=0.6g that is lower than the solubility limit of HCl in MCB.

Titration of the NaOH solution for neutralization of the degased HCl is reported no change for most of the cases. However in some cases with higher MDA concentration and high HCl excess amounts there was 65-90% success in absorbing the degased HCl. As the HCl detector did not show major change in detected HCl in the vent stream, 10-35% error in HCl component balance.

Table A-2- Summary of the Material balance for two Case Studies in Section 4-2

Process Variables			*MDA Relative Error(%)[1]*	*HCl in MCB Waste (g)*	*HCl degased absorbed in caustic Solution (g)*	*HCl Relative Error(%)[2]*
MDA Conc. wt%	*Flowrate*	*HCl excess %*				
0.5	***100***	***100***	*7.70*	*0.11*	*0*	*N/A*
1	***100***	***100***	*6.66*	*0.23*	*0*	*N/A*
2	***100***	***100***	*4.67*	*0.6*	*0*	*N/A*
3.5	***100***	***100***	*5.22*	*1.07*	*0*	*N/A*
5	***100***	***100***	*2.44*	*1.54*	*0.35*	*21*
0.5	***200***	***300***	*5.03*	*0.62*	*0*	*N/A*
1	***200***	***300***	*3.19*	*1.05*	*0*	*N/A*
2	***200***	***300***	*2.06*	*2.77*	*1.14*	*32*
3.5	***200***	***300***	*1.15*	*4.95*	*3.33*	*16*
5	***200***	***300***	*0.62*	*7.15*	*5.43*	*10*

1: Relative Error for MDA is calculated from $\frac{\mathrm{MDA_{in}} - \text{MDA existing in the solid product}}{\mathrm{MDA_{in}}} \times 100$.

2: Relative Error for HCl is calculated from $\frac{\mathrm{HCl_{degased}} - \mathrm{HCl_{Absorbed\ in\ the\ Caustic\ Solution}}}{\mathrm{HCl_{degased}}} \times 100$; where $\mathrm{HCl_{degased}}$ is the difference between the remaining HCl leaving the solid product and the maximum amount soluble in the waste MCB.

Appendix 2. Dissolution of Gaseous HCl in MCB

There are two sets of data provided in this appendix; first serie obtained from experimental data from the plant. Second serie is a simulated case study using VMGSim software.

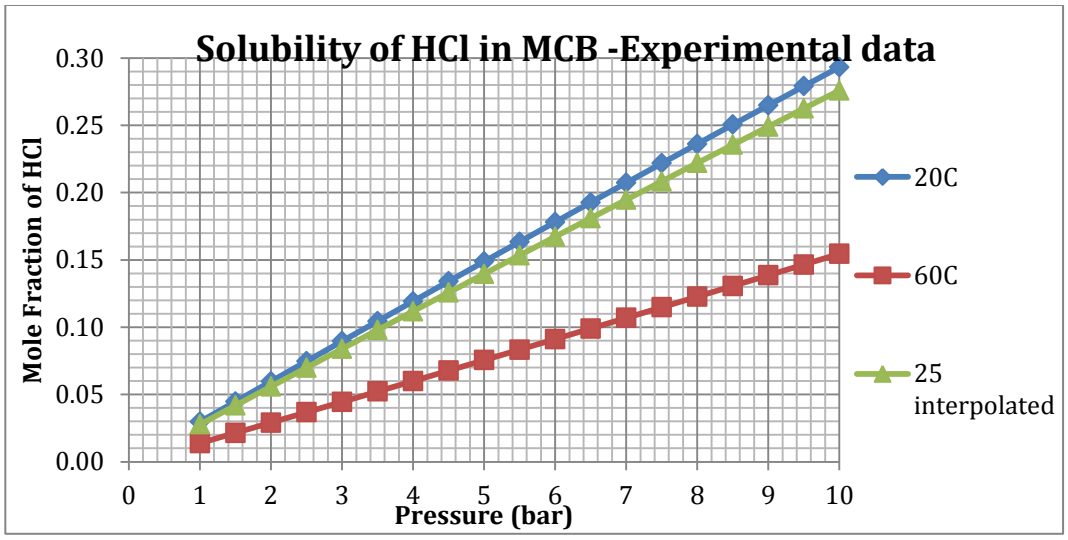

Figure A-1- Experimental chart of solubility of HCl in MCB vs. Pressure

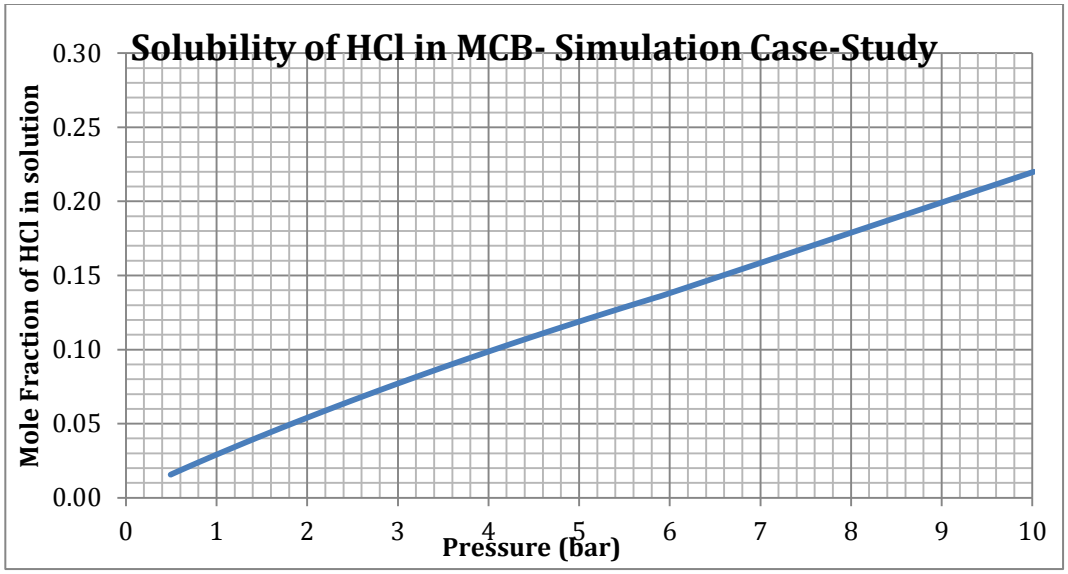

Figure A-2- Simulation result chart of solubility of HCl in MCB vs. Pressure

These two sets of data have less than 8% relative error to the mean value. By knowing the stoichiometric coefficients and HCl excess percent, system pressure must be set at a point that highest value of HCl flowrate to be dissolved completely in MCB. The highest MDA concentration selected to react with HCl is 5 wt% which needs 0.02 mol fraction HCl in the opposite

side of the CIJR to react based on stoichiometry of the reaction. 1000% HCl excess for this basis, 5 wt% MDA concentration, is equal to 0.1 mol fraction HCl in MCB, where in practice the highest excess percent of HCl gas was selected 700%. Therefore, according to the plots of the two series data, 4 bar gauge has an acceptable safety factor that keeps all the HCl dissolved in the MCB.

Appendix 3. Safe Work Procedure and Checklists

Safe Work Procedure: How to handle HCl gas cylinder in the lab and How to operate process of Aminehydrochloride salts' formation

Research Group:
Lab Location: #6120, CME Building
Created by: Navid F. Ershad
Supervisor: Dr. Suzanne Kresta
Date: October 12, 2011
Emergency Contact: Control center 780 492 5555

References:

1-Praxair MSDS for Hydrogen Chloride, anhydrous (P-460-F).

URL:http://www.praxair.com/praxair.nsf/0/214c050cecb3d6d885256a8600815177/$FILE/p4606f.pdf

2-PPG MSDS for Monochlorobenzene(MCB)

URL:http://gourabghosh.weebly.com/uploads/4/1/0/3/4103543/monochlorobenz.pdf

3-Sigma-Aldrich MSDS for: 4,4'-Methylenedianiline (MDA)

URL:http://www.sigmaaldrich.com/catalog/ProductDetail.do?D7=0&N5=SEARCH_CONCAT_PNO%7CBRAND_KEY&N4=92020424%7CSIGMA&N25=0&QS=ON&F=SPEC

4- Chemical Spill Procedure-AKA as Safe Work Procedure: minor chemical spill- by Andree Koenig

URL: https://cmesql.eche.ualberta.ca/safety/index.php/Chemical_Spill_Procedure

Part A- How to handle HCl gas cylinder in the lab

Contents

1. Scope

HCl gas cylinder with commercial name of Hydrogen chloride HC 2.0 (>99%) is provided by Praxair Canada. The major use of this gas is in semiconductor process, but can be used for other processes as well. In this lab, HCl is dissolved in MCB (monochlorobenzene) to react with DADPM (4,4'-Diamino diphenyl methane) blends in MCB. Operating of this gas must be done under high safe condition with safe procedures which will be discussed further.

2. Important Properties of gaseous HCl

Appearance: Colorless gas. Produces white fumes in moist air.

Odor: Pungent, suffocating

Physical State: Gas at normal temperature and pressure

Melting Point at 1 atm: -173.5°F (-114.2°C)

Boiling point at 1 atm: -121°F (-85°C)

Flash Point (test method): Not applicable.

Evaporation Rate (Butyl Acetate = 1): High

Flammability: Non-flammable

3. Potential Health Effects of gaseous HCl

HCl gas is toxic, corrosive, high-pressure liquid and gas; may cause liver and kidney damage. It can cause eye, skin, and respiratory tract burns. Self-contained breathing apparatus must be worn by rescue workers. Under ambient conditions, this colorless gas has a pungent, suffocating odor.

4 Emergency Procedures

4-1. First Aid Measures:

Skin Contact: Hydrogen chloride gas may severely irritate the skin, causing chemical burns with ulceration and scarring. Repeated exposure to vapors may produce dermatitis.

With prolonged or widespread contact, the skin may absorb harmful amounts of material.

In this case, immediately flush skin with plenty of water while removing contaminated clothing and shoes. Discard clothing and shoes.

Eye Contact: Exposure to the eye causes immediate pain and irritation with excess tear production and closure of the eyelids. The severity of the injury depends on the concentration and duration of contact and may range from slight excess redness and irritation of the conjunctiva to total corneal opacification and blindness.

In this case, immediately flush eyes thoroughly with warm water for at least 15 minutes. Hold the eyelids open and away from the eyeballs to ensure that all surfaces are flushed thoroughly. See a physician, preferably an ophthalmologist, immediately.

Inhalation: Overexposure to vapor concentrations moderately above 5 ppm irritates the upper respiratory tract. Concentrations ranging from 50-100 ppm are intolerable. High concentrations (as instance greater than 50 ppm) cause choking, coughing, burning of the throat, and severe irritation of the respiratory tract. Ulceration of the nose, throat, and larynx; laryngeal spasm; pulmonary edema; and general lung injury may also occur. Exposure to concentrations of 1500-2000 ppm is life-threatening. Liver and kidney injury has been reported after exposure to vapors.

If it happens, immediately remove to fresh air. If not breathing, give artificial respiration. If breathing is difficult, qualified personnel may give oxygen. Keep victim warm. Seek medical attention promptly.

Swallowing: Highly toxic. It may cause chemical burns of the mouth, throat, esophagus, and stomach, with severe pain, nausea, diarrhea, vomiting, dizziness, weakness, and collapse.

If it is swallowed, try to rinse mouth with water. Give two glasses of water. Do not induce vomiting. Call a physician.

NOTES TO PHYSICIAN: Keep victims of overexposure under medical observation for 24-48 hours. The hazards of this material are mainly due to its severely irritant and corrosive properties on skin and mucosal surfaces. There is no specific antidote. Treatment of overexposure should be directed at the control of symptoms and the clinical condition of the patient. Contact the Poison Control Center in your area for additional information on patient management and follow-up.

4-2: Exposure Control:

OSHA PEL[1]: 5 ppm; ACGIH TLV-TWA [2](2008): 2 ppm; IDLH[3]: 50 ppm

[1] OSHA PEL: Occupational Safety and Health Administration Permissible Exposure Level

[2] TLV-TWA: the allowable time-weighted average concentration for a normal 8-hour workday or 40-hour week. ACGIH (American Conference of Governmental Industrial Hygienists)

Odour threshold for HCl is less than 1 ppm. TLV-TWAs should be used as a guide in the control of health hazards and not as fine lines between safe and dangerous concentrations.

Engineering Controls:

Local Exhaust: Use a corrosion-resistant system with sufficient air flow to keep the hydrogen chloride concentration below the applicable exposure limits in the worker's breathing zone.

Mechanical Control:

-Not recommended as a primary ventilation system to control worker's exposure.

-A corrosion-resistant, canopy type, forced-draft fume hood may be preferred for some applications.

-Using a Gas Monitor is strongly recommended close to gas cylinder to find out any leakage.

-An appropriate fail safe valve is recommended to attached to the process, best point for that is just after regulator

Personal Protective Equipment:

Skin Protection: Wear work gloves for cylinder handling. Eye/Face Protection. Wear safety glasses when handling cylinders: vapor-proof goggles where contact with product could occur. Select per OSHA 29 CFR 1910.133. Metatarsal shoes for cylinder handling and protective clothing where needed. Select per OSHA 29 CFR 1910.132 and 1910.133. Regardless of protective equipment, never touch live electrical parts.

Respiratory Protection: A respiratory protection program that meet OSHA 29 CFR 1910.134, ANSI Z88.2, or MSHA 30 CFR 72.710 (where applicable) requirements must be followed whenever workplace conditions warrant respirator use. Use an air-supplied or air-purifying cartridge if the action

[3] IDLH: Immediately Dangerous to Life and Health

level is exceeded. Ensure the respirator has the appropriate protection factor for the exposure level. If cartridge type respirators are used, the cartridge must be appropriate for the chemical exposure.

4-3. Accidental Release Measures:

This gas is toxic, corrosive, high-pressure liquid and gas.

The following is steps to be taken if material is released or spilled in general:

Immediately evacuate all personnel from danger area. Do not approach area without self-contained breathing apparatus and protective clothing. Reduce vapors with fog or fine water spray. Shut off leak if without risk. Ventilate area of leak or move cylinder to a well-ventilated area. Prevent runoff from contaminating the surrounding environment. Toxic, corrosive vapors may spread from spill. Before entering area, especially a confined area, check atmosphere with an appropriate device. Reverse flow into cylinders may cause rupture.

Regularly check with Gas Detection Monitor to see leakage order. Three level risk is recommended based on gas release quantity and exposure control data:

A) Slightly over than 2ppm leakage (TLV TWA based on ACGIH):

This level should be controlled carefully by a person who is working with HCl gas. Exposure over this limit for 40-hour a week is not allowed. First, wear respirator, and then check for any failure in connections with moving sensor close to gas line, and let it stagnant close to each point for more than gas detector's response time to find out failure spot. Once it is found, shut down experiments and fix that spot.

B) Slightly Over 5ppm leakage (OSHA):

Evacuate the lab. Wear respirator and proper gloves and coat to get into lab and shut down set-up. Check with gas detector if HCl concentration is going down and lab is safe to enter. Try to find the leak point using purge gas to fix the problem, and start over with HCl when wearing respirator to see if there is no problem exists.

C) Far over OSHA limit and (Close to IDLH):

In this case, immediately evacuate the lab. Call 911 and safety persons in the campus. Stay away of the lab and don't let anybody to get close. Check with Gas Detector and report the situation to safety specialists and physician. Do not go back to the lab unless the lab is ventilated well.

4-4. Handling and Storage:

When handling the cylinder, do not breathe gas. Do not get vapor or liquid in eyes, on skin, or on clothing. Have safety showers and eyewash fountains immediately available. Protect cylinders from damage. Use a suitable hand truck to move cylinders; do not drag, roll, slide, or drop. Never attempt to lift a cylinder by its cap; the cap is intended solely to protect the valve. Never insert an object (e.g., wrench, screwdriver, and pry bar) into cap openings; doing so may damage the valve and cause a leak. Use an adjustable strap wrench to remove over-tight or rusted caps. Open valve slowly. If valve is hard to open, discontinue use and contact your supplier.

Precautions in storage are: Try to store and use with adequate ventilation. Firmly secure cylinders upright to keep them from falling or being knocked over. Screw valve protection cap firmly in place by hand. Store only where temperature will not exceed 125°F (52°C). Store full and empty cylinders separately. Use a first-in, first-out inventory system to prevent storing full cylinders for long periods.

5 Disposing of Material Safely:

Waste Disposal Method: Keep waste away from surrounding environment. Also, keep personnel away from the lab. If the gauge shows there is some gas existing in the cylinder and the experiments are done, contact gas supplier to return cylinder. Do not attempt to dispose of residual or unused quantities if there is any.

6 Step by Step Procedures for the Process;
Starting/operating/shut downing the experiments

6-1. Start-up: Follow these steps:

- Wear respirator, safety glasses, lab coat, and work gloves
- Tighten the cylinder either to the wall or a heavy bench to make sure it is physically stable
- Close the main valve tightly and remove the valve head to prevent any unwanted opening
- Attach the regulator (*) and close the valves
- Attach the process lines, and make sure the materials-especially metals- are compatible with HCl gas and also other reactants.
- Open the main valve gently and the first regulator and keep the second valve closed to operate during the process
- Make sure that every piece of equipment except for HCl cylinder and connecting tube is under fume hood, and ventilation system works properly.
- As outlet stream must be neutralized, check if product is vented to NaOH solution correctly; the outlet stream should be go thru a blow off valve(back pressure) and leads to a container witch is vented to a NaOH tank with a splash guard to prevent overloading. Then it can be vented to fume hood. Also ventilation must be checked with Gas Detection Monitor regularly to control NaOH saturation
- If applicable, check the status of gas detector and ask supervisor if it is calibrated
- Check fail safe valve condition in the set-up

(*): regulator must be compatible with HCl gas and corrosive resistant

6-2. Operating Process: As this process is dissolving HCl gas in MCB, make sure how much the gas flow rate should be to dissolve completely. Also, first run with gas side valve closed for a while, then open it to make sure there is no gas bubbles in the product. Note that gas detector is on and calibrated correctly. After opening the final valve for HCl, check its status to make sure process starts and is operated safely.

6-3.Shut down: After finishing data collecting, let the other stream continue following and close the HCl valve. Then other reactants' pumps can be stop from running. It is safer to wear respirator and safety glasses on.

6-4.Swapping/Disconnecting the Cylinder: In case of swapping the empty cylinder with a new one, or after finishing experiments in order to disconnecting the cylinder from process, it is mandatory to perform this action under a safe procedure. To suit that task, follow this procedure:

- Evacuate others from lab, it means everyone remaining in the lab should have respirator and proper gloves.
- Wear respirator, safety glasses, lab coat and work gloves
- Move the new cylinder close to the clamp and old cylinder and swap the cylinders and tighten the new one.
- Check the Gas Detection Monitor works
- Close the main(top valve)
- After evacuating the HCl gas accumulated in the line and regulator using the main safe process of set-up, close the regulator and detach that from old cylinder.
- Contact the cylinder provider to take out old HCl cylinder from the lab
- To start with new cylinder, see section 6.1.

7 Maintenance Procedures

Frequently check the regulator and gas condition. Make a check list contains of items like clamp stability condition, cylinder Pressure, fittings and connections, process pipeline, flow meter, respirator cartridge etc.

If applicable check gas monitor device, ventilation system, and process as well to make sure if there is any flaw in the system.

Part B- How to operate process of Aminehydrochloride(AHC) salts' formation

Contents

1. Scope:

The AHC formation process in the mentioned lab is a reaction between MDA (4,4'-Methylenedianiline) and gaseous HCl in MCB(Monochlorobenzene) solvent as environment. The two steps of the process simply can be named with blending and exposure of MDA/MCB blend to HCl. The reaction is operated in a jet reactor (CIJR) that inlets are MDA/MCB blend and HCl dissolved in MCB. As the whole process is operated under fume hood, there are not high safety risks in this procedure, but still safety precautions should be considered.

2. Important Properties of MDA and MCB:

2-1. MDA:

Description: 4,4'-Methylenedianiline AKA as 4,4′-Diaminodiphenylmethane. Light yellow crystalline solids in ordinary temperatures.

Melting range: 190-198°F (88-92°C)

Flash point: 446°F (230°C)- closed cup

2-2. MCB:

Description: Water-white, volatile, flammable, liquid at ordinary handling temperatures. It has a pleasant, almond-like odor.

Boiling Point: 268.9°F (131.6°C)

Flash Point: 81.5°F (27.5°C) - closed cup

Flammable limits in Air: Lower 1.3%, Upper 11%

Auto-ignition Temperature: 1094°F (590°C)

3. Hazards, Protection, First Aid and Storage of MDA and MCB:

3-1. MDA:

3-1-1. Hazards:

-Target organ effects-Excessive or chronic exposure may cause liver damage.
-Potentially Carcinogen; primary route of entry are skin contact and inhalation.

3-1-2. Protection:

Avoid all personal contact: Use chemical resistant gloves, goggles and outer clothing and launder any DADPM stained-clothing before reuse.

3-1-3. First Aid Procedure:

-Eye Contact: Flush with water for 15 minutes.
-Skin Contact: Wash thoroughly with soap and water.
-Inhalation: Remove to fresh air, get medical attention.
-Ingestion: Induce vomiting, contact physician.

3-1-4. Storage and Handling:

-Store away from sources of direct heat in a dry area

-For frequent use keep the container under fume hood

3-2. MCB

3-2-1 Hazards:

-Vapor and liquid extremely irritating to eyes and skin; may be absorbed through skin
-Harmful and fatal if inhaled; very toxic
- Flammable; keep away from sparks, flames and other sources of ignition

3-2-2 Protection:

-Avoid contact with eyes and skin; wear goggles and chemical suit
-Handle with mask and under fume hood; long-term exposure may cause kidney/liver injury
-Do not eat and drink in work area

3-2-3 First Aid Procedure:

-Eye Contact: Flush with warm water for at least 15 minutes
-Skin Contact: Run gentle stream of water for 15 minutes; use soap or skin cleanser
-Inhalation: Remove from area to fresh air; contact physician
-Ingestion: Do not induce vomiting; gently wipe inside of the mouth with water; contact emergency room

3-2-4 Storage and Handling:

-Store in a cool, dry, well-ventilated place; container must be closed and labeled.
-For frequent use, keep the container under fume hood.

4. Emergency Procedures:

Considering MDA and MCB properties and operating conditions in the lab, the only important risk is minor chemical spill that in this case, referring to

SWP titled Chemical Spill Procedure by Andree Koenig [4], there are some necessary steps to follow:

1- Put on personal protective equipment (PPE): You must be wearing proper PPE for the nature and the extent of the spill. Safety glasses, a lab coat and gloves are the absolute minimum PPE.

2- Assess difficulty of cleaning procedure: Assess the extent of the spill and the nature of the chemical. Make sure you have the proper PPE and that it is well maintained. Check that you have enough absorbent and that it is appropriate. Make sure you have back up in case something unexpected happens, or if the task is bigger than originally assessed.

3- Clean the spilled area: Cover the drain if there is a chance that the spill may reach it. If you do not have a drain cover, pour enough adsorbent to create a dam around the drain. Continue building the dam around the spill. When the spill is contained continue pouring the absorbent on the liquid until you can see that some of the absorbent is staying "dry", or that you have an excess of adsorbent.

Obtain a container big enough to put in all the used absorbent. If the liquid was a flammable liquid, only use non sparking tools. Use PPE and extreme caution.

Note: After you have started picking up the spill, if you feel the task is more than you can handle, or you feel you and others are at risk. Leave the lab and re-evaluate. You may call for assistance at any time.

4- Follow up: Send all used absorbent, contaminated gloves, contaminated broken glass to chemical waste disposal (Waste Disposal for the Laboratories). Reorder absorbent and any other supplies you used. Check that any equipment used (respirator as instance) is cleaned and ready to be used again if needed.

5. Operating Procedure Checklist

Make sure that the following items are checked:

1. Preparing before run:

- Respirator; Positive and negative pressure test and cartridge status
- Cylinder clamp is tightened properly
- Gas monitor calibrated less than 6 month ago
- Gas monitor battery has enough charge for the whole week
- HCl sensor cap is removed, and the sensor interface is clean
- Fume hood ventilation is working properly
- MCB and Blend stock is enough for the day's runs
- Caustic solution (NaOH) is in specific pH, and outlet tubing condition is in good condition
- Timer, wrenches and other necessary tools are available in the experiment area
- Pumps and mixer are plugged in and ready to use
- Every piece of equipment except for HCl cylinder and connecting tube must be under fume hood, and ventilation system works properly
- Purge gas has enough pressure
- Fill flow-meter and gas line with purge gas

2. Start-up: Follow these steps:

- Put respirator, safety glasses, lab coat, and work gloves on
- Check all tubing and connections and secure all loose ends
- Open the cylinder main valve gently, but leave the regulator and needle valve closed
- Turn the feed switch to MCB on both reactant sides
- Turn the product switch to waste
- Start the pumps (pure MCB run) in equilibrate flow

- Switch gas line to HCl to let purge gas out of the process line
- Open the regulator and needle valve and adjust desired HCl flow for the flow-meter
- Turn the feed switch to “Blend” and product switch to “Sample collector” and click the timer*

*: There will be a delay between this switch and arrival of good sample to the sample beaker. After running some tests, the switching procedure should be adapted to this delay

3. Shutdown: Follow these steps:

- Turn product switch to waste and click the timer
- Turn Feed switch to MCB
- Turn gas switch to purge gas and close the needle valve
- Close the regulator and main cylinder valve
- Turn switch to HCl and open the regulator and needle valve to remove accumulated HCl in the all equipment pieces, and then turn the switch into purge again -this step will remove all accumulated HCl in the line
- Turn off the pumps and if it is needed, pump methanol to clean the CIJR and product lines.
- Dispose of the waste and seal the samples for further characterization
- Check personal detector and record HCl exposure during the run.
- Record final pH of NaOH- by titration or pH-meter